

Control of Multiple Model Systems

Thesis by
Todd Murphey

In Partial Fulfillment of the Requirements
for the Degree of
Doctor of Philosophy



California Institute of Technology
Pasadena, California

2002

(Defended May 2, 2002)

We have not succeeded in answering all our problems. The answers we have found only serve to raise a whole set of new questions. In some ways we feel we are as confused as ever, but we believe we are confused on a higher level, and about more important things.

Bernt Øskendal

Stochastic Differential Equations:

An Introduction with Applications

Acknowledgements

There is no amount of thanks that could adequately show how much I appreciate everything Joel Burdick has done for me while wearing his many “hats.” As an advisor, he kept me interested while keeping me on track. As a research scientist, he is inspiring in his ability to actively seek new projects, and pursue them creatively. I would like to thank Richard Murray for keeping me honest, however painful it may have been at the time, during my presentations to his group. I was always pensive during the meetings themselves, but always came away with a better understanding of what questions I needed to answer. I would like to thank Jerry Marsden for pointing out how hard this topic would be and keeping the goals realistic. Moreover, it was largely due to his comments in my candidacy exam that Chapter 4 came about. I would like to thank Erik Antonsson and Pietro Perona for agreeing to be on my thesis committee and offering many helpful suggestions both in terms of my thesis and future directions of application. I would additionally like to thank Pietro Perona’s group for providing the vision software that made the feedback system we used possible.

I couldn’t have done half the things I did without Jim Radford. The countless insights he had while sitting in our office should warrant a place in this thesis. Combined with all his help in getting our computer system up and running, I owe him a debt not easily repaid. Hans Høeg made the beginning of my graduate school career fun and interesting and eventually inspired my interest in robotics. Without

him, I may have stayed forever a pure math geek instead of eventually graduating to an applied math geek. I should thank Kristi Morgansen for reading my thesis, offering many suggestions, and generally being amazingly supportive even though she had plenty to do herself. I cannot possibly express my gratitude to James Burgess, David Choi, and Andrew Homyk for doing an amazing job making the experiment, writing code, and helping me do the final experiments.

I would most especially like to thank my wife, Shelley, for all her support while I wrote this thesis. I hope she knows that there is no one in the world as beautiful and inspiring as she is.

Abstract:

This thesis considers the control of multiple model systems. These are systems for which only one model out of some finite set of models gives the system dynamics at any given time. In particular, the model that gives the system dynamics can change over time. This thesis covers some of the theoretical aspects of these systems, including controllability and stabilizability. As an application, “overconstrained” mechanical systems are modeled as multiple model systems. Examples of such systems include distributed manipulation problems such as microelectromechanical systems and many wheeled vehicles such as the Sojourner vehicle of the Mars Pathfinder mission. Such systems are typified by having more Pfaffian constraints than degrees of freedom. Conventional classical motion planning and control theories do not directly apply to overconstrained systems. Control issues for two examples are specifically addressed. The first example is distributed manipulation. Distributed manipulation systems control an object’s motion through contact with a high number of actuators. Stability results are shown for such systems and control schemes based on these results are implemented on a distributed manipulation test-bed. The second example is that of overconstrained vehicles, of which the Mars rover is an example. The nonlinear controllability test for multiple model systems is used to answer whether a kinematic model of the rover is or is not controllable.

Contents

1	Prelude	1
1.1	Relation to Previous Work and Summary of Contributions	3
1.2	Organization of Thesis	9
2	Intermezzo: Background	11
2.1	Differential Geometry	12
2.2	Nonsmooth Systems	14
2.2.1	Analysis of Discontinuous and Hybrid Systems	14
2.2.2	Equivalence of DEDRHSs to Differential Inclusions	17
2.2.3	Lyapunov Theorems of Clarke and Filippov	20
3	Theme I: Overconstrained Mechanical Systems	25
3.1	Lagrangian models	26
3.1.1	Motivation—A Two-Wheeled Bicycle	27
3.2	The Power Dissipation Methodology	29
3.3	Characteristics of the PDM	32
3.3.1	The PDM Leads to Multi-model Systems	34
3.4	Some Final Remarks on the PDM	37
4	Theme II: Kinematic Reducibility	39
4.1	$(\mathcal{U}, \bar{\mathcal{U}})$ Reducibility: The Smooth Case	40
4.2	Kinematic Reducibility for MMDA Systems	43
4.3	The PDM and $(\mathcal{U}, \bar{\mathcal{U}})$ Reducibility	48

4.4	Summary	49
5	Theme III: Controllability	50
5.1	Aside: Controlled Switching	51
5.2	Uncertain C^1 Stratified Systems	53
5.2.1	Background	55
5.2.2	Main Result	57
5.3	General MMDA Systems	61
5.3.1	Aside: Lipschitz Vector Fields	64
5.3.2	Main Result	67
5.3.3	Proof of Theorem 5.9	70
5.3.4	Proof of Theorem 5.10	73
5.4	Summary	79
6	Variation 1: Distributed Manipulation	81
6.1	Review of the Programmable Force Fields Approach	84
6.2	Modeling the Equilibrium Point of a Distributed Manipulation System	87
6.2.1	Equations of Motion	89
6.2.2	Simulations	91
6.2.3	More General Equations of Motion	92
6.3	Local Stability	94
6.3.1	XY Stability and θ Instability	94
6.3.2	Feedback for Distributed System	95
6.3.3	More General 2-Dimensional Arrays	96
6.3.4	Simulations	101
6.4	Aside: Fully-Actuated Distributed Manipulation	103
6.5	Global Stability	107
6.5.1	A LaSalle Result	108
6.5.2	Simulations	111
6.6	Experiments	113
6.6.1	Programmable Vector Field	114

6.6.2	Local Nonsmooth Feedback	114
6.6.3	Fully Actuated	116
6.6.4	Global Invariance	117
6.7	Methods for Estimating Contact States	118
6.7.1	Background - Scale-Independent Hysteresis Switching	119
6.7.2	Applications to Distributed Manipulation	124
6.8	Summary	132
7	Variation 2: Overconstrained Wheeled Vehicles	134
7.1	The Rocky 7 Mars Sojourner	134
7.2	A Simpler Rocky 7–The Kinematic Car	138
7.3	Simplifying the Rocky 7	139
7.3.1	Six Wheels and Two Steerable Wheels	140
7.3.2	Reduction 1	142
7.3.3	Reduction 2	145
7.4	Motion Primitives	148
7.4.1	Aside: Controlled Switching	149
7.4.2	Uncontrolled Switching	150
7.5	Summary	153
8	Finale: Conclusions	154
8.1	Summary	155
8.2	Future	156
A	Coda: Experimental Setup	160
A.1	Previous Experimental Setups	160
A.2	Fully Actuated Distributed Manipulator (FADM)	161
A.3	Algorithm for Nonsmooth Feedback	163
A.4	A Comment on Superposition of Forces	164
	List of Notation	170

List of Figures

2.1	A differential inclusion on a manifold	15
3.1	Planar bicycle	27
5.1	The fixed wheel kinematic car	52
5.2	Flows associated with a Lie bracket motion.	52
5.3	Cellular separation of kinematic states	54
5.4	Schematic of a set-valued Lie bracket motion.	56
5.5	Neighborhood of boundary submanifold.	58
5.6	Example of proof methodology	59
5.7	Controllability vs. noncontrollability	60
6.1	Parts on a distributed manipulator	83
6.2	Programmable vector field	85
6.3	Four node array centered at the origin	87
6.4	A wheel with the vector-dependent friction	88
6.5	X , Y , and θ trajectory of non-feedback system	92
6.6	X , Y , and θ trajectory of feedback system	103
6.7	Rigid body velocities	104
6.8	A LASALLE invariance theorem	108
6.9	A box being transported to $\{x, y, \theta\} = \{0, 0, 0\}$ from $\{3, 10, \frac{\pi}{4}\}$. . .	113
6.10	Experimental setup	113
6.11	Programmable vector field experiment	115
6.12	Under-actuated feedback control	116
6.13	Fully-actuated feedback control	117

6.14	Combining the programmable vector field with local feedback	118
6.15	A supervisory control system	120
6.16	A supervisory control system	124
7.1	Photo of Rocky 7 mars rover prototype	135
7.2	(a) kinematic car; (b) simplified Rocky 7.	136
7.3	The kinematic car	138
7.4	6 driven wheels, 2 steerable wheels	141
7.5	1 driven and steered wheel, 2 passive wheels	142
7.6	2 driven and steered wheels, 1 passive wheel	146
7.7	SR7 with constant wheel angle and speed	149
7.8	(a) X and Y variables; (b) θ variables of the FWKC bracket-like motion.	150
7.9	a) X and Y variables of Simulation 1 b) θ variable of Simulation 1 .	150
7.10	a) X and Y coordinates of a Lie Bracket Motion of Rocky 7 b) θ motion	151
7.11	a) X and Y Coordinates for Simulation 2 b) θ for Simulation 2	152
A.1	Force Superposition	161
A.2	Front and Underside of the FADM System	162
A.3	Cartoon of Experiment	162
A.4	Algorithm for Nonsmooth Feedback	164
A.5	One of the cells	165
A.6	8 cell configuration of FADM system	166
A.7	FADM computer interface	167
A.8	Superposition experiment	168

List of Tables

1.1	Different combinations of smooth and nonsmooth control theory . . .	2
3.1	The Lagrangian dynamics of the planar bicycle	28
5.1	Different Chow's Theorems with the same condition	80
6.1	Advantages and disadvantages of supervisory control	123
A.1	Nonsmooth control law	165
A.2	List of control laws for regions I-VIII	168
A.3	List of control laws for regions 0 – $\frac{7\pi}{4}$	169

Chapter 1

Prelude

The music of the heavens being eternal, Leonardo understood that friction is absent from the state of grace. Thus confined to this mortal world, friction is a consequence of original sin.

Brian Armstrong-Helouvry *Control of Machines with Friction*

The product of original sin or not, friction is a reality in our world. And one of the fundamental problems friction introduces is that of nonsmoothness. That is, when one introduces friction into a model of a system, equations that were C^∞ or even analytic become Lipschitz continuous, continuous, or even discontinuous. One of the ways friction can introduce these errors is by producing *forces of constraint*—forces that ensure some constraint is satisfied. For instance, the wheels of a car enforce no sliding constraints both in the direction the wheel is turning and in the direction perpendicular to the wheel. One can often use these constraints to produce a tractable model for a system.

However, it is sometimes the case that the system is *overconstrained*—the system cannot satisfy all of its constraints at once. In this case, the contact state can introduce discontinuities into the equations of motion. Such a system can be modeled as a *multiple model* system. These are systems for which only one model out of some finite set of models gives the system dynamics at any given time. In

<p style="text-align: center;">Smooth Dynamics Smooth Control</p> <p>All of classical control falls here. Linear, nonlinear, and most of optimal control.</p>	<p style="text-align: center;">Smooth Dynamics Nonsmooth Control</p> <p>Bang-bang control and functional analytical notions of controllability, reachability, and solvability are here.</p>
<p style="text-align: center;">Nonmooth Dynamics Smooth Control</p> <p>Addressed in this thesis.</p>	<p style="text-align: center;">Nonsmooth Dynamics Nonsmooth Control</p> <p>Addressed in this thesis.</p>

Table 1.1: Different combinations of smooth and nonsmooth control theory

particular, the model that gives the system dynamics can change over time. In the case of overconstrained systems, these different models correspond to a subset of the constraints being satisfied. There are then several questions. How does one model such a system? Given a model, how does one design control laws that incorporate the salient features of the overconstrained system without being so complicated that they cannot be analyzed? Overconstrained systems often have discontinuous dynamics. Because of these nonsmooth terms, controllers based on C^∞ analysis often fail. This thesis is concerned with aspects of how to treat nonsmooth and discontinuous systems, motivated by concerns of intermittent contact, overconstrained systems, and, in general, multiple model systems. This thesis focuses on developing analytical tools and control system design for these systems. These include tests for controllability, kinematic reducibility, and stability. Moreover, these tools are used in the context of two important examples and include case studies in the form of simulations and experiments for illustration.

1.1 Relation to Previous Work and Summary of Contributions

This thesis has its roots in many different areas of control. Roughly speaking, it lies at an intersection of some of the classical areas of smooth control and nonsmooth control. Consider Table 1.1. A great deal of work has been done on control of smooth systems using smooth control (in fact, all of classical control falls into this category). Additionally, substantial areas of research are dedicated to control of smooth systems using nonsmooth control schemes. Hybrid control, bang-bang control, and some nonlinear control techniques fall in this category. However, relatively little work has been done in the control of nonsmooth systems using smooth control or in control of nonsmooth systems using nonsmooth control. This thesis falls in the latter two categories. Here an overview is given of the history behind the results in this thesis. Only brief descriptions are given here and generally more in-depth descriptions will be given as they are needed. The contributions of this thesis address both theoretical and practical aspects of the control of overconstrained systems. Some of this work has already appeared in previous papers (see [61, 62, 63, 64, 65, 66, 67]). These contributions and their relationship to previous work will be the focus of the remainder of this section.

Modeling Overconstrained Systems

One of the primary difficulties in modeling overconstrained systems is developing a model that incorporates the essential dynamical effects while remaining tractable. In general, the work in two papers in particular will be used as the starting point for developing equations of motion for overconstrained systems. In Alexander and Maddocks [3], the power dissipation method is used to develop equations of motion for overconstrained systems. However, they did not show any formal characteristics of the resulting first order discontinuous differential equations. Peshkin and Sander-son [72] showed at an intuitive level the relationship between solutions to the power dissipation method and solutions to Newton's equations. This thesis formalizes even

further the power dissipation approach used by Alexander and Maddocks [3] and Peshkin and Sanderson [72]. Rather than using “slow moving” assumptions, a more geometric approach is taken and the work in Lewis [44] is extended to the case of multiple model systems. Additionally several key properties of solutions to the power dissipation method are shown. In particular, it is shown that it has unique solutions almost always and that these solutions are easily characterized by the constraints. Most importantly, it is shown that the power dissipation method implies that the dynamic states can be completely described by the contact states of the object, where by contact state I mean the current stick/slip state of all potential contacts in the system.

Nonsmooth Analysis

Historically, nonsmooth analysis first became important within the context of optimal control. Probably the most important set of results in this area in the last 50 years was the Pontryagin maximum principle (see [74]). Later, after the importance of set-valued analysis became more clear, Filippov wrote one of the first systematic treatments of discontinuous differential equations (see Filippov [27]). This treatise includes basic conditions of existence and uniqueness, notions of a derivative, and stability results for differential inclusions. Later, Clarke extended many of these notions by introducing, among other things, what is now termed the Clarke Generalized Differential (see [20, 19]). Recently, much of Pontryagin’s work has been extended by Sussmann in [81] by generalizing packet variations to abstract variations so as to have a more general notion of optimality. Aubin [6] has contributed significantly in the areas of computation for differential inclusions. Only in the past few years have several authors studied the application of nonsmooth analysis to understanding dynamics best modeled by discontinuous vector fields. For instance, both Marques [56] and Moreau and Panagiotopoulos [59] discuss detailed models of friction, viscous flow, and impacting bodies using analysis techniques largely coming from the formalism developed in [20, 19, 27]. This formalism is used throughout the thesis to prove extensions of existing control techniques relevant to multiple model

systems.

Kinematic Reducibility

Kinematic reducibility answers whether or not the description of a mechanical system can be reduced to a kinematic one. In [44], a necessary and sufficient local condition was derived for such a reduction to be possible, although the reduction is not given explicitly. Nevertheless, the reduction is often clear by inspection. One of the purposes of this thesis is to extend tests of controllability to the case of overconstrained systems. Using formal properties of the power dissipation method, extensions of the work in Lewis [44] relevant to the class of nonsmooth systems in this thesis are proved. In particular, it is shown that it is sufficient that the dynamics of each contact state be kinematically reducible for the overconstrained system to be kinematically reducible.

Controllability

One of the most fundamental theorems in nonlinear control, Chow's theorem (in [18]) states that if the involutive closure of the distribution of a drift free control system spans \mathbb{R}^n , then the system is locally controllable. Roughly, a system is locally controllable if it can go anywhere in a small neighborhood of a point without leaving that neighborhood. This important theorem gives insight into many different areas of control, including wheeled vehicles, robotic fish, and satellite control. One of the purposes of this thesis is to extend tests of both controllability and of kinematic reducibility to the case of overconstrained systems. Again, using the formal properties of the power dissipation method, extensions of the work in Chow [18] relevant to the class of nonsmooth systems considered in this thesis are proved. In particular, it is shown that a set-valued Lie bracket is appropriate for a controllability test.

Distributed Manipulation

Distributed manipulation is the study of how to affect the motion of an object through the use of many points of contact with actuators. Typically, these actuators

are small, inexpensive mechanisms that combined can produce large net effects on the object being considered. Moreover, such distributed manipulation can be fault tolerant because removing or breaking one actuator does not jeopardize the overall system performance. Lastly, distributed manipulators can potentially perform a large number of tasks in parallel. Distributed manipulation has many implementations. For instance, MEMS (microelectromechanical systems) Technology can be used to make an actuator array where high numbers of micro-scaled actuators move and control objects that rest on them. Although MEMS technology is not explicitly considered in this thesis, this is one of the examples I ultimately have in mind.

The problem of using a highly articulated, large input space to control a relatively small number of outputs has only recently become significant. Its significance has largely been brought about by the ability to machine at extremely small scales at a relatively low cost (such as MEMS) and the availability of basically unlimited computational resources. An overview of some of these recent developments can be found in [10]. One of the difficulties inherent in a many input/few output system is a control synthesis problem—how does one get all the inputs to “cooperate” in such a way to get the desired output? There have been several approaches to this, ranging broadly over a set of theoretical techniques. An open loop approach pioneered by Böhringer et al. has been to use a programmable force field to control an object on an array of actuators. The basic idea is to idealize the discrete array of actuators to a continuous distribution of actuation, which can be written down explicitly as a force field. Then design based on the mass distribution of the object being controlled is used to control the object (see [9, 11, 12, 13]). This work has been extended significantly by Kavraki in [79] and other works. Another approach pioneered by Luntz et al. in [48, 49, 52, 53] uses closed loop control based on the same fields developed by Böhringer and Kavraki. Naturally, a tremendous amount of work has been done in the area of fabrication and design of arrays of actuators (see, for instance, [7, 29, 40, 41, 43, 55, 77]), but as this thesis is not concerned with fabrication, I would like to refer the reader to these references and [10] and the references therein.

One of the problems with the preceding control strategies is that they do not take into account the contact state of the distributed actuators as they make and break contact with the object being controlled. This thesis considers distributed manipulation as a nonsmooth problem, with kinematics defined by the power dissipation method. In particular, the open loop control strategies in [9, 11, 12, 13, 79] are analytically shown to lead to unstable rotational dynamics, a result well known in practice. Then it is shown that in the presence of feedback the system is stabilizable. In fact, if the actuators are fully actuated (can steer in any direction and rotate with any velocity), it is shown that an analytical smooth control law is appropriate for controlling these systems. However, when the actuators are not fully actuated, the system can be exponentially stabilized using discontinuous feedback. Moreover, it is shown that global exponential stability can be achieved even if feedback is only available in a small neighborhood of the desired equilibrium point. This technique involves “patching” together the open loop control philosophy of [9, 11, 12, 13, 79] and closed loop philosophy just mentioned. All these results are validated both in simulation and on an experimental apparatus. Although the test-bed used is quite large (approximately a square meter with only 9 actuators), it approximates some of the difficulties encountered at the micro-actuator scale. This test-bed is used as an example of a distributed system, and it is shown that many of the techniques used by Böhringer, Kavraki, and others are not always appropriate approximations because of the overconstrained nature of the problem. The feedback control laws are then implemented using visual feedback.

Nonholonomic Motion Planning

Control of what are termed term *essentially nonlinear* systems—systems which do not have controllable linearizations—has been an active area of research for many decades. An important subclass of these systems, nonholonomic systems, has been studied intensively in many works which not related here. Instead, for an overview I recommend Kolmanovsky and McClamroch [39]. For an excellent example of a nontrivial nonholonomic system, Lewis et al. [46] is very good. For somewhat more

in depth analysis I recommend Bloch et al. [8]. Since the work here is most closely related to the problem of controllability and stabilization of a vehicle, the work here starts from a formalism and uses many results found in Murray et al. [69, 70, 82]. Lastly, there has been quite a lot of work done on stabilizing nonholonomic systems using discontinuous feedback laws. In particular, Hespanha et al. [35] uses many of the same ideas I will use in this thesis for control of overconstrained systems, and I owe many of the insights in this thesis to their work.

This thesis considers the control of overconstrained wheeled vehicles. In particular, a chapter focuses on the example of the Rocky 7 Mars rover, a prototype Mars rover exploratory vehicle. Such a vehicle is overconstrained because of the nature of its nonholonomic constraints. Moreover, because each of the individual contact states for the wheels reduces to a nonholonomic problem, the system is essentially nonlinear. The controllability theory developed in earlier chapters is used to show under what conditions overconstrained vehicles are controllable. There are, in fact, conditions under which they do not meet the sufficiency condition for a system to be controllable. Some preliminary results regarding the stabilization of such vehicles are developed and simulations are provided.

Other Application Areas

Although this thesis does not specifically consider application areas beyond those just mentioned, the theory developed in this thesis is relevant to a number of other areas. In particular, systems with dynamic graphs are an important area of study. These are systems that have a graph structure describing the interconnection of various components of the system. This graph structure can change over time, hence making the system a multiple model system if changing the graphs changes the dynamics. An example is a system of vehicles that communicate with each other to accomplish some joint task that requires cooperation between the vehicles. This cooperation is enabled through the use of feedback. Each individual vehicle enacts a controller that is a function of not just that vehicles state but also of the state of some set of other vehicles' states. With a fixed communication pattern, certain

properties of what is called its connectivity matrix can be used to analyze stability of the overall connected system. However, if each vehicle can only communicate with some subset of the vehicles around it (for instance, within a certain radius), then over time the vehicles with which it communicates will change, possibly in an unpredictable manner. This means that any stability analysis must include the dynamics of the graph as well as of the individual vehicles. The theoretical part of this thesis offers insight into how to analytically treat such discrete changes in the description of the system.

Summary

I do not claim that the nonsmooth analysis approach is the only, or even the best, way to understand and control overconstrained systems. However, this thesis demonstrates both analytically and in experiment that such an approach leads to control laws which are both provably correct and practical with respect to implementation. These assertions are backed with simulations and experimentation. The strength of this theory is that with relatively little background one can analyze previously largely intractable problems.

1.2 Organization of Thesis

This thesis is organized into eight chapters and an appendix. Chapter 2 gives some of the necessary background for the succeeding chapters. Chapter 3 introduces the power dissipation method, which gives us the ability to model overconstrained systems as first order discontinuous ordinary differential equations. Chapter 4 discusses the first major result of the thesis, which answers the question, “When can the dynamic model of a complex mechanical system involving multiple contact states be reduced to a kinematic model?” This validates to a large extent the methodology given in Chapter 3 by giving a rigorous relationship between the governing equations produced by the the power dissipation method and the original Lagrangian system. Chapter 5 analyzes the issue of controllability for overconstrained systems. It essen-

tially gives two different versions of an extension of Chow's Theorem, starting with the strongest assumptions and the easiest proof. The chapter continues with a much more general result. Chapter 6 discusses in depth the application to distributed manipulation. Not only are stability theorems proved for distributed manipulators, but additionally include significant experiments using a distributed manipulation test-bed. The control designs developed in the chapter are demonstrated on this system. Chapter 7 discusses the more difficult case of an overconstrained vehicle, where the individual contact dynamics lead to what are termed essentially nonlinear dynamics. An overconstrained vehicle is used as an example, and controllability results developed earlier are used to see under what circumstances such a vehicle is controllable. Additionally, some preliminary results on stability for such systems are presented. Finally, Chapter 8 is the conclusion, and has an extensive section on the worthwhile topics not addressed in this thesis. The List of Notation and Bibliography are at the end of the thesis.

Chapter 2

Intermezzo: Background

Everything of importance has been said before by somebody who did not discover it.

Alfred North Whitehead

This chapter reviews some of the mathematical concepts that are used in subsequent chapters. Background materials appropriate to specific applications are relegated to the chapter where they are appropriate. Rather than giving a complete background in differential geometry or in nonsmooth analysis, I give an abbreviated overview which will establish notation and give some intuition about the more important results (with respect to this thesis) in each area. I give a very brief introduction to differential geometry in Section 2.1 to establish notation. Since nonsmooth analysis is not as mature a field as classical smooth analysis, I provide a more thorough summary of important theorems in Section 2.2. I attempt to relate the my intuition while also giving a rigorous presentation. The presentation of this material is primarily based on Clarke ([20, 19]) and Filippov ([27]), although this presentation certainly benefits from the work of Sussmann ([80, 81]) as well as many others. Section 2.2.1 gives an overview of hybrid systems and “switching” dynamical systems. Section 2.2.2 discusses the relationship between differential equations with

discontinuous right-hand sides (hereafter referred to as DEDRHSs) and differential inclusions. Section 2.2.3 compares and contrasts the Lyapunov theorems of Clarke and Filippov.

2.1 Differential Geometry

I assume the reader is familiar with the basic notation and formalism of differential geometry and nonlinear controllability theory (see [68, 76]). There are many good references on differential geometry (for instance, [1, 14, 23, 28, 85]), and I would like to direct the reader to them for more information. I would like to review the following definitions and classical theorems so that it may be clear where we are starting from. Let Q be an n -dimensional configuration space, and TQ its associated $2n$ -dimensional tangent bundle. The space of inputs, \mathcal{U} , is m -dimensional. If a map is k times differentiable, we will say it is C^k . Moreover, denote the real numbers by \mathbb{R} , the rational numbers by \mathbb{Q} , and the natural numbers by \mathbb{N} .

The governing mechanics of classical nonholonomic systems can in many cases be put into the form of a drift free affine system:

$$\dot{q} = g_1(q)u_1 + g_2(q)u_2 + \cdots + g_m(q)u_m \quad (2.1)$$

where $q \in \mathbb{R}^n$ is the system's state space, (u_1, \dots, u_m) are the controls, and g_1, \dots, g_m are analytic vector fields termed the *control vector fields*. Controllability tests for such systems are based on the following definitions.

Definition 2.1. A vector space V over the \mathbb{R} is a *Lie Algebra* if there exists a bilinear operation $[\cdot, \cdot] : V \times V \rightarrow V$ satisfying skew symmetry and the Jacobi identity. That is, $[v, w] = -[w, v]$ and $[v, [w, z]] + [z, [v, w]] + [w, [z, v]] = 0$.

A Lie algebraic structure has proven to be extremely useful in many applications. Here, it is desirable to give the space of vector fields a Lie algebra structure, and do so by defining the *Lie bracket*.

Definition 2.2. The *Lie bracket* between two smooth vector fields f and g on Q is defined to be

$$[f, g](q) = \frac{\partial g}{\partial q} f(q) - \frac{\partial f}{\partial q} g(q) \quad (2.2)$$

Definition 2.3. The *distribution* associated with a set of vector fields $\{g_1, \dots, g_m\}$ to be

$$\Delta = \text{span} \{g_1, g_2, \dots, g_m\},$$

where the span is defined over the set of real valued functions on \mathbb{R}^n

A distribution is said to be *regular* if the dimension of $\Delta(q)$ does not vary with q . It is said to be *involutive* if it is closed under the Lie Bracket operation. Involutivity implies that the Lie Brackets of the basis elements of the distribution are contained with the distribution. The *involutive closure* of a distribution is the smallest involutive distribution containing Δ , and is denoted by $\overline{\Delta}$. The constraints considered in this thesis are *nonholonomic* constraints. Nonholonomic constraints can be written in the form of

$$\omega(q)\dot{q} = 0, \quad (2.3)$$

where $\omega(q)$ consists of covectors (also called *one forms*) acting on the elements of $T_q Q$.

Two theorems play a fundamental role in much of differential geometry and nonlinear control theory. The first, one of the most important results of elementary differential geometry, relates involutive distributions to integral manifolds.

Theorem 2.1 (Frobenius). *A regular distribution is integrable if and only if it is involutive.*

Therefore, from a controls perspective, integrability is undesirable. It leads to the restriction of the control system to a submanifold. Instead, we want a condition that guarantees the control system in Equation (2.1) can be driven anywhere on the configuration manifold Q . This leads to the following definition of controllability.

Definition 2.4. We say a drift free control system of the form in Equation 2.1 is

controllable if for any $q_0, q_f \in \mathbb{R}^n$ there exists a $T > 0$ and $u : [0, T] \rightarrow \mathcal{U} \subset \mathbb{R}^m$ such that $q(0) = q_0$ and $q(T) = q_f$.

A system is *locally controllable* if there exists a neighborhood \mathcal{N} of q such that the system is controllable for any $q_0, q_f \in \mathcal{N}$. The next theorem relates controllability of a system to the closure of its distribution. Chapter 5 focuses on extending this theorem to a class of nonsmooth systems. The main controllability test for systems of the form Equation (2.1) is

Theorem 2.2 (Chow [18]). *The control system 2.1 is locally controllable at $q \in \mathbb{R}^n$ if $\bar{\Delta}_q = T_q\mathbb{R}^n$.*

2.2 Nonsmooth Systems

This section covers some of the basic aspects of the theory of nonsmooth systems. In particular, it covers the different contexts in which discontinuity can arise, when the need for set-valued differentials becomes apparent, and finally some standard stability theorems for differential equations with discontinuous right-hand sides (DE-DRHSs). The primary reference for this material is Filippov [27].

2.2.1 Analysis of Discontinuous and Hybrid Systems

There are two main philosophies in control that give rise to discontinuous behavior in a system. By the far the more well known is that of hybrid control. In this control strategy, one has a finite number of controllers, each relevant to different scenarios in the configuration space of the control system. The fields of sliding mode control, hybrid automata, and supervisor based adaptive control all fit within this philosophy. A lesser known philosophy, and the one I will use, is essentially that of model reduction. Given some complicated system that can be bounded by a conservative approximation of the dynamics, this conservative approximation can be used to design control laws. Consider Figure 2.1. Here we see a point q on the sphere S^2 , and the associated tangent plane T_qS^2 at q . Typically a dynamical system on the sphere would be described by the flow of a single vector in T_qS^2 .

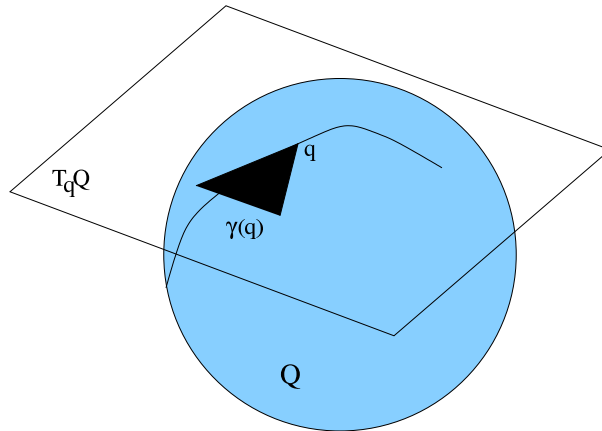


Figure 2.1: A differential inclusion on a manifold

For reasons that will be clear shortly, the governing equations are modeled as a set $\gamma(q) \subset T_q S^2$. This set will typically be convex, leading to a scenario where solutions to the dynamical equations are no longer unique. Therefore, we only require that the time derivative of the system flow lies within the set $\gamma(q)$ shown in the figure.

The vectors of ordinary differential equations are now replaced by sets, vector fields are replaced by differential inclusions, and existence and uniqueness of solutions is replaced only by existence. Moreover, in this context, sets can arise due to disturbances as well as inputs. This thesis will primarily use sets to model specific classes of disturbances, those that arise due to switching contact states. In particular, it will arise as a natural way of viewing *multiple model* systems. These are systems where the actual plant governing the dynamics of the system is only known to lie in some set \mathcal{P} of potential plants. Switching between plants can occur arbitrarily. \mathcal{P} is in our case finite, but can be countably infinite or even a continuum. More general classes of disturbances may be modeled as sets in this framework.

Discontinuities in t

Many people have looked at the case when the discontinuity of the right-hand side of a differential equation is solely dependent on time t . Most often, the discontinuity in this case is a result of controller design. That is, in optimal control, the optimal solution may be a function $\phi(t)$ which takes its values in $\{-1, 1\}$ (known as “bang-

bang” control). It may also arise when actual control input, say an alternating current, is necessarily discontinuous. In this case, the mathematical treatment of the discontinuity can almost entirely be treated by the Caratheodory case. In the Caratheodory case, the original system is

$$\dot{x} = f(x, t),$$

which is known to be equivalent to

$$x(t) = x(t_0) + \int_{t_0}^t f(x(s), s) ds. \quad (2.4)$$

If the function $f(x, t)$ is only discontinuous in t (and continuous in x), then functions satisfying Equation 2.4 can be considered solutions of $\dot{x} = f(x, t)$. Then, using the concept of the Lebesgue integral, one obtains the definition of a solution in the sense of Caratheodory. This is not terribly different from the normal definition. Moreover, since it is not the case with which I am primarily concerned, I will not comment further on it. Complete treatments of the Caratheodory case can be found in [21].

Discontinuities in x and t

Now consider differential equations with discontinuities with respect to x and t . Even in this case, there are two relatively important distinctions to be made. In one case, one can use the state to *decide* when discontinuities should occur. For instance, the entire methodology of sliding mode control falls into this category (see [83] for example). In the other case one has no control over when the discontinuities occur. That is, in the first case, the discontinuities are an effect of feedback, whereas in the second case they are a result of environmental factors. We will see later that the dynamics of overconstrained mechanical systems can be viewed as this latter kind of problem. Physically, one can think of using differential inclusions or differential equations with discontinuous right-hand side(s) (DEDRHS) as a type of model reduction. Take, for instance, the case of friction. The interplay between “stick” and “slide” is a phenomenally complicated problem, but the decision to only

include those two states and not model the transition is a philosophical statement about how much one thinks the transition is of vital importance to understanding the control problem. In general, we expect that detailed modeling of friction will not be very fruitful, so instead we do this “model reduction” to the discontinuous case. That said, I acknowledge that if one looks at a fine enough scale, dynamics we model as discrete should actually be continuous. (Alternatively, if one goes to an even finer scale, the molecular level, one could argue that then no dynamics are actually continuous, and that they are in fact discrete!)

Given discontinuities in x and t , it is reasonable to ask what one should count as admissible solutions. Solution concepts are complicated in the case of DEDRHS largely due to the strong coupling between the physical meaning of a solution and its mathematical existence. Here are the main ideas that need to be considered (primarily from [27]).

1. The continuous case should be a special case of the discontinuous case.
2. For the case when discontinuities only occurs in t , there should only be the solution $x(t) = \int_{t_0}^t f(x, s) ds$.
3. The definition must be physically meaningful.
4. Solutions that uniformly converge must converge to a solution.
5. Change of variables of a solution must also be a solution.

Examples 2.1 and 2.2 show that in order to realize these properties, one must allow the solution to satisfy a differential inclusion, rather than satisfy a single-valued differential equation.

2.2.2 Equivalence of DEDRHSs to Differential Inclusions

First consider two illustrative examples. In the first, we will see that even when we can explicitly calculate the solution to a DEDRHS, we will see that this solution does not satisfy the differential equation. In the second example, we see that generalizing

the condition for satisfying the differential equation is the right approach, and see that in fact differential inclusions provide the right existence properties.

Example 2.1

Consider the following example of a differential equation with a discontinuous right-hand side.

$$\dot{x} = 1 - 2 \operatorname{sgn}(x), \quad (2.5)$$

where sgn is the sign function which takes values

$$\operatorname{sgn}(x) = \begin{cases} 1 & \text{for } x > 0 \\ 0 & \text{for } x = 0 \\ -1 & \text{for } x < 0 \end{cases}$$

The solution to this differential equation can be found explicitly. We know that for $x < 0$, $\dot{x} = 3$, and that for $x > 0$ we have $\dot{x} = -1$. Therefore, the solution looks like (purposefully omitting the case $x = 0$ for now):

$$x(t) = \begin{cases} 3t + c_1 & \text{for } x > 0 \\ -t + c_2 & \text{for } x < 0 \end{cases} \quad (2.6)$$

Now we have the question of how to continue the solution past the point $x = 0$. Notice that $x = 0$ is an equilibrium point for this system. This implies that $\dot{x} = 0$. But if we substitute in $x = 0$ in Equation 2.5, we get $\dot{x} = 1!$ \diamond

We are now faced with a question as to what is the best way to include $x(t) = 0$ as a solution. However, the only way to get the differential equation to make sense at $x = 0$ is to have $\operatorname{sgn}(x) = \frac{1}{2}$, an untenable solution. Consider the generalization of Example 2.1 in Example 2.2:

Example 2.2

We now consider the DEDRHS:

$$\dot{x} = 1 - a \operatorname{sgn}(x) \tag{2.7}$$

This equation leads to requiring that $\operatorname{sgn}(x) = 1/a$, which leads to $\operatorname{sgn}(x)$ not being well defined. There are two possible ways to resolve this dilemma. The classical way is to only require that the solution satisfies Equation 2.5 almost always (*a.a.*). The problem with this is that it makes it then difficult to talk about equilibria. More importantly, the solutions in the case of Example 2.5 *do not* satisfy the inclusion everywhere, because the solution $x = 0$ is stable. This definition would only work if we knew that the solutions would pass through $x = 0$ transversely, thus ensuring the “almost always” condition. Instead, we allow the function $\operatorname{sgn}(\cdot)$ to become a multivalued map defined by

$$\left\{ \begin{array}{ll} \operatorname{sgn}(x) = 1 & \text{for } x > 0 \\ \operatorname{sgn}(x) = [-1, 1] & \text{for } x = 0 \\ \operatorname{sgn}(x) = -1 & \text{for } x < 0 \end{array} \right\}$$

In this way we produce the natural necessary condition for equilibrium, that $0 \in F(x_0)$, which can then be tested for stability using other techniques. \diamond

There are two interesting properties of the system in Example 2.2 which are quite different from solutions to ordinary differential equations. First, solutions are not unique. The point $x = 0$ has multiple solutions running through it. In fact, in this case, *all* solutions pass through it as $t \rightarrow \infty$. Second, solutions reach the origin in *finite* time. This is clear from the solution in Equation 2.6.

Returning to the original goal of this section, which is to formalize the relationship between DEDRHSs and differential inclusions, consider the differential equation

$$\dot{x} = f(x, t), \tag{2.8}$$

where f is piecewise continuous in some domain G , $x \in \mathbb{R}^n$, $\dot{x} = \frac{dx}{dt}$, and M is a set of measure zero upon which the function f is discontinuous. As in Filippov [27, page 50], we say that a map is a solution to Equation 2.8 if it satisfies the differential inclusion

$$\dot{x} \in F(x, t), \tag{2.9}$$

where $F(x, t)$ is convex and appropriately defined to approximate whatever physical process in which we are interested. The solution is required to be an absolutely continuous vector-valued function $x(t)$ which satisfies Equation 2.9 almost everywhere (*a.e.*). (Note that the solution to Equation 2.5 does satisfy the inclusion everywhere.) Aside from the fact that on G/M $F(x, t)$ must be single valued and equal to $f(x, t)$, there is no a priori restriction on the definition of $F(x, t)$.

Remark 2.1

Note that if we have no information about the stability or lack of stability of the set M , Example 2.5 illustrates why we cannot arbitrarily allow $F(x, t)$ to be single valued, but must instead make the conservative allowance that on the boundary $F(x, t)$ is some multivalued map. In the case of time delay systems and dry friction systems, it is traditionally accepted to define $F(x_0, t)$ to be the convex hull of all possible values of the limit as the limit approaches the boundary M upon which x_0 lies. See [59] and [56] for more information on the interplay between the detailed modeling of friction and the use of differential inclusions. \diamond

2.2.3 Lyapunov Theorems of Clarke and Filippov

As previously mentioned, there are two important camps of nonsmooth analysis, at least from the author's perspective. These stem from the point of view of Clarke and Filippov, respectively, and although their work overlaps in many ways, they have decidedly different interests philosophically. The most important difference is the reason that the set-valued natures of their problems arise. For Clarke, from the

perspective of control, set-valued maps arise in the form of an equation:

$$\dot{x} \in F(x, u) \tag{2.10}$$

where $u \in \mathcal{U}$. \mathcal{U} can be thought of as the space of admissible inputs for the system $\dot{x} = F(x, u)$. He then uses this structure to show the existence of stabilizing controllers, as in [20].

On the other hand, Filippov views these things quite differently. Motivated by the need to have a reasonable definition of a *solution* of Eq. (2.10), he is implicitly thinking of a system where the dynamics are known (and smooth) almost everywhere, but must be extended to the set-valued case in order to guarantee existence of solutions. Example 2.1 and Example 2.2 are examples of this dilemma.

This fundamental difference in their perspectives on the world of differential inclusions leads to similarly stated but radically different theorem meanings. Shortly, we will see Lyapunov theorems based on the work of both Clarke and Filippov, and will illustrate the fundamental differences between them. First we need to define some notions of stability.

Definition 2.5. The equilibrium point $x = 0$ is *uniformly stable* if for all $\epsilon > 0$ there exists $\delta > 0$, independent of t_0 , such that the trajectories $\Phi(t, t_0, x_0)$ of the system satisfy $\|x_0\| < \epsilon \Rightarrow \|\Phi(t, t_0, x_0)\| < \delta \forall t > t_0$.

Definition 2.6. The equilibrium point $x = 0$ is *uniformly asymptotically stable* if it is uniformly stable and for all $\epsilon, \delta > 0$ there exists $T \geq 0$, independent of t_0 , such that the trajectories $\Phi(t, t_0, x_0)$ of the system satisfy $\|x_0\| < \epsilon \Rightarrow \|\Phi(t, t_0, x_0)\| < \delta \forall t > T + t_0$.

Definition 2.7. The equilibrium point $x = 0$ is *locally exponentially stable* if there exists constants $\alpha, \beta > 0$ and a neighborhood U of the origin such that the trajectories $\Phi(t, t_0, x_0)$ of the system are bounded by

$$\|\Phi(t, t_0, x_0)\| \leq \beta \|x_0\| e^{-\alpha(t-t_0)} \quad \forall t_0, \forall x_0 \in U$$

Definition 2.8. For any of the notions of stability in Definitions 2.5, 2.6, and 2.7, we say a differential inclusion is *strongly stable* if every solution of the differential inclusion is stable, and we say that it is *weakly stable* if there exists a solution of the differential inclusion which is stable.

Additionally define the upper and lower derivatives of a function as:

Definition 2.9. The upper and lower derivatives for a function $V(t, x) \in C^1$ are defined, respectively, by

$$\dot{V}^* = \sup_{y \in F(t, x)} (V_t + \nabla V y) \quad \dot{V}_* = \inf_{y \in F(t, x)} (V_t + \nabla V y) \quad (2.11)$$

Consider Filippov's theorem, Theorems 2.3, and Clarke's theorem, Theorem 2.4¹.

Theorem 2.3 (Filippov's Lyapunov Theorem). *Let, in a closed domain $D(t_0 \leq t < \infty, |x| \leq \epsilon_0)$, the differential inclusion $\dot{x} \in F(t, x)$ satisfy the basic conditions of existence (from [27]) and $0 \in F(t, 0)$; in this domain, let there exist functions $V(t, x) \in C^1, V_0(x) \in C$ for which*

$$V(t, 0) = 0, V(t, x) \geq V_0(x) > 0 (0 < |x| < \epsilon_0)$$

Then:

- 1) *If $\dot{V}^* \leq 0$ in D , the solution $x(t) = 0$ of the inclusion $\dot{x} \in F(t, x)$ is stable.*
- 2) *If, moreover, there exist functions $V_0(x), V_1(x) \in C, W(x) \in C$ (for $|x| \leq \epsilon_0$) and*

$$0 < V_0(x) \leq V(t, x) \leq V_1(x), \dot{V}^* \leq -W(x) < 0,$$

$$(0 < |x| < \epsilon_0), V_1(0) = 0$$

¹I should note that I have rewritten Clarke's theorem so that both will use the same notation and to generally make the relationship between them more explicit.

then the solution $x(t) = 0$ is asymptotically stable.

3) Finally, if there exist $k_1, k_2, k_3, c > 0$ such that

$$V_0(x) \geq k_1 \|x\|^c$$

$$V_1(x) \leq k_2 \|x\|^c$$

$$W(x) \geq k_3 \|x\|^c$$

then the solution $x(t) = 0$ is exponentially stable.

Theorem 2.4 (Clarke's Lyapunov Theorem). *Let, in a closed domain $D(t_0 \leq t < \infty, |x| \leq \epsilon_0)$, the differential inclusion $\dot{x} \in F(t, x)$ satisfy the basic conditions of existence and $0 \in F(t, 0)$; in this domain, let there exist functions $V(t, x) \in C^1, V_0(x) \in C$ for which*

$$V(t, 0) = 0, V(t, x) \geq V_0(x) > 0 (0 < |x| < \epsilon_0)$$

Then:

1) If $\dot{V}_* \leq 0$ in D , then for every $(t_0, x_0) \in D$ there exists a solution $x(t)$ with $x(t_0) = x_0$ of the inclusion $\dot{x} \in F(t, x)$ which is stable.

2) If, moreover, there exist functions $V_0(x), V_1(x) \in C, W(x) \in C$ (for $|x| \leq \epsilon_0$) and

$$0 < V_0(x) \leq V(t, x) \leq V_1(x), \dot{V}_* \leq -W(x) < 0,$$

$$(0 < |x| < \epsilon_0), V_1(0) = 0$$

then for every $(t_0, x_0) \in D$ there exists a solution $x(t)$ with $x(t_0) = x_0$ which is asymptotically stable.

3) Finally, if there exist $k_1, k_2, k_3, c > 0$ such that

$$V_0(x) \geq k_1 \|x\|^c$$

$$V_1(x) \leq k_2 \|x\|^c$$

$$W(x) \geq k_3 \|x\|^c$$

then for every $(t_0, x_0) \in D$ there exists a solution $x(t)$ with $x(t_0) = x_0$ which is

exponentially stable.

It is most likely apparent to the reader that not only do these theorems greatly resemble classical Lyapunov theorems, but that they are also nearly identical, except that one is *robustness* theorem and the other is a *existence* theorem. That is, Theorem 2.3 shows that all trajectories go to the origin as time goes to infinity. However, Theorem 2.4 shows that there exists a solution with the desired properties. I will complete this introduction by applying Theorem 2.3 to a relatively simple example.

Example 2.3 First-Order Time-Varying Stability

Consider the example:

$$\dot{x} = -(a + \cos^2(t))x$$

where $a > 0$. This system is, of course, asymptotically stable, as can be seen from looking at it as a time-varying system. However, the purpose of this example is to convince the reader that in some cases differential inclusions are a more natural way to prove stability. In this case, we can replace $\cos^2(t)$ with the set $[0, 1]$ and we get

$$\dot{x} = -(a + [0, 1])x.$$

Choose a Lyapunov function, say $V = x^2$, and get

$$\dot{V} = \frac{\partial V}{\partial x} \dot{x} = 2x \cdot (-(a + [0, 1])x) = -2(a + [0, 1])x^2$$

which is strictly less than 0 for all values in $[0, 1]$. Then, by Theorem 2.3, the resulting system is asymptotically stable. The beauty of this example is that it is a smooth system which *can* be solved using classical techniques, but has a much cleaner solution when thought of from the vantage point of differential inclusions. ◇

Chapter 3

Theme I: Overconstrained Mechanical Systems

It ain't what a man don't know that makes him a fool, but what he does know that ain't so.

Josh Billings

This chapter presents techniques for deriving equations of motion for overconstrained mechanical systems. The goal is to capture essential features of the mechanics of overconstrained systems in a tractable way. The power dissipation method, abbreviated PDM, will be used for determining first order governing equations for an overconstrained system. The basic ideas behind this method were first proposed in the context of overconstrained wheeled systems Alexander and Maddocks [3]. It has been used successfully to model many types of systems (see, for instance, [73]). Moreover, preliminary work has been done at an intuitive level showing the relationship between equations of motion coming from the PDM and equations of motion coming from a Lagrangian framework (see [72]). One of the purposes in this chapter and Chapter 4 is to develop this relationship. Section 3.1 describes a Lagrangian approach, and points out some of the additional complexities the Lagrangian approach brings with it. Section 3.1.1 presents an example to explain some of the intuition behind using this method. Section 3.2 formally states the power dissipa-

tion method. Section 3.3 gives some important characteristics of PDM solutions which will be used later. Section 3.4 gives some final remarks on this method and how it will be used.

3.1 Lagrangian models

Constrained mechanical systems can be modeled using conventional Lagrangian mechanics through the use of Lagrange multipliers. Consider a generic mechanical system with n contacts, whose contact state can vary. It will therefore have 2^n possible contact states. Let $L(q, \dot{q})$ denote the Lagrangian (kinetic minus potential energy) of the overconstrained system. If the i^{th} contact is not slipping, then this constraint on the mechanical system's motion can be expressed as $\omega_i(q)\dot{q} = 0$. If the i^{th} contact is slipping, then the Coulomb law governs the reaction force at that contact: $F_i^R = -\frac{v_i}{\|v_i\|}\mu_i N_i$, where μ_i , N_i , and v_i are respectively the Coulomb friction coefficient, normal force to the ground, and slipping velocity of the contact at the i^{th} contact. Hence, the system's equations of motion are described by:

$$\frac{d}{dt} \left(\frac{\partial L}{\partial \dot{q}} \right) - \frac{\partial L}{\partial q} + \sum_{i \in \mathcal{S}} F_i^R + \sum_{j \notin \mathcal{S}} \lambda_j \omega_j^T(q) = T \quad (3.1)$$

where \mathcal{S} is the *slipping set*, the $\{\lambda_j\}$ are undetermined Lagrange multipliers, and T are the generalized applied forces. That is, $k \in \mathcal{S}$ if the k^{th} contact is slipping. If the k^{th} contact is not slipping, λ_k corresponds to the reaction force necessary to maintain the no-slip constraint at the k^{th} contact. There are two primary practical problems with the Lagrangian approach. First, one must solve for the Lagrange multipliers—a tedious task that often leads to complex equations. Second, an additional (and often complicated) analysis is necessary to determine which contacts are slipping at any given instant. I will discuss the reduction of these equations of motion to first order equations of motion in Chapter 4. That chapter shows that the power dissipation method has the appropriate “quasistatic” solutions, which are kinematic.

3.1.1 Motivation—A Two-Wheeled Bicycle

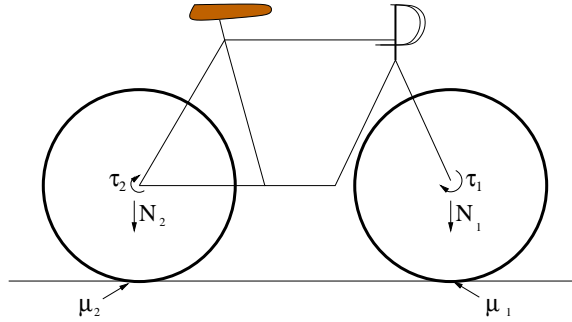


Figure 3.1: Planar bicycle

As an example, consider the planar bicycle (Fig. 3.1). The downward normal force on each wheel will depend on the bicycle's weight distribution. Assume that each wheel is actuated, with torques τ_1 and τ_2 , and that each of the wheels may slip (depending upon the ground reaction force). Using Eq. (3.1) and solving for the Lagrange multipliers, there are four equations of motion, each corresponding to a different contact state. Let $q = [x, \theta_1, \theta_2]^T$, where θ_1 is the front wheel angle and θ_2 is the rear wheel angle. Then the dynamics are as shown in Table 3.1. Here I is a wheel's moment of inertia about its rotational axis, ρ is total bicycle mass, R is the wheel radius, and $F_i^R = -\frac{\dot{x} - R\dot{\theta}_i}{\|\dot{x} - R\dot{\theta}_i\|} \mu_i N_i$. If λ_i is the reaction force for each contact, the Coulomb friction model implies that the boundary between slipping and nonslipping states occurs at some value of $\lambda_i = \lambda_{nom}$, thereby implying that the λ space is divided into regions of different slipping states. Generally, for an n -contact system, the slipping regions are separated by hyperplanes which bound a hypercube. The problem of state determination arises from the inherently complicated dependency of λ on the current state. In the case of the planar bicycle, we compute that

$$\lambda_1 = \frac{I(\tau_1 - \tau_2) - R^2 \rho \tau_1}{R(R^2 \rho + 2I)}$$

$$\lambda_2 = \frac{I(\tau_2 - \tau_1) - R^2 \rho \tau_2}{R(R^2 \rho + 2I)}.$$

Moreover, the critical λ_{nom} takes the value $\mu_i N_i$. This fact implies that the bound-

$$\ddot{q} = \begin{bmatrix} \frac{R}{2I+\rho R^2} \\ \frac{1}{2I+\rho R^2} \\ \frac{1}{2I+\rho R^2} \end{bmatrix} \tau_1 + \begin{bmatrix} \frac{R}{2I+\rho R^2} \\ \frac{1}{2I+\rho R^2} \\ \frac{1}{2I+\rho R^2} \end{bmatrix} \tau_2 \quad (3.2)$$

$$\ddot{q} = \begin{bmatrix} \frac{F_1^R}{I+\rho R^2} \\ \frac{-RF_1^R}{I} \\ \frac{RF_1^R}{I+\rho R^2} \end{bmatrix} + \begin{bmatrix} 0 \\ \frac{1}{I} \\ 0 \end{bmatrix} \tau_1 + \begin{bmatrix} \frac{R}{I+\rho R^2} \\ 0 \\ \frac{1}{I+\rho R^2} \end{bmatrix} \tau_2 \quad (3.3)$$

$$\ddot{q} = \begin{bmatrix} \frac{F_2^R}{I+\rho R^2} \\ \frac{RF_2^R}{I+\rho R^2} \\ \frac{-RF_2^R}{I} \end{bmatrix} + \begin{bmatrix} \frac{R}{I+\rho R^2} \\ \frac{1}{I+\rho R^2} \\ 0 \end{bmatrix} \tau_1 + \begin{bmatrix} 0 \\ 0 \\ \frac{1}{I} \end{bmatrix} \tau_2 \quad (3.4)$$

$$\ddot{q} = \begin{bmatrix} \frac{F_1^R+F_2^R}{\rho} \\ \frac{-F_1^R R}{I} \\ \frac{-F_2^R R}{I} \end{bmatrix} + \begin{bmatrix} 0 \\ \frac{1}{I} \\ 0 \end{bmatrix} \tau_1 + \begin{bmatrix} 0 \\ 0 \\ \frac{1}{I} \end{bmatrix} \tau_2 \quad (3.5)$$

Table 3.1: The Lagrangian dynamics of the planar bicycle

ary of these regions is terrain dependent. I.e., the hypercube delineation of switching regions is a purely local phenomena. The analysis based on Lagrangian mechanics would suggest that there are *four* possible contact states, corresponding to Equation (3.2) where neither wheel is slipping, Equation (3.3) where wheel A is slipping, Equation (3.4) where wheel B is slipping, and Equation (3.5) where both wheels are slipping.

3.2 The Power Dissipation Methodology

To analyze control system performance, one would like models for overconstrained mechanical systems that faithfully capture the system’s essential physics, and that are tractable and amenable to control and motion planning analysis. In particular, we are interested in models that have the salient features we are interested in, while still avoiding some of the complications associated with the full Lagrangian modeling process. I should point out, however, that many of the techniques described in this thesis are not only relevant to the reduced system, but are additionally applicable to the full Lagrangian modeling framework. Nevertheless, as an interim step, consider the conceptually easier “quasi-static” or “kinematic” states of an overconstrained system. In pursuit of this goal, I will use a “power dissipation model” (PDM) approach to model the governing dynamics of a mechanical system. This method typically produces unique models that are relatively easy to compute, and to which one can apply nonsmooth control system analysis methods. Since the method is a quasi-static modeling method, it produces first-order governing equations, instead of second order equations that are associated with Lagrange’s equations. The primary disadvantage is that the method only applies to quasi-static systems.

Let q denote the configuration of the system, consisting of the object’s planar location. Let $\omega(q)$ be one forms acting on TQ . It is well known that the relative motions between the object and a point of contact can be modeled in the form $\omega(q)\dot{q}$. If $\omega(q)\dot{q} = 0$, then the contact is not slipping (i.e., it is nonholonomic), while if $\omega(q)\dot{q} \neq 0$, then $\omega(q)\dot{q}$ describes the slipping velocity of the contact point.

In general, from kinematic considerations, one or more of the contact points must be in a slipping state. The *power dissipation function* measures the object's total frictional energy dissipation due to contact slippage.

Definition 3.1. The *Dissipation* or *Friction Functional* for an n -contact state is defined to be

$$\mathcal{D} = \sum_{i=1}^n \mu_i N_i | \omega_i(q) \dot{q} | \quad (3.6)$$

with μ_i and N_i being the Coulomb friction coefficient and normal force at the i^{th} contact, which are assumed known.

In the case of wheeled vehicles, $\omega^i(q)\dot{q}$ represents the velocity of the i^{th} wheel's point of contact with the ground. Alexander and Maddocks showed that \mathcal{D} is convex as a function of \dot{q} ; therefore its local minima are global minima [3]. Let us revisit the planar bicycle example. Note that the minimum of \mathcal{D} must occur at a nondifferentiable point of \mathcal{D} , since the function is monotone everywhere else. By direct comparison of the two nondifferentiable states, which correspond to one wheel not slipping or the other wheel not slipping, the minimum is associated with whichever has a lower value of μN . Consequently, the zero level set of the function

$$\Psi(g) = \mu_1 N_1 - \mu_2 N_2$$

determines which state the bicycle's kinematics lie in. This determination becomes nonunique when $\mu_1 N_1 = \mu_2 N_2$. This model has only two states, making it much simpler to analyze than the Lagrangian model. Additionally, the governing equations take the simplified form:

$$\dot{x} = R u_i \quad (3.7)$$

where i is the wheel not slipping. With sufficiently many contacts between the object and the manipulating surface, it will often be true that one or more contacts must slip during object motion, thereby dissipating energy. I.e., no motion exists where all of the contacts can be simultaneously slipless. These ideas lead to the following formal statement.

Power Dissipation Principle: An object's motion at any given instant is the one that minimizes \mathcal{D} with respect to \dot{q} .

The *power dissipation method* assumes that the object's motion at any given instant is the one that instantaneously minimizes power dissipation due to contact slippage.

Remark 3.1

I should comment further on the relationship between the kinematics that the power dissipation method predicts and the dynamics predicted by the Lagrangian approach. Consider a particle subject to some holonomic constraint (that is, the particle is moving on some surface). If there is friction between the particle and the surface, then if the particle slips against the surface there will be a reaction force due to friction. The Lagrangian analysis would suggest that there are two possible states—one slipping and one not slipping. The PDM predicts that the particle will not slip, however, so it misses some dynamics predicted by the Lagrangian framework. At the same time, however, the dynamics it does predict (those with no slipping) are consistent with a Lagrangian analysis.

In the case of an overconstrained system with inputs, the PDM leads to more interesting dynamics than those of a particle on a surface (which doesn't move at all). In the case where one can divide all elements q of the configuration manifold Q into two components $q = (g, r)$ (where we refer to g as the group variable and r as the shape variable), Equation (3.6) implies that the PDM will predict \dot{g} given a set of \dot{r} . The variable \dot{r} corresponds to the inputs u_i and \dot{g} corresponds to the motion in $SE(2)$ in the case of planar motion. The important thing to note is that in general \dot{g} will be nonzero if \dot{r} are nonzero. \diamond

To compare the PDM method to conventional Lagrangian analysis, consider the bicycle with torque inputs on both the front wheel A and the back wheel B . The PDM analysis (which we will see in Section 3.2), using velocities as the wheel inputs instead of torques, suggests that there are only two different contact states

corresponding to either A or B slipping as compared to the four contact states the Lagrangian model predicts. Equations (3.2) and (3.5) both imply that the inertial terms dominate the system's dynamics, thereby violating the quasi-static assumption. Equation (3.5) implies that the bicycle is skidding out of control. The conditions corresponding to Equation (3.2) are unlikely to be found in an actual system, as this implies that both contacts must be driven at *exactly* compatible speeds, or the normal forces are so high that they dominate the contact speeds instead of the contact speeds determining the motion. In the case of Equation (3.2) where the speeds are exactly the same speed, the dimension of the subspace spanned by the constraints drops in any case, implying that constraint is essentially duplicated (I will discuss this more later, as it turns out this is a good way of designing controllers for certain high input systems). Therefore the power dissipation will give results satisfying this constraint even if it is practically unlikely. This leaves the second two states in Equations (3.3) and (3.4), which are the same as those found in Equation (3.7) using the power dissipation model. This is an indication of how the quasi-static assumption helps to simplify our problem, while yielding similar insights to Lagrangian analysis.

3.3 Characteristics of the PDM

This section describes some of the main properties of solutions to the PDM. In particular, we will see that the PDM gives rise to *multiple model driftless affine* systems. Chapter 4 explores formally the relationship between the governing equations coming from the PDM and the governing equations coming from the Lagrangian framework. These traditionally arise in the context of adaptive control (see Section 6.7), but are additionally well suited to our case.

Definition 3.2. A control system Σ is said to be a *multiple model driftless affine system (MMDA)* if it can be expressed in the form

$$\Sigma : \quad \dot{q} = f_1(q)u_1 + f_2(q)u_2 + \cdots + f_m(q)u_m \quad (3.8)$$

where for any q and t , $f_i \in \{g_{\alpha_i} | \alpha_i \in I_i\}$, with I_i an index set, g_{α_i} analytic in (q, t) for all α_i , and the controls $u_i \in \mathbb{R}$ are piecewise constant and bounded for all i . Moreover, letting σ_i denote the “switching signals” associated with f_i (which will be referred to as “MMDA maps”),

$$\begin{aligned} \sigma_i : Q \times \mathbb{R} &\longrightarrow \mathbb{N} \\ (q, t) &\longrightarrow \alpha_i \end{aligned}$$

then the σ_i are measurable in (q, t) .

An MMDA is a driftless affine nonlinear control system where each control vector fields may “switch” back and forth between different elements of a finite set. The σ_i which regulate this switching may not be known, so we have no guarantees about the nature of the switching except that it is measurable. Note that it is easy to see that f_i is measurable in (q, t) since σ_i is measurable and the g_{α_i} are analytic. In our case, this switching corresponds to the switching among different contact states (i.e., different sets of slipping contacts) due to variations in contact geometry and surface friction properties. Moreover, so that we can distinguish between the overall control system and the smooth control systems that comprise it, define the following.

Definition 3.3. Let Σ be an MMDA control system. Then we define $\Sigma_{\sigma_1, \sigma_2, \dots, \sigma_n}$ to be the individual control systems made up of

$$\Sigma_{\sigma_1, \sigma_2, \dots, \sigma_m} : \dot{q} = g_{\sigma_1} u_1 + g_{\sigma_2} u_2 + \dots + g_{\sigma_m} u_m$$

We will additionally refer to a system as a *multiple model* system if it is an MMDA system with $u_m = 1$. That is, it is an MMDA system with a drift term. In the next section it is shown that the PDM generically leads to MMDA systems as in Definition 3.2.

3.3.1 The PDM Leads to Multi-model Systems

Ideally the dissipation function defined in Definition 3.1 would always have a unique minimum. Unfortunately, as shown by the planar bike's indeterminacy in the case of $\mu_1 N_1 = \mu_2 N_2$, a unique minimum cannot be expected. This section shows that the power dissipation approach generically leads to MMDA systems, which generically exhibit unique minimum in \mathcal{D} . Alexander and Maddocks [3] show that the dissipation model is convex, so local minima are global minima, should they exist. They also show that if such a minimum exists, it must exist at a point of nondifferentiability of \mathcal{D} . However, there may be other points at which the minimum is obtained. Let $\Omega = \{\omega_1, \dots, \omega_m\}$ and $\mathcal{Q} = \{\dot{q}_1, \dot{q}_2, \dots, \dot{q}_r\}$ where \dot{q}_k is the kinematic solution to a non-overconstrained subset $\Omega' \subset \Omega$ consisting of $n - m$ constraints, i.e.,

$$\Omega' \dot{q}_k = \begin{bmatrix} \omega_{k_1} \\ \vdots \\ \omega_{k_{m-n}} \end{bmatrix} \dot{q}_k = 0.$$

This means that \mathcal{Q} consists of $\binom{n}{n-m}$ points for which no directional derivatives of \mathcal{D} exist and that we therefore only have a finite number of points to check in order to find the minima. It is straightforward to show that these minima must *at least* occur at points in \mathcal{Q} . See, for instance, Clarke [19]. Reorder \mathcal{Q} so that $\mathcal{D}(\dot{q}_1) \leq \mathcal{D}(\dot{q}_2) \leq \dots \leq \mathcal{D}(\dot{q}_r)$. Although \mathcal{Q} has at least one of the minima achieved by \mathcal{D} , it does not necessarily contain all of them. In fact, if more than one element of \mathcal{Q} is a minimum, then every element of the convex hull of these minima are also minima. Hence, if there is more than one solution, there are an infinite number of solutions. Unfortunately, the condition $0 \in \partial \mathcal{D}$ is only necessary for a minimum, but the next proposition proves that in the case of the function \mathcal{D} , it is also sufficient.

Proposition 3.1. *If \dot{q}_1 and \dot{q}_2 both minimize the dissipation functional found in Definition 3.1, then so does $\text{co}\{\dot{q}_1, \dot{q}_2\}$.*

Proof:

Assume $\mathcal{D}(\dot{q}_1) = \mathcal{D}(\dot{q}_2) = a$ and $\delta \in [0, 1]$. Then

$$\begin{aligned} \mathcal{D}(q) (\delta \dot{q}_1 + (1 - \delta) \dot{q}_2) &= \sum_{i=1}^n \mu_i N_i |\omega_i (\delta \dot{q}_1 + (1 - \delta) \dot{q}_2)| \\ &\leq \delta \sum_{i=1}^n \mu_i N_i |\omega_i (\dot{q}_1)| + (1 - \delta) \sum_{i=1}^n \mu_i N_i |\omega_i (\dot{q}_2)| = a \end{aligned}$$

Assume that \mathcal{D} is strictly less than $\mathcal{D}(\dot{q}_1)$ somewhere in $\text{co}\{\dot{q}_1, \dot{q}_2\}$. Then $\exists \delta'$ such that $\mathcal{D}(\delta' \dot{q}_1 + (1 - \delta') \dot{q}_2)$ is at a minimum by an extension of Rolle's Theorem for the real line. Then $\dot{q}' = \delta' \dot{q}_1 + (1 - \delta') \dot{q}_2$ is at a point where \mathcal{D} is nonsmooth in all its directional derivatives [3] (because \mathcal{D} is monotone elsewhere). This implies that $\dot{q}' \in \mathcal{Q}$ and that $\mathcal{D}(\dot{q}') < \mathcal{D}(\dot{q}_1)$, thus violating our assumption that $\mathcal{D}(\dot{q}_1)$ is a minimum of \mathcal{D} . Therefore $\mathcal{D}(q) (\delta \dot{q}_1 + (1 - \delta) \dot{q}_2) = a \forall \delta \in [0, 1]$. The proof for higher numbers of \dot{q}_i having equal dissipation is by induction on this argument. \blacksquare

This result formalizes the intuition that if the power dissipated is equal for two velocities \dot{q}_i , then all possible trajectories whose velocity lies in the convex hull of the \dot{q}_i will satisfy the minimum also. That is, in the nongeneric case when \mathcal{D} does not have a unique minimum, we can still bound the object's motion. Now $\text{co}\{\dot{q}_i, i \in J\}$ is a set of points on which \mathcal{D} is nondifferentiable, just not in all directions. It therefore still meets the criterion to be a minimum [3]. Now let us consider the extent to which the function \mathcal{D} having a unique minimum is generic. We denote the function space of the coefficient of friction by Ξ , the function space of normal forces by \mathcal{N} .

Proposition 3.2. *Assume $\mathcal{D} : (\mathcal{U}, \Xi, \mathcal{N}, TQ) \rightarrow \mathbb{R}$ is of the form in Definition 3.1 and that the μ is measurable in x and t . Then the dissipation functional \mathcal{D} has a unique minimum almost always (i.e., except on a set of measure 0 relative to the space $(\mathcal{U}, \Xi, \mathcal{N}, TQ)$)*

Proof:

Case 1: If \dot{q}_1 is a unique minimum in \mathcal{Q} , then it is the unique global minimum

since Alexander and Maddocks showed that the minimum must occur in \mathcal{Q} by our definition of \mathcal{Q} .

Case 2: If $\exists \dot{q}_1$ and \dot{q}_2 such that both are minima, then by Proposition 3.1, we know that $co\{\dot{q}_1, \dot{q}_2\}$ also minimizes the \mathcal{D} . However, this only occurs when $(u_i, N_j, \mu_k) \in \mathcal{U} \times \mathcal{N} \times \Xi$ satisfy the constraint $\mathcal{D}(\dot{q}_1) = \dots = \mathcal{D}(\dot{q}_n)$. This implies that the constraint is only satisfied on a set of measure 0 in the space $\mathcal{U} \times \mathcal{N} \times \Xi$. ■

That is, the PDM will almost always lead to a unique set of governing equations. The reader should note that the proof of Proposition 3.2 is only useful if we have already found \mathcal{Q} , and moreover for a high number of states it may be very difficult to find the minimum of \mathcal{Q} . This problem, thus stated, bears more than a passing resemblance to the simplex method found in LP theory and techniques from that theory can be applied to the problem of finding the minimum of the function \mathcal{D} in the presence of high numbers of contact states. Also note that in the non-overconstrained case of $n - m$ constraints, the dissipation method leads to the classical kinematic solution. Proposition 3.2 allows us to now state what we mean by the dissipation functional leading generically to an MMDA system.

Corollary 3.3. *The multivalued map $\mathcal{F} : TQ \rightarrow TQ$ implicitly defined by $\mathcal{D}(\dot{q}) = \min(\mathcal{D})$ is single valued almost everywhere.*

Corollary 3.3 implies that we can generically expect the power dissipation method to lead to a uniquely defined set of kinematics. In particular, it implies that the dissipation modeling approach will generically give a well defined set of kinematics, and that it will almost never lead to an indeterminate system. This makes rigorous the comment made in [3] referring to the physical expectation of continually switching back and forth between the dominance of one wheel or another, rather than staying in an indeterminate state. See [25] for a discussion of implicitly defined multivalued maps. Corollary 3.3 is additionally the relationship between solutions to minimizing \mathcal{D} and MMDA systems. The power dissipation function has a unique minimum almost always, so we have unique solutions almost always. In cases when we do not have unique solutions we have a point of discontinuity in the governing equations.

Moreover, we will see in Chapter 4 that the contact states the PDM predicts are $(\mathcal{U}, \overline{\mathcal{U}})$ reducible, implying among other things that there is no drift. However, I cannot justify the requirement that σ be measurable in (q, t) . It is unclear what requirements on $(\mathcal{U}, \Xi, \mathcal{N}, TQ)$ are necessary to guarantee that the switching signal σ is measurable. I will use the fact that σ is measurable extensively in Chapter 5, so it must be viewed as an additionally necessary assumption to make the problems I am considering more tractable. Moreover, it is unclear how to interpret what it would physically mean for σ to not be measurable.

Remark 3.2 Sets of Measure 0

I should discuss sets of measure 0 and their physical meaning. Intuitively, sets of measure 0 can be as sparse as disjoint points in Q or as replete as a submanifold of Q . As an example, consider a vehicle moving on some smooth terrain. In its full three-dimensional ambient space, a vehicle is always constrained to a set of measure 0, yet that set is precisely where the interesting dynamics occur. Therefore, the dynamics which occur on this set of measure 0 cannot be dismissed. On the other hand, sets of measure 0 can represent arbitrary algebraic relationships between parameters and the state space. Unless there is some reason to believe that these relationships are necessarily satisfied, we can feel physically motivated in asserting they will never occur. This is the case that I am considering, and therefore I feel that the preceding results do imply the genericity I assert. Nevertheless, the important thing to keep in mind is that whether or not these sets are important in the analysis is a *physical assumption*, not a mathematical result. For a reference on measure theory, see [2]. \diamond

3.4 Some Final Remarks on the PDM

Here I make some final comments on the power dissipation method. Consider Equation (3.7), the kinematic equations for the planar bicycle. If we define $u_2 = u_1$, then

the system is never overconstrained. In this way, we can take a system that is overconstrained turn it into a non-overconstrained problem. In doing so, we additionally reduce the number of control inputs we need to design. This structure will be put to advantage in Chapter 6 in an application to distributed manipulation. However, as we will see in Chapter 7, there are times when such a simplification is not possible. We call these situations *essentially overconstrained*.

I do not claim that the PDM is a better model than the full Lagrangian setup, only that it is more tractable. It produces first order equations of motion that are amenable to analysis, as we will see in the next chapters. Moreover, the fact that it allows us to compute explicit controllers that work on a real experiment is an indication of its validity. Nevertheless, eventually the work in this dissertation will need to be extended to apply to full Lagrangian mechanical systems, as even in the example of the planar bike there are important dynamic states not accounted for in the PDM. Chapter 4 explores more formally, via the concept of $(\mathcal{U}, \bar{\mathcal{U}})$ reducible mechanical systems, the relationship between the PDM and Lagrangian analysis.

Chapter 4

Theme II: Kinematic Reducibility

It is far better to foresee even without certainty than not to foresee at all.

Henri Poincare

This chapter strengthens the relationship between the governing equations produced by the power dissipation method from Chapter 3 and the dynamics given by the Euler-Lagrange equations (Equation (3.1)) for the case of overconstrained systems. This relationship is phrased in terms of “reducibility”, that is, the ability to reduce equations of motion for mechanical systems down to first order equations of motion. In particular, the notion of $(\mathcal{U}, \bar{\mathcal{U}})$ -reducibility formalizes what is meant by kinematic reducibility. It is basically the requirement that all paths on TQ coincide in the right way with paths on Q when they are projected onto Q . The definition can be found near the end of Section 4.1. Lewis [44] proved that the symmetric product could be used to provide a local test for reducibility, which I will define rigorously in a moment. Lewis’ result is extended to the case of overconstrained mechanical systems that are modeled as multiple model systems. The result states that if all of the individual models comprising the multiple model system are $(\mathcal{U}, \bar{\mathcal{U}})$ reducible, then the multiple model system is $(\mathcal{U}, \bar{\mathcal{U}})$ reducible. This result is later applied to the case of multiple model mechanical systems and it is shown that the kinematics derived from the power dissipation method correspond to $(\mathcal{U}, \bar{\mathcal{U}})$ reducible dynamics

derived from the Lagrangian mechanics. This verifies that the PDM is consistent with Lagrangian mechanics in the appropriate context. Section 4.1 reviews the results from Lewis [44]. Section 4.2 gives the theorem statement and proof regarding $(\mathcal{U}, \overline{\mathcal{U}})$ -reducibility of multiple model mechanical systems. The proof methodology will basically be the following. For each model that makes up a multiple model mechanical system, we will have reduced equations that come from Lewis [44]. Any map that has its time derivative in the convex hull of all these model equations is a solution to the multiple model mechanical system. These solutions will be approximated with a limit of solutions that are piecewise explicitly known to be $(\mathcal{U}, \overline{\mathcal{U}})$ reducible. Then they will be reduced to first order equations and a result from Filippov [27] will be used to show that the limit of these in the reduced space is also a solution. Then the process is reversed to show that for any solution to the MMDA system there is a solution to the multiple model mechanical system.

4.1 $(\mathcal{U}, \overline{\mathcal{U}})$ Reducibility: The Smooth Case

For mechanical systems, I will consider inputs $u : [0, T] \rightarrow \mathbb{R}^m$ that are essentially bounded and Lebesgue integrable. In Lewis [44], it was assumed that the inputs were absolutely continuous since piecewise continuous inputs imply that one can change the systems velocity instantaneously. With inertia this can only occur given infinite forces. However, in the cases relevant to the systems described in this thesis, state transitions are being *approximated* with piecewise continuous signals. This is a common approximation in many areas of physical modeling—for example, the study of impacting bodies often includes this assumption. Therefore, I will only require that absolute continuity hold almost everywhere in my subsequent treatment.

Definition 4.1. $f : [a, b] \rightarrow \mathbb{R}^m$ is *absolutely continuous* if for each $\epsilon > 0 \exists \delta > 0$ such that for every finite collection $\{(t_i, t'_i)\}_{1 \leq i \leq N}$ of non-overlapping intervals in $[a, b]$ with the property that

$$\sum_{i=1}^N |t'_i - t_i| < \delta \text{ we have } \sum_{i=1}^N \|f(t'_i) - f(t_i)\| < \epsilon$$

This implies Df exists almost everywhere. Let us define some of the basic notions from differential geometry, including the covariant derivative, the distribution, and the symmetric product. As in Lewis [44], I restrict my attention to *simple mechanical systems* whose Lagrangian takes the form $\mathcal{L} = K.E. - V$. Assume that Q is an n -dimensional configuration manifold, and g is a riemannian metric on Q defining the kinetic energy. Also, since many of the applications of interest are systems with no potential energy (such as flat terrain problems), let us simplify to the case where $\mathcal{L} = K.E.$ (i.e., $V = 0$).

First, some more definitions are necessary so that the symmetric product can be defined. Denote by v_q elements in the tangent space of Q at q , T_qQ . Assuming that the potential energy is zero, the system Lagrangian is $\mathcal{L} = \frac{1}{2}g(v_q, v_q)$. Next we recall Christoffel symbols so that we can define the covariant derivative and then the symmetric product.

Definition 4.2. The *Christoffel symbols* for the Levi-Civita connection ∇ are

$$\Gamma_{jk}^i = \frac{1}{2}g^{il} \left(\frac{\partial g_{jl}}{\partial q^k} + \frac{\partial g_{kl}}{\partial q^j} - \frac{\partial g_{jk}}{\partial q^l} \right) \quad (4.1)$$

where the standard convention of implied summation over repeated indices is used unless otherwise stated and upper indices indicate the inverse.

Now we can define the covariant derivative and finally the symmetric product.

Definition 4.3. In coordinates, the *covariant derivative* of Y with respect to X is

$$\nabla_X Y = \left(\frac{\partial Y^i}{\partial q^j} X^j + \Gamma_{jk}^i X^j Y^k \right) \frac{\partial}{\partial q^j} \quad (4.2)$$

Definition 4.4. The *symmetric product* between two vector fields X and Y is defined to be

$$\langle X : Y \rangle = \nabla_X Y + \nabla_Y X \quad (4.3)$$

Given a metric g on the manifold Q and inputs u^a , it is possible to show that the Euler-Lagrange equations can be written in the form:

$$\nabla_{c'(t)} c'(t) = u^a(t) Y_a(c(t)) \quad (4.4)$$

where $t \rightarrow c(t)$ is a path on Q and $c'(t) = \frac{d}{dt} c(t)$. On the other hand, given input velocities \bar{u}^α , kinematic equations can be written in the form:

$$\dot{q}(t) = \bar{u}^\alpha(t) X_\alpha(q(t)) \quad (4.5)$$

Let $\{Y_1, \dots, Y_m\}$ and $\{X_1, \dots, X_{\bar{m}}\}$ be two sets of vector fields on TQ for $m, \bar{m} \in \mathbb{N}$. Denote by D_{dyn} the distribution spanned by the vector fields $\{Y_1, \dots, Y_m\}$ and by D_{kin} the distribution spanned by the vector fields $\{X_1, \dots, X_{\bar{m}}\}$. Although the formulation is not presented here, I will use the fact that mechanical systems with constraints can be written in the form of Equation (4.4) [45]. The next definition formalizes the class of admissible solutions to Equation (4.4) and Equation (4.5).

Definition 4.5. If we have a control system $\dot{q} = f(q, u)$ on Q and u coming from some space of inputs $U \subseteq \mathbb{R}^m$, a $(\mathcal{U}, \mathcal{T})$ -solution is a pair (c, u) , where $u : [0, T] \rightarrow U$ and $c : [0, T] \rightarrow Q$ satisfy $c'(t) = f(c(t), u(t))$.

Let

$$\begin{aligned} \tau_Q : TQ &\rightarrow Q \\ (v_q, q) &\rightarrow q \end{aligned}$$

be the tangent bundle projection. We now can define what it means for a mechanical system of the form in Equation (4.4) to be $(\mathcal{U}, \bar{\mathcal{U}})$ reducible to Equation (4.5).

Definition 4.6. Let ∇ be an affine connection on Q , and let \mathcal{U} and $\bar{\mathcal{U}}$ be two families of control functions. The system in Equation (4.4) is $(\mathcal{U}, \bar{\mathcal{U}})$ -reducible to the system in Equation (4.5) if the following two conditions hold:

- i) for each $(\mathcal{U}, \mathcal{T})$ -solution (η, u) of Equation (4.4) with initial conditions $\eta(0)$

in the distribution D_{kin} , there exists a $(\bar{\mathcal{U}}, \mathcal{T})$ -solution (c, \bar{u}) of Equation (4.5) with the property that $c = \tau_Q \circ \eta$;

- ii) for each $(\bar{\mathcal{U}}, \mathcal{T})$ -solution (c, \bar{u}) of Equation (4.5), there exists a $(\mathcal{U}, \mathcal{T})$ -solution (η, u) of Equation (4.4) with the property that $\eta(t) = c'(t)$ for almost every $t \in [0, T]$.

Let $\chi^\infty(D)$ denote those C^∞ vector fields taking values in the distribution D . The following theorem states the local test for Equation (4.4) to be $(\mathcal{U}, \bar{\mathcal{U}})$ reducible to Equation (4.5).

Theorem 4.1 (Lewis [44]). *Let ∇ be an affine connection, and let Y_1, \dots, Y_m and $X_1, \dots, X_{\bar{m}}$ be vector fields on a manifold Q . The control system in Equation (4.4) is $(\mathcal{U}, \bar{\mathcal{U}})$ reducible to a system of the form in Equation (4.5) if and only if the following two conditions hold:*

- i) $\text{span}_{\mathbb{R}}\{X_1(q), \dots, X_m(q)\} = \text{span}_{\mathbb{R}}\{Y_1(q), \dots, Y_{\bar{m}}(q)\}$ for each $q \in Q$ (in particular, $\bar{m} = m$)*
- ii) $\langle X : Y \rangle \in \chi^\infty(D_{dyn})$ for every $X, Y \in \chi^\infty(D_{dyn})$.*

As noted in Lewis [44], the symmetric product plays a similar role in establishing $(\mathcal{U}, \bar{\mathcal{U}})$ reducibility to the Lie bracket in establishing controllability. The goal in the next section will be to extend Theorem 4.1 to the case of multiple model systems. It will turn out that such an extension is relatively straightforward and has natural interpretations both in terms of the symmetric product and in terms of the individual models making up the multiple model system.

4.2 Kinematic Reducibility for MMDA Systems

This section considers the problem of whether or not a dynamic multiple model system is kinematically reducible to an MMDA system. Let us start with a statement that should not be surprising. Lemma 4.2 states that if the solution to the

dynamic equations only has switches which are separated by some small amount of time (making the switching signal piecewise continuous), the resulting solution is also kinematically reducible. Recall from Chapter 3 that a multiple model system is an MMDA system with $u_m = 1$, i.e., it has a drift term.

Lemma 4.2. *Let Σ be a multiple model system such that the switching signal σ is piecewise constant. Then, Σ is $(\mathcal{U}, \bar{\mathcal{U}})$ reducible iff $\Sigma_{\sigma_i, \dots, \sigma_j}$ are all $(\mathcal{U}, \bar{\mathcal{U}})$ reducible.*

Proof:

Since σ is piecewise constant, we know that the number of times that σ changes are countable. Therefore, let the times when σ changes its value be $\{t_1, t_2, \dots\}$ for i in some index I . Then on the intervals (t_i, t_{i+1}) Σ is $(\mathcal{U}, \bar{\mathcal{U}})$ reducible, making it $(\mathcal{U}, \bar{\mathcal{U}})$ reducible almost always. It therefore satisfies the requirements of Definition 4.6. ■

I will use this theorem to prove Theorem 4.4, which says that solutions to the differential inclusion defined by multiple model systems are kinematically reducible if and only if the individual models are kinematically reducible. Before proving the next theorem I will use the following result from Filippov [27].

Theorem 4.3 (Filippov [27]). *Let $\mathbf{f} : Q \times \mathbb{R} \rightarrow TQ$ be a set-valued map and let $\{\Phi_i\}$ be a sequence of solutions to the differential inclusion*

$$\dot{q} \in \mathbf{f}(t, q) \tag{4.6}$$

such that $\lim_{i \rightarrow \infty} \Phi_i \rightarrow \Phi$. Then Φ is also a solution to Equation (4.6).

I will use Theorem 4.3 several times in the proof of Theorem 4.4. Roughly speaking, I will show how to use piecewise continuous $(\mathcal{U}, \bar{\mathcal{U}})$ reducible solutions of the multiple model mechanical system as approximations to arbitrary elements of \mathbf{f} , and then use Theorem 4.3 to show that their kinematic counterparts on TQ must also converge to an element of the differential inclusion defined on TQ .

Theorem 4.4. *A multiple model system Σ is $(\mathcal{U}, \overline{\mathcal{U}})$ reducible iff $\Sigma_{\sigma_i, \dots, \sigma_j}$ are all $(\mathcal{U}, \overline{\mathcal{U}})$ reducible.*

Proof:

First note that it is obviously necessary that all the individual models be $(\mathcal{U}, \overline{\mathcal{U}})$ reducible in order for the resulting multiple model mechanical system to be reducible, because otherwise a perfectly valid solution to a multiple model mechanical system is the smooth, non-reducible solution. So let us show sufficiency. We must therefore show that when the individual models are $(\mathcal{U}, \overline{\mathcal{U}})$ reducible, the MMDA system satisfies parts *i)* and *ii)* of Definition 4.6.

(i) A multiple model mechanical system has the form

$${}^{g_l}\nabla_{c'(t)}c'(t) \in u^\alpha {}^lY_\alpha(c(t)) \quad (4.7)$$

where $l \in \Lambda$ is the index for a given model, g_l is the metric appropriate to that model, ${}^{g_l}\nabla$ is the affine connection associated with g_l , and ${}^lY_\alpha^i$ is the i^{th} component of vector field representing the force input corresponding to u^α of the l^{th} model of the multiple model system. Equation (4.7) is equivalent to

$$\ddot{q}^i + {}^{g_l}\Gamma_{jk}^i \dot{q}^j \dot{q}^k = u^\alpha {}^lY_\alpha^i. \quad (4.8)$$

Setting ${}^l\mathcal{Y}_\alpha^i = -{}^{g_l}\Gamma_{jk}^i \dot{q}^j \dot{q}^k + u^\alpha {}^lY_\alpha^i$ and $\mathbf{Y}_\alpha^i = \text{co}\{{}^l\mathcal{Y}_\alpha^i : l \in L\}$ we get that

$$\ddot{q}^i \in \mathbf{Y}_\alpha^i \quad (4.9)$$

For a given solution Φ of Equation (4.9) we know that $\frac{d}{dt}\Phi \in \mathbf{Y}$, so we can choose a selection of \mathbf{Y} which is locally representative of the time evolution. Denote this selection by $s(\mathcal{Y})_\alpha^i \in \mathbf{Y}$. Therefore,

$$s(\mathcal{Y})_\alpha^i = \delta_1 Y_{\alpha_1}^i + \delta_2 Y_{\alpha_2}^i + \dots + \delta_m Y_{\alpha_m}^i \quad (4.10)$$

such that $\delta_j > 0$ and $\sum_j^m \delta_j = 1$. Let us denote the composition of a flow Φ with itself n times by Φ^n . That is,

$$\Phi^n(q) = \Phi \circ \Phi \circ \dots \circ \Phi \circ \Phi(q). \quad (4.11)$$

Dropping the index i , choose the following map to approximate the flow of the selection $s(\mathcal{Y})_\alpha^i$:

$$\Phi_{dyn}^{t,n}(q) \stackrel{def}{=} \left(\Phi^{\delta_1 Y_{\alpha_1} \frac{t}{n}} \circ \Phi^{\delta_2 Y_{\alpha_2} \frac{t}{n}} \circ \dots \circ \Phi^{\delta_m Y_{\alpha_m} \frac{t}{n}} \right)^n (q) \quad (4.12)$$

$\Phi_{dyn}^{t,n}(q)$ consists of flows along $(\mathcal{U}, \bar{\mathcal{U}})$ reducible mechanical systems. Moreover, it is a solution of Equation (4.9) on TQ which is absolutely continuous almost everywhere for every n . Lastly, it converges to the selection $s(\mathcal{Y})$ as $n \rightarrow \infty$. That is, by construction we get

$$\lim_{n \rightarrow \infty} \Phi_{dyn}^{t,n} = \Phi^{Y_\alpha}$$

By assumption, we know that each segment $\Phi^{\delta_i Y_{\alpha_i} \frac{t}{n}}$ of $\Phi_{dyn}^{t,n}$ is $(\mathcal{U}, \bar{\mathcal{U}})$ -reducible. Therefore, for every choice of n , $\Phi_{dyn}^{t,n}$ is $(\mathcal{U}, \bar{\mathcal{U}})$ reducible by Lemma 4.2. This then gives us, for each n , a corresponding map on Q :

$$\Phi_{kin}^{t,n}(q) \stackrel{def}{=} \tau_Q \circ \Phi_{dyn}^{t,n}(q) = \left(\Phi^{\delta_1 X_{a_1} \frac{t}{n}} \circ \Phi^{\delta_2 X_{a_2} \frac{t}{n}} \circ \dots \circ \Phi^{\delta_m X_{a_m} \frac{t}{n}} \right)^n (q) \quad (4.13)$$

where each $\Phi^{\delta_i X_{a_i} \frac{t}{n}}$ is the reduced equations of $\Phi^{\delta_i Y_{\alpha_i} \frac{t}{n}}$. Moreover, from Theorem 4.3 we know that $\lim_{n \rightarrow \infty} \Phi_{kin}^{t,n}$ exists and that its limit is a solution to

$$\dot{q} \in u^a \mathbf{X}_a \quad (4.14)$$

where $\mathbf{X}_a = \text{co}\{ {}^l X_a \mid l \in L \}$, ${}^l X_a$ are the reduced equations for a given model in Equation (4.5). Therefore, part *i*) of Definition 4.6 is satisfied.

(ii) This has the same essential steps as the above argument, but now we start with the kinematic solution and work towards a dynamic solution. Starting with the

kinematic solutions from Equation (4.5), we know that for the model with index l :

$$\dot{q}^i = u^a \ l X_a^i \quad (4.15)$$

Therefore, this MMDA system has kinematics of the form in Equation (4.14). Let us choose an arbitrary solution of Equation (4.14), and choose the selection $s(X_a)$ to be locally representative of the time evolution. That is, locally, we have Φ^{X_a} , for $X_a \in \mathbf{X}_a$. As before, we construct a sequence of solutions converging to Φ^{X_a} . By construction, $\Phi_{kin}^{t,n}$ satisfies this. We must show there exists a η solution with

$$\frac{d}{dt} \Phi^{X_a} = \eta.$$

We know that

$$\lim_{n \rightarrow \infty} \Phi_{kin}^{t,n} = \Phi^{X_a}(q_0, t)$$

and that for every n and $\Phi_{kin}^{t,n}$ there exists a corresponding $\Phi_{dyn}^{t,n}$ (as defined in (i) above). Taking the limit of this, we have

$$\lim_{n \rightarrow \infty} \Phi_{dyn}^{t,n} = \Phi^{Y_\alpha},$$

which is a solution of Equation (4.9), again by Theorem 4.3. Taking the derivative of both sides, we get (after repeated application of the chain rule)

$$\frac{d}{dt} \Phi^{Y_\alpha} = \frac{d}{dt} \lim_{n \rightarrow \infty} \Phi_{dyn}^{t,n} = \lim_{n \rightarrow \infty} \frac{d}{dt} \Phi_{dyn}^{t,n} = \lim_{n \rightarrow \infty} \Phi_{kin}^{t,n}$$

so part *ii*) is satisfied. ■

Notice that the proof of Theorem 4.4 relied heavily on specifically constructing a solution with the desired properties based on *known* solutions to the individual models comprising the multiple model system. This is the key idea in proving that an MMDA system is kinematic, but we will see in Chapter 5 that it is insufficient for the purposes of proving controllability.

4.3 The PDM and $(\mathcal{U}, \bar{\mathcal{U}})$ Reducibility

This section addresses the relationship between the models produced by the power dissipation methodology and the kinematically reducible states of a generic mechanical system. First, however, I prove the following simple corollary to the work found in Lewis [45]. A reasonable question to ask is, given a metric g for some mechanical system and some set of constraints described by one forms ω_j , what are sufficient conditions for the resulting system to be $(\mathcal{U}, \bar{\mathcal{U}})$ reducible? Lemma 4.5 gives one sufficient condition which is invariant with respect to the metric g .

Lemma 4.5. *Given a “constraint distribution” D_{con} which annihilates the constraints ω_j and an input distribution D_{dyn} , if $D_{dyn} = D_{con}$ the mechanical system described by $\nabla_{\dot{q}}\dot{q} = uY$ is $(\mathcal{U}, \bar{\mathcal{U}})$ reducible.*

Proof:

Denote by ∇ the connection and by $\bar{\nabla}$ the constrained connection defined by the Lagrange-d’Alembert principle (see Lewis [44] for details of this construction). We know that

$$\bar{\nabla}_X Y \in D_{con} \quad \forall Y \in D_{con} \text{ and } X \in \mathcal{T}(\mathcal{M}),$$

which implies

$$\bar{\nabla}_X Y + \bar{\nabla}_Y X \in D_{con} \quad \forall X, Y \in D_{con}.$$

This in turn implies by Theorem 4.1 that $\nabla_{\dot{q}}\dot{q} = uY$ is $(\mathcal{U}, \bar{\mathcal{U}})$ reducible. ■

Therefore, $(\mathcal{U}, \bar{\mathcal{U}})$ reducibility of a multiple model mechanical system is guaranteed *regardless of the metric g* when the constraint distribution is covered by the input distribution. Moreover, from the previous chapter we already know that the power dissipation model only admits solutions where this is true. This allows us to interpret the use of the power dissipation method. The power dissipation is a way of choosing a more tractable *subset* of contact states from the full Lagrangian contact mechanics. In other words, when we make the “quasistatic” assumption, we are

merely restricting our attention to $(\mathcal{U}, \bar{\mathcal{U}})$ reducible systems. Moreover, when the reaction forces due to friction do not lie in D_{kin} , then those contact states are not $(\mathcal{U}, \bar{\mathcal{U}})$ reducible. Consider, for instance, the planar bicycle example in Section 3.1.1. The only contact state which does not satisfy the requirements of Lemma 4.5 is that where both wheels are slipping. The other three states are precisely the states that the power dissipation method predicts. However, I should be very clear that this only shows that the power dissipation captures $(\mathcal{U}, \bar{\mathcal{U}})$ reducible states when $D_{con} = D_{kin}$. That is, the correspondence only goes one direction: all PDM contact states are kinematic states, but not all kinematic states can be predicted by the PDM. There are examples of mechanical systems which are $(\mathcal{U}, \bar{\mathcal{U}})$ reducible by virtue of properties of the metric g . For examples of such systems, see Lewis [44].

I should also remark on the relationship between Theorem 4.1 and Theorem 4.4. In the smooth case, $(\mathcal{U}, \bar{\mathcal{U}})$ reducibility is basically equivalent to geodesic invariance (for details, see Lewis [44]). However, in the nonsmooth case there is no well defined notion of geodesic invariance. Nevertheless, I was able to extend the notion of $(\mathcal{U}, \bar{\mathcal{U}})$ reducibility relatively easily. Therefore, the concept of $(\mathcal{U}, \bar{\mathcal{U}})$ reducibility is in some sense more general than that of geodesic invariance.

4.4 Summary

I would like to end this chapter with a comment on the relationship between this result and the controllability result found in the next chapter. One of the intuitive aspects of Theorem 4.4 is precisely that it is sufficient for each model to be $(\mathcal{U}, \bar{\mathcal{U}})$ reducible in order to guarantee that the multiple model mechanical system is $(\mathcal{U}, \bar{\mathcal{U}})$ reducible. That is, piecewise $(\mathcal{U}, \bar{\mathcal{U}})$ reducibility is enough. However, in the case of controllability, this no longer holds. An MMDA system can switch amongst individually controllable systems in such a way as to destroy controllability. This will be the focus of the next chapter.

Chapter 5

Theme III: Controllability

I am sufficiently proud of my knowing something to be modest about my not knowing everything.

Vladimir Nabokov

This chapter focuses on the issue of controllability of MMDA systems. Understanding controllability for MMDA systems is a first step in understanding what techniques we must employ to stabilize such systems. The issue of controllability for such systems has not been extensively addressed. While controllability was not studied by Hespanha, Liberzon, and Morse [35], they did consider a related stabilization problem arising from a kinematic nonholonomic vehicle with parametric uncertainty. Goodwine and Burdick [32] developed a local controllability test for systems of the form in Definition 3.2 when the switching boundaries and configuration space have an a priori known stratified structure. While they did not study multiple model systems, Rampazzo and Sussmann [75] have recently developed a nonsmooth version of Chow’s theorem that applies to Lipschitz vector fields. The results obtained in [75] have strong analogues with the result presented here. Section 5.1 gives a controllability condition for an MMDA system where the switching signal is controlled. Section 5.2 provides conditions for controllability when we assume that the “switching” boundaries (where the model changes as trajectory crosses it) are

locally at least C^1 and unknown. Section 5.3 presents conditions for controllability for an even broader class of MMDA systems. This condition is the same as the one found in the Section 5.2. These results are summarized in Section 5.4 in Table 5.1.

As an example of a physical system where these concepts are important, Chapter 7 uses the results of this chapter to analyze the issue of controllability of a simple model of an overconstrained wheeled vehicle. This model is inspired by novel high-mobility wheeled robots (e.g, the Mars Sojourner) that operate in rough terrain.

5.1 Aside: Controlled Switching

In this section I will temporarily take an aside to consider controllability in the case when the switching signal can be directly controlled. Certainly, for a system where the individual models are controllable, one may choose to stay with one smooth system and use its controllability to achieve overall system controllability. However, when none of the individual models are controllable, can switching be used to achieve controllability? Not surprisingly, the answer is yes, as we will see illustrated below.

Let $\overline{\Delta}_{\sigma_i}$ denote the involutive closure of the control vector field distribution associated with switching state σ_i . When $\overline{\Delta}_{\sigma_i}$ is full rank, controllability is immediately realized, as one can (with the assumption of complete control over the switching process) switch to the controllable state σ_i . Conventional results for smooth systems then apply to this state. However, if none of the $\overline{\Delta}_{\sigma_i}$ are full rank, then controllability may still exist, but is not obvious. To motivate this situation, consider the example in Fig 5.1. This *fixed wheel kinematic car* (FWKC) has three wheels, of which only the middle is driven. None of the wheels are steerable: the back one remains straight, and the front remains at a constant angle of $\pi/4$. I include the mechanical arm above the body as an example of a mechanism that can control switching. As the arm moves forward and backward, it can shift the center of mass sufficiently to switch the vehicle into a new dynamic state—i.e., the arm position determines which wheel is slipping. Each dynamic state by itself is uncontrollable, though we shall see that this system is indeed controllable. While this example

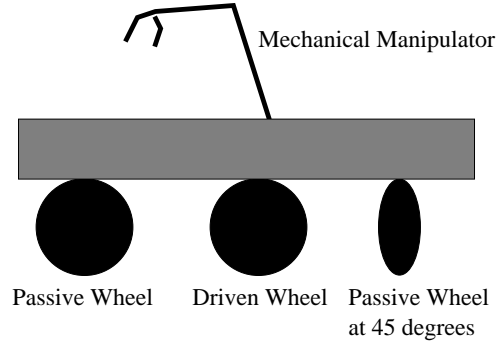


Figure 5.1: The fixed wheel kinematic car

generally has no practical value, it is illustrative of the idea, and may possibly represent the vehicle in a singular configuration of its suspension or a state of steering actuator failure. Based on the power dissipation approach, the governing dynamics of this vehicle are

$$\dot{q} = g_\sigma(q)u_1 \quad \sigma : (q, t) \rightarrow \{1, 2\}$$

$$g_1 = \begin{bmatrix} \frac{1}{\sqrt{2}} \cos(\theta) \\ \frac{1}{\sqrt{2}} \sin(\theta) \\ 1 \end{bmatrix}, \quad g_2 = \begin{bmatrix} \cos(\theta) \\ \sin(\theta) \\ 0 \end{bmatrix}.$$

Recall that the classical Lie bracket between two differentiable vector fields, which does not have any meaning in this multiple model context, is equivalent to

$$[f, g](q) = \lim_{\varepsilon \rightarrow 0} \frac{1}{\varepsilon^2} \left(\Phi_\varepsilon^{-f} \circ \Phi_\varepsilon^{-g} \circ \Phi_\varepsilon^f \circ \Phi_\varepsilon^g(q) - q \right)$$

where Φ_ε^f represents the flow along f for time ε . The total flow can be seen schematically in Fig. 5.2.

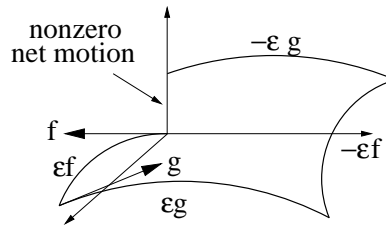


Figure 5.2: Flows associated with a Lie bracket motion.

The interpretation of the Lie bracket as a flow makes the following extension to the switched case almost trivial. Rather than forming the Lie Bracket between two separate smooth control input vector fields, form a Lie Bracket of a control input vector field $f_i u_i$ where $f_i \in \{g_i | i \in \{1, 2\}\}$. Do this by setting $u = 1$ for $0 \leq t < 2\varepsilon$ and $u = -1$ otherwise, while $i = 1$ for $0 \leq t < \varepsilon$ and $3\varepsilon \leq t \leq 4\varepsilon$, $i = 2$ otherwise. This produces the flow seen in Figure 5.2. This simple *controlled switched Lie bracket (CSLB)* can therefore be used to control the mechanism. This leads us to the following corollary of Chow's Theorem.

Corollary 5.1. *Consider an MMDA system of the form Definition 3.2, where the switching signals σ_i can be controlled directly. Let Δ_{σ_i} denote the distribution of the control vector fields associated with state σ_i . Let $\overline{\Delta}_{H,\sigma}$ denote the involutive closure of $\cup_i \Delta_{\sigma_i}$. The system is locally controllable if $\overline{\Delta}_{H,\sigma} = T_q \mathbb{R}^n$ for all q .*

The proof of this corollary is similar to a standard proof of Chow's Theorem (see [76] for example) with the modification that the flows are produced by a switching vector field. In other words, the switching acts like a control that can only take on a finite number of values (in the case of the FWKC, only two values). For this reason I omit details of the proof.

Applying this result to the FWKC, the Lie bracket along with the vector fields g_1 and g_2 are found to be

$$g_1 = \begin{bmatrix} \frac{1}{\sqrt{2}} \cos(\theta) \\ \frac{1}{\sqrt{2}} \sin(\theta) \\ 1 \end{bmatrix}, \quad g_2 = \begin{bmatrix} \cos(\theta) \\ \sin(\theta) \\ 0 \end{bmatrix}, \quad [g_1, g_2] = \begin{bmatrix} -\sin \theta \\ \cos \theta \\ 0 \end{bmatrix}.$$

This leads to a full span of the three-dimensional vector space. Therefore the FWKC is controllable. Simulations in Section 7.4 bear out this result.

5.2 Uncertain C^1 Stratified Systems

This section develops a local controllability result for Multiple Model Driftless Affine (MMDA) control systems. The controllability result can be interpreted as a non-

smooth extension of Chow’s theorem, and uses a set-valued Lie bracket. This section considers systems of the form in Definition 3.2 with the added requirement that switching can only occur through crossing a C^1 manifold. I.e., the control vector fields may change amongst a finite collection of vector fields, each representing a model, P , in a set of models \mathcal{P} . In the case studied in this section, the changes between models are determined by a collection of C^1 continuous submanifolds $\{N_k\} \subset \mathbb{R}^n$, $k = 1, \dots, p$. Fig. 5.3 depicts the state space of a simple example,

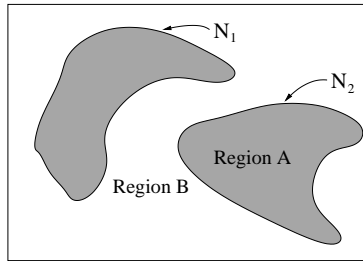


Figure 5.3: Cellular separation of kinematic states

where two different regions, A and B, correspond to different governing equations. The region boundaries are denoted by N_1 and N_2 . Within each region, the governing model is unique. As the system trajectory flows from one region to the other, its governing equations change at the boundary. The difficulty addressed in this section lies in the fact that the regions’ geometries may be a priori completely unknown, and moreover may be local in nature, i.e., Fig. 5.3 may correspond to an arbitrarily small neighborhood of the operating point. Moreover, allow the $\{N_k\}$ to lie anywhere in \mathbb{R}^n with an arbitrary, but countable, number of intersections between submanifolds.

The goal, then, is to have a theory which incorporates the arbitrary nature of these regions, and to produce algorithms which are not sensitive to this kind of switching. Such systems are intimately related to multiple model systems such as studied in [35]. However, I should emphasize that the “switching” which occurs when the trajectory $q(t)$ crosses state space boundaries is *not* like the switching phenomena found in [15], [47], [24], or [87], or as typically studied in the hybrid control systems literature (e.g., [71, 5]). In these studies, the switching is part of a control strategy to be implemented in the controller. Rather, it is switching

induced by environmental factors, such as variations in the contact state between rigid bodies. Systems of this sort are actually quite common in engineering practice (see Chapter 7 for an example). As a first step in understanding such systems, we would like a local controllability test that works in the presence of a priori unknown switching behavior.

5.2.1 Background

The goal of this section is to extend Chow's Theorem to the MMDAs of Definition 3.2. I will use several aspects of the formalism of [27] for investigating the properties of ODEs with discontinuous right-hand sides. Eq. (3.8) can be viewed as a differential inclusion, i.e., a system of the form $\dot{q} \in F$, where F is a set-valued multi-function. For equations of the form $\dot{q} = f(q)$ with f discontinuous in q at a point q_* , one must generally allow f to take on the convex hull of limit values $\lim_{q \rightarrow q_*} f$ at q_* in order to guarantee existence of solutions (see [27, Chapter 2] for details). To account for this issue at the switching boundaries, define the following at each q :

$$\mathbf{f}_i(q) = \text{co}\{f_i(q)\} = \text{co}\{g_{\alpha_i}(q) | \alpha_i \in I_i(q)\}. \quad (5.1)$$

where $I_i(q)$ is the set of limiting values of $f_i(q)$ at q , and $\text{co}\{\cdot\}$ denote the convex hull of a set. For notational convenience, let $s_i(\mathbf{f}_i)$ denote a *selection* of $\mathbf{f}_i(q)$ —i.e., a choice of a particular element in $\mathbf{f}_i(q)$. Let S_{i_1, i_2, \dots, i_k} denote the set of all possible selections from $\mathbf{f}_{i_1}, \dots, \mathbf{f}_{i_k}$.

The result presented here uses the notion of a set-valued Lie bracket. Rampazzo and Sussmann [75] also used a set-valued Lie bracket to prove the controllability of a driftless affine control system whose single valued governing equation includes Lipschitz control vector fields. They showed that this choice of Lie bracket is a General Differential Quotient of the product of exponentials formulation of a Lie bracket. Although these two applications seem different, the choice of Lie bracket is the same, and the resulting nonsmooth versions of Chow's theorem are analogous. Rampazzo and Sussmann [75] use the following Lie bracket definition, adapted appropriately:

Definition 5.1. Let f_1 and f_2 be as in Def 3.2. I.e., $f_i \in \{g_{\alpha_i} | \alpha_i \in I_i(q)\}$. The Lie bracket of f_1 and f_2 is defined as

$$[f_1, f_2](q) = \text{co}\left\{\lim_{j \rightarrow \infty} (Df_1(q_j) \cdot f_2(q_j) - Df_2(q_j) \cdot f_1(q_j))\right\} \quad (5.2)$$

for all sequences $\{q_j\}_{j \in \mathbb{N}}$ such that

1. f_1 and f_2 are differentiable $\forall q_j$,
2. $\lim_{j \rightarrow \infty} q_j = q$,
3. the limit of (5.2) exists.

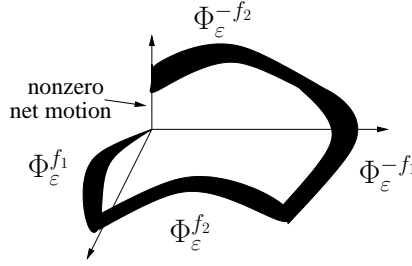


Figure 5.4: Schematic of a set-valued Lie bracket motion.

This concept is illustrated in Figure 5.4.

As noted in [75], this has the skew symmetry properties associated with the Lie bracket. Note that this Lie bracket is a set-valued object, which can be shown to be both compact and convex. Definition 5.1 is appropriate to the case where the dynamics are single valued in open neighborhoods, but multi-valued on “switching boundaries.” In the case where $f = \text{co}\{f_i\}$ and $g = \text{co}\{g_j\}$ on the boundary submanifold N_k , it is straightforward to show that $[f, g] = \text{co}\{[f_i, g_i]\}$. Once again for notational convenience, let $s_{ij}([\mathbf{f}_i, \mathbf{f}_j])$ denote a selection of $[\mathbf{f}_i, \mathbf{f}_j]$ and S_{ij} denote the set of all possible such selections. To analyze the controllability of MMDAs, define:

Definition 5.2. Let f_i be as in Def 3.2 and \mathbf{f}_i as in Eq. (5.1). Define a distribution

$\Delta_{s_1 s_2 \dots s_n}(q)$ as

$$\Delta_{s_1 s_2 \dots s_n}(q) = \text{span}\{v \mid v = s_i(\mathbf{f}_i(q)), \quad i = 1, \dots, n\} \quad (5.3)$$

I.e., $\Delta_{s_1 s_2 \dots s_n}(q)$ is formed from a particular selection of vectors from each $\mathbf{f}_i(q)$.

Define the distribution $\Delta(q)$ as

$$\Delta(q) = \bigcap_{S_{1, \dots, n}} \Delta_{s_1 s_2 \dots s_n}(q) \quad (5.4)$$

I.e., $\Delta(q)$ is formed by intersecting the $\Delta_{s_1 s_2 \dots s_n}(q)$ over all possible selections of $\mathbf{f}_1(q), \dots, \mathbf{f}_n(q)$. Next define

$$\Delta^1(q) = \bigcap_{S_{12, 13, \dots}} (\text{span}\{v \mid v = s_{ij}([f_i, f_j])\}) \quad (5.5)$$

and analogous higher order distributions formed from higher order set-valued Lie brackets. Finally, define $\overline{\Delta}(q)$ as

$$\overline{\Delta}(q) = \Delta(q) \cup \Delta^1(q) \cup \dots \quad (5.6)$$

5.2.2 Main Result

Before stating and proving the section's main result, I would like to describe the underlying intuition. Fig 5.5 shows the local geometry of the state space in the vicinity of a point q_* on a switching boundary. The shaded cone represents \mathbf{f}_i , the set of possible control vector field selections that might occur when u_i is activated. In particular, if $\mathbf{f}_i(q_*) \cap TN_1(q_*) = 0$, activating u_1 will ensure that the trajectory of Σ can escape N_1 for any selection in $\mathbf{f}_i(q_*)$. Then one can apply the classical Chow's theorem to get local controllability. The goal is to apply the preceding idea to the case where q_* lies at the intersection of an arbitrary, but countable, number of switching boundaries.

Theorem 5.2. *Let $\{N_k\} \subset \mathbb{R}^n$ be a countable set of C^1 submanifolds, Σ be a control system as in Definition 3.2 where the governing equations are determined by crossing*

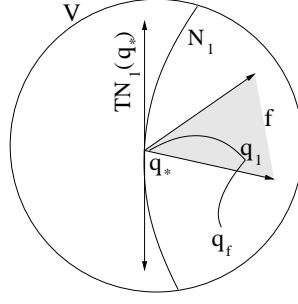


Figure 5.5: Neighborhood of boundary submanifold.

submanifolds in $\{N_k\}$, and q_* be a point such that $\overline{\Delta}(q_*) = \mathbb{R}^n$. Then Σ is small time locally controllable at q_* .

Proof:

Proceed by recursion on p_{q_*} , the number of submanifolds of $\{N_k\}$ intersecting at q_* . Assume V is an open subset of \mathbb{R}^n , $q_0, q_f \in V$, and $T > 0$. Moreover, assume that $\overline{\Delta}(q_*) = \mathbb{R}^n$.

First, let $p_{q_*} = 0$. That is, assume that q_* does not lie in any submanifold of the set $\{N_k\}$. Then all the f_i in Definition 3.2 are single valued, and $[\cdot, \cdot]$ is therefore single valued, and the classical Chow's theorem holds as in Theorem 2.2. Therefore the system is small time locally controllable.

For purposes of clarity, before going on to the recursion step, let $p_{q_*} = 1$ (i.e., $q_* \in N_i$ for some i). Order the indices of $\{N_k\}$ so that $q_* \in N_1$. Now $\overline{\Delta} = \mathbb{R}^n$ implies that there exists \mathbf{f}_i such that $\mathbf{f}_i \cap TN_1 = 0$ (if $\mathbf{f}_i \cap TN_1 \neq 0$ for all i , then elements of TN_1 are common to all \mathbf{f}_i , implying by Definition 5.2 that $\overline{\Delta}(q_*)$ does not span \mathbb{R}^n). The condition $\mathbf{f}_i \cap TN_1 = 0$ implies that there exists $u_i : [0, \frac{T}{2}] \rightarrow \mathbb{R}^n$ such that $q(0) = q_0$, $q(\frac{T}{2}) = q_1$ where $q_1 \in V/N_1$ (i.e. input u_i will move the system off of N_1 to some point q_1 not on N_1 regardless of the selection from \mathbf{f}_i). By Theorem 2.2 $\exists u_i^0 : [\frac{T}{2}, T] \rightarrow \mathbb{R}^n$ such that $q(\frac{T}{2}) = q_1, q(T) = q_f$. This implies that the choice of

$$u_i = \begin{cases} u_i^1, & \text{if } 0 < t < \frac{T}{2} \\ u_i^0, & \frac{T}{2} < t \leq T \end{cases}$$

satisfies the condition $q(0) = q_*$, $q(T) = q_f \forall q_f \in V$.

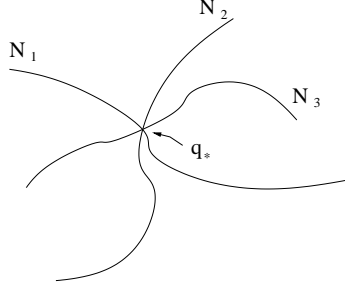


Figure 5.6: As an example of the proof methodology, q_* lies at the intersection of N_1, N_2, N_3 . $\bar{\Delta} = \mathbb{R}^n$ guarantees that the system trajectory can at least be made to move away from the intersection $N_1 \cap N_2 \cap N_3$.

Intuitively, it seems that as $p_{q_*} \rightarrow \infty$ it will be more and more difficult for Σ to be controllable. This difficulty, however, is embedded in the definition of $\bar{\Delta}$, for if there exists a selection restricting the flow of Σ to a submanifold, then by definition $\bar{\Delta}$ does not span \mathbb{R}^n .

Assume that for some k the above proposition holds. Then for $k + 1$ submanifolds intersecting at q_* , if $\bar{\Delta} = \mathbb{R}^n$ then there exists \mathbf{f}_i such that $\mathbf{f}_i \cap TN_{k+1} = 0$. Therefore, as before, there exists $u_i^{k+1} : [0, \frac{T}{k}] \rightarrow \mathbb{R}^n$ such that $q(0) = q_0$, $q(\frac{T}{k}) = q_k$ where $q_k \in V/N_{k+1}$. By assumptions on the case k there exists $u_i^k : [\frac{T}{k}, T] \rightarrow \mathbb{R}^n$ such that $q(\frac{T}{k}) = q_k$, $q(T) = q_f$, where

$$u_i^k = \begin{cases} u_i^k, & \text{if } \frac{T}{k+1} < t < \frac{2T}{k+1} \\ \vdots \\ u_i^0, & \frac{kT}{k+1} < t \leq T \end{cases} \quad (5.7)$$

This implies that

$$u_k = \begin{cases} u_i^{k+1}, & \text{if } 0 < t < \frac{T}{k+1} \\ \vdots \\ u_i^0, & \frac{kT}{k+1} < t \leq T \end{cases} \quad (5.8)$$

satisfies the condition $q(0) = q_*$, $q(T) = q_f$. It is therefore true for all $k > 0$. \blacksquare

An advantage of this approach is the geometric simplicity of the controllability

condition. On the other hand, we are restricted to the assumption that the submanifolds $\{N_k\}$ determine the governing equations. In the next section I will get rid of the C^1 manifold requirement, and show controllability for MMDA systems using an entirely different technique based in large part on methods developed by Sussmann.

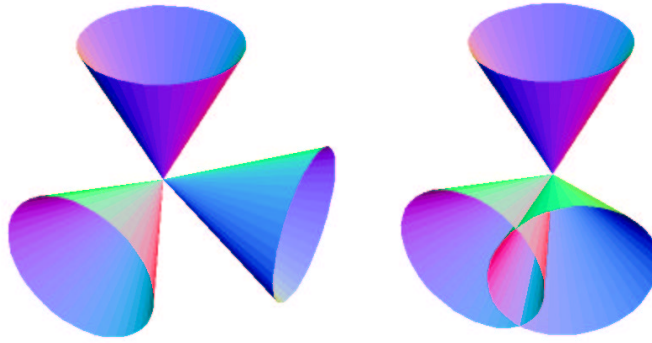


Figure 5.7: Controllability vs. noncontrollability

Intuitively, Theorem 5.2 says that if we have some set of n nominally independent control directions, there exists a switching sequence which can make two control directions the same if and only if their associated convex hulls intersect. Therefore, worst-case scenario switching can make the system locally uncontrollable if the convex hulls associated with sufficiently many MMDA vector fields intersect. One advantage of this approach is that it does lead to such a geometrically simple interpretation of the controllability condition. If a system fails this controllability test, then this does not imply that the system is not controllable, only that it is not locally controllable. Theorem 5.2 can also, of course, be extended to a global controllability result by patching together open neighborhoods between two points q_0 and q_f . See Sastry [76, page 516] for details. However, in many cases such as the one considered in Chapter 7, we are interested in local controllability so that fine maneuvering can be achieved. An equivalent statement of Theorem 5.2 can be found in Corollary 5.3, where an algebraic, as opposed to a geometric, condition for necessary and sufficient conditions on controllability is found.

Corollary 5.3. *Given the assumptions in Theorem 5.2 and writing \mathbf{f}_i as $\mathbf{f}_i =$*

$co\{v_1, \dots, v_l\} = \sum_{i=1}^n \delta_i v_i$ such that $\sum_{i=1}^n \delta_i = 1$ and $\delta_i \in [0, 1]$, then the control system is locally controllable if $rank(\overline{\Delta}(\mathbf{f}_1, \dots, \mathbf{f}_k)) = n \forall \{\delta_1, \delta_2, \dots, \delta_{l_{total}}\} \in [0, 1]^{l_{total}}$

5.3 General MMDA Systems

Now let us consider the following dilemma: Section 5.2 provides a test for controllability, but i) it uses the C^1 boundary assumption, and more importantly ii) its proof does not give any intrinsic insight into how to treat discontinuous systems. It uses a constructive technique similar to the proof of Chow's Theorem found in [76], but it does not lead to explicit control laws. What we desire is a proof more similar to the original proof of Chow's Theorem (found in [18]) which uses the open mapping properties of smooth maps. Therefore, let us now proceed with a more topological approach to controllability which will allow us to both get a more general result and significant insight into the proper formalism for dealing with MMDA systems (and Multiple Model systems in general).

I will cover some of the basic formalism found in [81] needed to prove the next result. In particular, I need the notion of a *GDQ* (Definition 5.4) which can be thought of as a generalized differential. I will use an open mapping theorem for *GDQs* from [80] to prove this extension of Chow's theorem. Denote a set-valued map by the triple $(S, T, Gr(\mathbf{h}))$, where S is the source set (denoted by $So(\mathbf{h})$), T is the target set (denoted by $Ta(\mathbf{h})$), and $Gr(\mathbf{h})$ is the set $\{(s, t) | s \in S, t \in T \text{ with } \mathbf{h}(s) = t\}$. When S and T are understood, I will denote such a map merely by $\mathbf{h}(s)$, where if $s \in S$, $\mathbf{h}(s) = \{t | (s, t) \in Gr(\mathbf{h})\}$. Denote the set of all set-valued maps from S to T by $SVM(S, T)$. Define $SVM_{comp}(S, T)$ to be the subset of $SVM(S, T)$ whose members are set-valued maps having compact graph.

Given a set-valued map \mathbf{h} , we say that a sequence $\{\mathbf{h}_j\}_{j \in \mathbb{N}}$ of set-valued maps with compact graph *inward graph converges* (denoted by $\mathbf{h}_j \xrightarrow{igr} \mathbf{h}$) to \mathbf{h} (also a set-valued map with compact graph) if for every open subset $\Omega \subseteq S \times T$ such that $Gr(\mathbf{h}) \subseteq \Omega$ there exists a $j_\Omega \in \mathbb{N}$ such that $Gr(\mathbf{h}_j) \subseteq \Omega$ whenever $j \geq j_\Omega$. Moreover, define the *flow* of \mathbf{h} , $\Phi^{\mathbf{h}}$, to be the set-valued map from $\Omega \times \mathbb{R}$ to Ω whose value,

for a given $(q_0, t) \in \Omega \times \mathbb{R}$, is the set of all $y \in \Omega$ such that there exists an integral curve $q(t) : [0, T] \rightarrow \Omega$ of \mathbf{h} satisfying $\dot{q} \in \mathbf{h}$ almost everywhere which is defined on some subinterval $[0, T] \subseteq \mathbb{R}$ such that $t \in [0, T]$, $q(0) = q_0$, and $q(t) = y$.

Definition 5.3. Let X and Y be metric spaces. A *regular set-valued map* from X to Y is a set-valued map \mathbf{f} such that for every compact subset $K \subset X$ the restriction $\mathbf{f}|_K$ is a set-valued map with compact graph, and is a limit, in the sense of inward graph convergence, of a sequence of continuous single-valued maps from K to Y .

That is, regularity of a set-valued map requires that the map must be approximated by single-valued continuous maps. I now introduce the extended notion of the differential of a map, the generalized differential quotient (GDQ).

Definition 5.4. Let $\mathbf{f} : \mathbb{R}^m \rightarrow \mathbb{R}^n$ be a set-valued map, and let Λ be a nonempty compact subset of $\mathbb{R}^{n \times m}$. Let S be a subset of \mathbb{R}^m . We define Λ to be a *generalized differential quotient (GDQ)* of \mathbf{f} at $(q, \mathbf{f}(q))$ in the direction of S , if for every positive real number δ there exist U and \mathbf{g} such that:

1. U is a compact neighborhood of $q \in \mathbb{R}^m$ and $U \cap S$ is compact.
2. \mathbf{g} is a regular set-valued map from $U \cap S$ to the δ -neighborhood Λ^δ of Λ in $\mathbb{R}^{n \times m}$.
3. $\mathbf{g}(q) \cdot q \subseteq \mathbf{f}(q)$ for every $q \in U \cap S$.

If Λ is a GDQ of \mathbf{f} at $(q, \mathbf{f}(q))$ in the direction of S we write $\Lambda \in GDQ(\mathbf{f}, q, \mathbf{f}(q), S)$. That is, $GDQ(\mathbf{f}, q, \mathbf{f}(q), S)$ is the set of all GDQs of \mathbf{f} at $(q, \mathbf{f}(q))$ in the direction of S . I should note that *GDQ* theory is a generalized differentiation theory in the sense of [20]. Moreover, the *GDQ* theory has a strong directional open mapping property which I will use later to prove controllability.

Theorem 5.4 (Open Mapping Theorem [80]). *Let C be a convex cone in \mathbb{R}^m . Let $\mathbf{f} : \mathbb{R}^m \rightarrow \mathbb{R}^n$ be a set-valued map, and let $\Lambda \in GDQ(\mathbf{f}; 0, 0, C)$. Let D be a closed convex cone in \mathbb{R}^n such that $D \subseteq \text{Interior}(\mathcal{L}C) \cup \{0\}$ for every $\mathcal{L} \in \Lambda$ (where $\mathcal{L}C$ is the cone produced by the linear operator \mathcal{L} acting on C). Then there exists*

a convex cone $\Delta \subseteq \mathbb{R}^n$ such that $D \subseteq \text{Interior}(\Delta) \cup \{0\}$, and positive constants $\bar{\varepsilon}, \kappa$ having the property that if $y \in \Delta$ and $\|y\| \leq \bar{\varepsilon}$, then there exists a $q \in C$ such that $\|q\| \leq \kappa\|y\|$ and $y \in \mathbf{f}(q)$. Moreover, the cone Δ and the constants $\bar{\varepsilon}, \kappa$ can be chosen so that if $y \in \Delta$ and $\|y\| = \varepsilon \leq \bar{\varepsilon}$ then there exists a compact connected subset Z_y of $(C \cap \overline{\mathbb{B}^n}(\kappa\varepsilon))$ (where $\mathbb{B}^n(r)$ is the closed ball of radius r in \mathbb{R}^n), and $ry \in \mathbf{f}(q)$ whenever $0 \leq r \leq 1$ and (q, r) belong to Z_y .

This basically says that if all possible selections of the GDQ of a map are surjective at q , then the map is open is at q . I will now give an example to illustrate the previous theorem.

Example 5.1 Open Mapping Example

Consider the map¹

$$f(x) = x + \sin\left(\frac{1}{x}\right).$$

The Clarke Generalized Differential (CGD) of $f(x)$ at $x = 0$ is

$$CGD(f(x))|_{x=0} = 1 + [-1, 1] = [0, 2].$$

CGDs are GDQs, but by the open mapping theorem for GDQs all elements of the GDQ must be surjective. Since $0 \in CGD(f)$, we can make no conclusions about the open mapping properties of this map. However, it is possible to prove that 0 is a GDQ of $\sin(\frac{1}{x})$ at $x = 0$, which implies that 1 is a GDQ of $f(x)$ at $x = 0$. Therefore, $GDQ(f, 0, f(0), \mathbb{R})$ is full rank for all elements of the GDQ, implying that the map f is open at $x = 0$. This illustrates the power of the GDQ approach: one need only find a *sufficiently small* GDQ in order to establish the open mapping property of a map. Therefore, the nonuniqueness of GDQs is actually an advantage analytically. The primary disadvantage is that one must have a guess of what the GDQ is, and then go about showing that it satisfies the definition of a GDQ. ◇

¹I would like to thank Hector Sussmann for suggesting and discussing this example with me over email.

I will end this introduction to GDQs with the intuitive result that the classical differential of a map is a GDQ of that map whenever the classical differential is well defined.

Theorem 5.5 ([75]). *If $F : \mathbb{R}^n \longrightarrow \mathbb{R}^m$ is a continuous map, $q \in \mathbb{R}^n$, and F is classically differentiable at q , then $\{DF(q)\} \in GDQ(F, q, F(q), \mathbb{R}^n)$.*

I use the notation $\{DF(q)\}$ to emphasize the fact that DF is itself a set-valued map.

5.3.1 Aside: Lipschitz Vector Fields

In this section I describe a result in [75] and apply their result to a simple example.

Define a linear map $L^f(q_*) : \mathbb{R}^n \times \mathbb{R} \rightarrow \mathbb{R}^n$ by

$$L^f(q_*)(v, r) = v + rf(q_*) \quad (5.9)$$

for $v \in \mathbb{R}^n$ and $r \in \mathbb{R}$. This first result shows that a single valued continuous (but not necessarily Lipschitz) vector field, f , is a GDQ of its flow, Φ^f . Although this is obvious for vector fields with unique flows, it is nontrivial for continuous vector fields without unique flows.

Theorem 5.6 ([75]). *Assume Ω is an open subset of \mathbb{R}^n , $f : \Omega \longrightarrow \mathbb{R}^n$ be a continuous vector field on Ω , and $q_* \in \Omega$. Then the set $\{L^f(q_*)\}$ is a GDQ of Φ^f at $(q_*, 0)$ in the direction \mathbb{R}^n .*

The next result uses a set-valued Lie bracket (in fact, the same one used in the previous section) to take brackets of Lipschitz vector fields. The set of these elements forms a GDQ of Ξ defined below.

$$\Xi^{f,g}(q, \varepsilon) = \begin{cases} \psi^{f,g}(q, \sqrt{\varepsilon}, \sqrt{\varepsilon}) & \text{if } \varepsilon \geq 0 \\ \psi^{f,g}(q, \sqrt{-\varepsilon}, \sqrt{-\varepsilon}) & \text{if } \varepsilon \leq 0 \end{cases} \quad (5.10)$$

where $\psi^{f,g}(q, t, s) = \Phi^{-sg} \circ \Phi^{-tf} \circ \Phi^{sg} \circ \Phi^{tf}(q)$.

Theorem 5.7 ([75]). *Assume Ω is an open subset of \mathbb{R}^n , f and g are locally Lipschitz vector fields on Ω , and $q_* \in \Omega$. Then the set $\{L^w(q_*) | w \in [f, g]\}$ is a GDQ of the map $\Xi^{f,g}$ at $(q_*, 0)$ in the direction \mathbb{R}^n .*

We now arrive at the sufficient condition for controllability developed for Lipschitz vector fields. It basically says that if the continuous vector fields and the Lipschitz vector fields combined with every possible elements of the Lie bracket of Lipschitz vector fields span \mathbb{R}^n , then the system is controllable.

Theorem 5.8 ([75]). *Assume Ω is an open subset of \mathbb{R}^n and that $f_1, \dots, f_m, g_1, \dots, g_r$ are vector fields on Ω with f_i continuous and g_j locally Lipschitz. Let Σ be the driftless control system*

$$\Sigma : \dot{q} = \sum_{i=1}^m u_i f_i(q) + \sum_{j=1}^r v_j g_j(q)$$

with control constraints $|u_i|, |v_j| \leq 1$. Let q_ be a point of Ω such that, for every choice $V = \{v_{kl}\}_{1 \leq k < l \leq r}$ of members $v_{kl} \in [g_k, g_l](q_*)$ the set of vectors*

$$\{f_i(q) : i = 1, \dots, m\} \cup \{g_j(q) : j = 1, \dots, r\} \cup \{v_{kl}(q) : k = 1, \dots, r-1, l+k+1, \dots, r\}$$

linearly spans \mathbb{R}^n . Then Σ is locally controllable from q_ in small time. More precisely, there exists a positive constant A having the property that for every sufficiently small r it is possible to reach every point within a distance smaller than r from q_* in time not exceeding $A\sqrt{r}$ by means of a piecewise constant bang-bang control such that at each time t only one of the quantities u_i, v_j is nonzero.*

I do not give a proof in full because I will use many of the same techniques in the proof of Theorem 5.12. Having shown that both of the previous set-valued objects are GDQs of their respective maps, [75] then use the considerable machinery developed in [80] to prove controllability using an open mapping theorem developed therein.

Remark 5.1 Characteristics of Lipschitz Vector Fields

I should comment on the relationship between this result and the one I will show in the next section. In proving Theorem 5.8, Rampazzo and Sussmann [75] used the following key facts about Lipschitz vector fields to arrive at their result:

1. Lipschitz vector fields are almost everywhere differentiable.
2. Lipschitz vector fields are regularizable.
3. Solutions to ODE's with Lipschitz vector fields are guaranteed to exist for small time and satisfy a local linear growth criterion.

These characteristics are shared by MMDA systems. MMDA systems are almost everywhere differentiable. Due to the fact that they are almost everywhere analytic they are regularizable. Moreover, we know that solutions exist for MMDA systems and that they satisfy local linear growth conditions by [27]. The main point here is that MMDA systems have the key properties Lipschitz vector fields have with respect to the proof of Theorem 5.8. \diamond

I now present an example system to illustrate the usefulness of the result in the case of Lipschitz vector fields. Choose a Lipschitz extension of a nonholonomic integrator, although what the reader should keep in mind is a carangiform fish with drag - see [60]:

Example 5.2 Lipschitz Nonholonomic Integrator

Let

$$f = \begin{bmatrix} 1 \\ 0 \\ y \end{bmatrix} \quad g = \begin{bmatrix} 0 \\ 1 \\ ax + |x| \end{bmatrix}$$

Due to the presence of $|x|$ in the equation, classical analysis does not allow give us a well defined Lie bracket. So instead we turn to Sussmann's formalism.

Taking the bracket $[f, g]$ as defined in Definition 5.1, we get

$$\begin{aligned}
\lim_{x_i \rightarrow x} Df \cdot g - Dg \cdot f &= \begin{bmatrix} 0 & 0 & 0 \\ 0 & 0 & 0 \\ 0 & 1 & 0 \end{bmatrix} \begin{bmatrix} 0 \\ 1 \\ ax + |x| \end{bmatrix} - \begin{bmatrix} 0 & 0 & 0 \\ 0 & 0 & 0 \\ a + \lim_{x_i \rightarrow x} \frac{\partial |x|}{\partial x} & 0 & 0 \end{bmatrix} \begin{bmatrix} 1 \\ 0 \\ y \end{bmatrix} \\
&= \begin{bmatrix} 0 & 0 & 0 \\ 0 & 0 & 0 \\ 0 & 1 & 0 \end{bmatrix} \begin{bmatrix} 0 \\ 1 \\ ax + |x| \end{bmatrix} - \begin{bmatrix} 0 & 0 & 0 \\ 0 & 0 & 0 \\ a + [-1, 1] & 0 & 0 \end{bmatrix} \begin{bmatrix} 1 \\ 0 \\ y \end{bmatrix} \\
&= \begin{bmatrix} 0 \\ 0 \\ 1 - (a + [-1, 1]) \end{bmatrix}
\end{aligned}$$

Hence, at the origin, as long as $a \notin [0, 2]$, the system is controllable. If, however, $a \in [0, 2]$ we can draw no conclusion. \diamond

5.3.2 Main Result

I will show that MMDA systems share these characteristics and that, with relatively minor extensions, one can prove a theorem analogous to Theorem 5.8. Note that the three key properties mentioned in Remark 5.1 are not only true of the set-valued maps, but of their GDQs as well. This allows us to take higher-order brackets without resorting to stronger regularity conditions (such as those found in [75]). I will first prove that a set-valued map f from an MMDA system is a GDQ of its flow. Then I will prove that the Lie bracket defined in Definition 5.1 is indeed a GDQ for an appropriately defined map. This will in turn allow us to prove the desired theorem. I will leave the proofs of these to Sections 5.3.3 and 5.3.4.

Theorem 5.9. *Assume Ω is an open subset of \mathbb{R}^n , f is an MMDA vector field on Ω as in Definition 3.2, and $q_* \in \Omega$. Then the set $L^{\mathbf{f}}$, defined by*

$$L^{\mathbf{f}}(q_*)(v, r) = v + rf(q_*) \quad \text{for } f \in \mathbf{f}, \quad (5.11)$$

is a *GDQ* of the set-valued map $\Phi^{\mathbf{f}}$ at $(q_*, 0)$ in the direction of \mathbb{R}^n .

I will then show that $[f, g]$ from Definition 5.1 is a *GDQ* of the map:

$$\Xi^{\mathbf{f}, \mathbf{g}}(q, \varepsilon) = \begin{cases} \psi^{f, g}(q, \sqrt{\varepsilon}, \sqrt{\varepsilon}) & \text{if } \varepsilon \geq 0 \\ \psi^{f, g}(q, \sqrt{-\varepsilon}, \sqrt{-\varepsilon}) & \text{if } \varepsilon \leq 0 \end{cases} \quad (5.12)$$

for $f \in \mathbf{f}$ and $g \in \mathbf{g}$, and where $\psi^{f, g}(q, t, s) = \Phi^{-sg} \circ \Phi^{-tf} \circ \Phi^{sg} \circ \Phi^{tf}(q)$. Note that Ξ is set-valued since \mathbf{f} and \mathbf{g} are set-valued. Moreover, this definition implies a type of symmetry in the switching which we cannot necessarily always expect to have. However, even with this assumption, this result significantly extends the one found in the previous section.

Theorem 5.10. *Assume Ω is an open subset of \mathbb{R}^n , \mathbf{f} and \mathbf{g} are MMDA vector fields on Ω as in Definition 3.2, and $q_* \in \Omega$. Then the set $\{L^w(q_*) | w \in [\mathbf{f}, \mathbf{g}]\}$ is a *GDQ* of the map $\Xi^{\mathbf{f}, \mathbf{g}}$ at $(q_*, 0)$ in the direction of \mathbb{R}^n .*

I would like to reiterate that because MMDA systems are almost everywhere analytic, higher order brackets are well defined. This is due to the fact that the *GDQ* of $[\mathbf{f}, \mathbf{g}]$ (with \mathbf{f} and \mathbf{g} coming from an MMDA system) is again almost everywhere analytic. Therefore, we can take unlimited brackets, whereas Theorem 5.8 allows only first order brackets. In this way, discontinuous systems with enough regularity in their description can actually be more transparently controllable than single-valued Lipschitz systems, a result which is somewhat surprising! Moreover, we can take higher order brackets of some Lipschitz vector fields as well. For instance, $|x|$ can be treated as an MMDA map that switches at $x = 0$. Having shown both of those are *GDQs* of their respective maps, I will use the considerable machinery developed in [80] to prove controllability using an open mapping theorem developed therein. Here is a restricted version of the chain rule here, adapted to the case of *GDQs*.

Theorem 5.11 (Chain Rule for *GDQs* [80]). *Let X_1, X_2, X_3 be finite-dimensional real linear spaces, and let $q_i \in X_i$ $i \in \{1, 2, 3\}$. For $i = 1, 2$, let $\mathbf{f}_i : X_i \rightarrow X_{i+1}$ be a set-valued map from X_i to X_{i+1} . Let C_i be a closed convex cone in X_i and let S*

be a linear subspace of X_2 spanned by C_2 , and let Π be a linear projection from X_2 onto S . Finally, assume that $\Lambda_i \in GDQ(\mathbf{f}_i, q_i, \mathbf{f}_i(q_i), S)$ and $\mathbf{f}_1(q_1 + C_1) \subseteq q_2 + C_2$. Then

$$\Lambda_2 \circ \Pi \circ \Lambda_1 \in GDQ(\mathbf{f}_2 \circ \mathbf{f}_1, q_1, \mathbf{f}_2 \circ \mathbf{f}_1(q_1), S)$$

where

$$\Lambda_2 \circ \Pi \circ \Lambda_1 = \{L_2 \circ \Pi \circ L_1 : L_2 \in \Lambda_2, L_1 \in \Lambda_1\}.$$

This leads us to the following sufficient condition for MMDA systems to be controllable. The proof is analogous to that found in [75], with small modifications made for the existence of higher order brackets. It relies on constructing a map composing flows of all the MMDA fields and their associated brackets. Then one uses the theory in [80] to show that this map is open, thus showing controllability.

Theorem 5.12. *Let Σ be a control system as in Definition 3.2, and q_* be a point such that $\bar{\Delta}(q_*) = \mathbb{R}^n$, where $\bar{\Delta}(q_*)$ is defined in Definition 5.2. Then Σ is small time locally controllable at q_**

Proof:

Start by making a slight change of notation, and letting $\Phi^f(q, \epsilon)$ be denoted by $\Phi_\epsilon^f(q)$. Moreover, denote the bracket of two maps f_i and f_j by f_{ij} . Define the map $\Theta_\epsilon^m(q)$ by:

$$\Theta_\epsilon^m(q) = \Phi_\epsilon^{f_1} \circ \Phi_\epsilon^{f_2} \circ \dots \circ \Phi_\epsilon^{f_n} \circ \Phi_\epsilon^{f_{12}} \circ \Phi_\epsilon^{f_{13}} \circ \dots \circ \Phi_\epsilon^{f_{(n-1)n}} \circ \dots \circ \Phi_\epsilon^{f_{(n-m)(n-m+1)\dots n}}$$

Taking the GDQ of $\Theta_\epsilon^m(q)$ at q_* and applying the Chain Rule for GDQs, we get that $\Theta_\epsilon^m(q)$ is open if $\bar{\Delta} = \mathbb{R}^n$. (see [80]) Then, by standard arguments in [68] we get that Σ is controllable. ■

5.3.3 Proof of Theorem 5.9

Before I begin, I need to define some operators and quantities. Choose a δ neighborhood of q_* to be U . Then define the following:

$$\Lambda(q - q_*, t) = \{L^f(q_*)(q - q_*, t) + E_{(q - q_*, t), p - q - tf(q_*)}^{n+1, n}(q - q_*, t)\} \quad (5.13)$$

such that $p \in \Phi^f$, $f \in \mathbf{f}$ and where $E_{q, p}^{m, n}(u) = \frac{\langle q, u \rangle}{\|q\|^2} p$ for $q \in \mathbb{R}^m$, $p \in \mathbb{R}^n$, and $u \in \mathbb{R}^m$. Extend the definition of Λ to $t = 0$ by defining $\Lambda(q, t) = \{L^f(q_*)\}$ (that is, the set of L^f with $f \in \mathbf{f}$ at q_*).

I shall prove this theorem by directly showing that \mathbf{f} is a GDQ of Φ^f . To do so I need only show that \mathbf{f} satisfies the properties of Definition 5.4. The proof goes in three stages:

1. Show $\Lambda(q_* - q_*, t) \cdot (q - q_*) \subseteq \Phi^f$ for a sufficiently small neighborhood of $q_* \in \mathbb{R}^n$.
2. Show Λ is a map from neighborhoods of q_* to Λ^δ .
3. Show Λ is regular.

Choose \hat{p} so that $\hat{p} > 0$ and

$$\hat{V} \stackrel{def}{=} \{q \in \mathbb{R}^n : \|q - q_*\| \leq \hat{p}\} \subseteq \Omega. \quad (5.14)$$

Let $\bar{k} = \sup\{\|f(q)\| : q \in \hat{V}\}$. For every ρ_1, ρ_2 define

$$\omega(\rho_1, \rho_2) \stackrel{def}{=} \sup\{\|f(q) - f(q')\| : \|q - q'\| \leq \rho_1, \|q - q_*\| \leq \rho_2, \|q' - q_*\| \leq \rho_2\}. \quad (5.15)$$

Define $\bar{\rho}$ such that $\bar{\rho} > 0$, $(2 + \bar{k})\bar{\rho} \leq \hat{p}$, and $\omega((1 + \bar{k})\bar{\rho}, \hat{p}) \leq \delta$. Finally, let

$$\bar{V} \stackrel{def}{=} \{q \in \mathbb{R}^n : \|q - q_*\| \leq \bar{\rho}\} \quad (5.16)$$

and

$$\bar{W} = \bar{V} \times [-\bar{\rho}, \bar{\rho}]. \quad (5.17)$$

Now to the proof.

Proof:

1) Let $M \in \Lambda(q, t)$ and (q, t) be in a sufficiently small ϵ -ball of $(q_*, 0)$ (i.e., $(q, t) \in (q_* + B_{\epsilon_1}, B_{\epsilon_2})$ with B_ϵ denoting a ball of ϵ radius and ϵ_1 and ϵ_2 sufficiently small).

Let $f \in \mathbf{f}$. Then $q_* + M(q - q_*, t) =$

$$\begin{aligned} & q_* + L^f(q_*)(q - q_*, t) + E_{(q-q_*, t), p-q-tf(q_*)}^{n+1, n}(q - q_*, t) \\ &= q_* + q - q_* + tf(q_*) + p - q - tf(q_*) = p. \end{aligned}$$

So $\Lambda((q - q_*), t) \cdot (q - q_*) \subseteq \Phi^{\mathbf{f}} \forall f \in \mathbf{f}$.

2) We must show that $d(\Lambda, L^{\mathbf{f}}(q_*)) < \delta$, where $d(\cdot, \cdot)$ is the Hausdorff set distance function defined by

$$d(A, B) = \max \left(\max_{b \in B} \min_{a \in A} d(a, b), \max_{a \in A} \min_{b \in B} d(a, b) \right). \quad (5.18)$$

with A and B sets and $d(a, b)$ is the Euclidian distance function. (Note that this is *not* the standard notion of the distance of from a point to a set. In this case, the distance between two sets will only be zero if they are the same. (That is, of course, up to sets of measure 0.) I will abuse notation somewhat by allowing $d(\cdot, \cdot)$ to denote the distance between sets, distance from a point to a set, and the distance from a point to a point, and depend on context to make the correct interpretation clear.) Let $M \in \Lambda(q, t)$ and let $\xi : [0, t] \rightarrow \Omega$ be an integral curve of \mathbf{f} such that $\xi(0) = q$ and $\xi(t) = p$. Then,

$$\sup \|M - L^{\mathbf{f}}(q_*)\| = \sup_{f \in \mathbf{f}} \frac{\|p - q - tf(q_*)\|}{(\|q - q_*\|^2 + t^2)^{\frac{1}{2}}}. \quad (5.19)$$

For all $f \in \mathbf{f}$ we know that

$$\|p - q - tf(q_*)\| = \left\| \int_0^t (f(\xi(s)) - f(q_*)) ds \right\|.$$

Moreover, we know that

$$\|\dot{\xi}(s)\| \leq \max(\sup\{\|f_i(q)\| : q \in \hat{V}\} : i \in I) = \bar{k}$$

so

$$\|f(\xi(s) - f(q_*))\| \leq \omega((1 + \bar{k})\rho, \hat{\rho})$$

where ω is defined in Equation (5.15). This then implies

$$\|p - q - tf(q_*)\| \leq |t|\omega((1 + \bar{k})\rho, \hat{\rho}) \quad \forall f \in \mathbf{f}$$

which means that

$$\|p - q - tf(q_*)\| \leq |t|\delta \quad \forall f \in \mathbf{f}.$$

Thus, we can show Equation (5.19) must be small for t and $\|q - q_*\|$ sufficiently small, showing that $d(\Lambda, L^{\mathbf{f}}(q_*)) < \delta$.

3) I need to show that $\Lambda : \overline{W} \rightarrow \text{Lin}(\mathbb{R}^{n+1}, \mathbb{R}^n)$ (where $\text{Lin}(U, V)$ is the set of all linear maps from a vector space U to a vector space V and \overline{W} is defined in Equation (5.17)) is a regular set-valued map. This reduces to showing that the restriction of Λ to a compact subset K is compact and then showing that Λ is a limit, in the sense of inward graph convergence, of single-valued continuous maps.

First, let us show that $\Lambda|_K$ is compact. Choose a sequence of (q_j, t_j) such that $q_j \rightarrow q_*$ and $t_j \rightarrow t_0$ as $j \rightarrow \infty$. We know that (q_*, t_0) is in \overline{W} because \overline{W} is compact. The (q_j, t_j) clearly define a corresponding set of p_j for all $f \in \mathbf{f}$ through the absolutely continuous map Φ^f . Moreover, observe that the limit p_* of p_j is in the flow of f , Φ^f , that is, $p \in \Phi^f$. Let $M_{q,t,p} = \{L^f(q_*) + E_{(q-q_*,t),p-q-tf(q_*)}^{n+1,n} : f \in \mathbf{f}\}$ and let $M^i = M_{q_i,t_i,p_i}$. Then we know that M^j has a limit in Λ by the continuity of $M \in \Lambda$ (which is continuous because L and E are continuous). Therefore, Λ is compact.

Now let us show that Λ is the limit of single-valued continuous maps. We know that MMDA systems are almost everywhere differentiable. This implies that we can

construct regularizations of f at all points of discontinuity, where the regularization of the transition of f from f_i to f_j at q_* is defined by

$$f_{ij}^\zeta = \int_{\mathbb{R}^n} \phi(h) f(q + \zeta) dh \quad (5.20)$$

where $\phi(h) \geq 0$, is C^∞ , $\int_{\mathbb{R}^n} \phi(h) = 1$, $\phi(h) = 0$ for $\|h\| > 0$, and $\zeta > 0$. This forms a finite set of regularizations. These regularizations form the smooth single valued maps which converge in the sense of inward graph convergence to Λ as $\zeta \rightarrow 0$. ■

5.3.4 Proof of Theorem 5.10

To prove that the Lie bracket as described in Definition 5.1 is a *GDQ* of Ξ as defined in Equation 5.10 I will utilize some of the additional tools found in [81]. In particular, I will use a general sufficient condition for a set to be a *GDQ* of a map (Theorem 5.13) to show that the set-valued Lie bracket is a *GDQ* of Ξ . However, before I can state these theorems, I will need a few more definitions. A *cone* in a real linear space X is a nonempty subset $C \subset X$ such that $r \cdot c \in C$ whenever $c \in C$, $r \in \mathbb{R}$, and $r \geq 0$. Changing notation slightly from previous sections, I will refer to the flow of f starting from q_* from time a to time b as $\Phi_{a,b}^f$. Use $Traj(f)$ to refer to all trajectories of f , and use $Traj_c(f)$ to refer to all $\xi \in Traj(f)$ whose domain is a compact interval. Let $\mathcal{C}(1)$ be the set of all cones in \mathbb{R} and $\mathcal{C}(2)$ be the set of all cones in \mathbb{R}^2 that are products $C_+ \times C_-$, where $C_+ \in \mathcal{C}(1)$ and $C_- \in \mathcal{C}(1)$. Lastly, denote by $\xi_*(t)$ a trajectory of f at time t . I will additionally need the notion of a variational generator to state Theorem 5.13. If $\xi : [a, b] \rightarrow \mathbb{R}^n$ is a continuous curve, and $\alpha > 0$, define $\mathcal{T}^n(\xi, \alpha) \stackrel{def}{=} \{(q, t) : q \in \mathbb{R}^n, a \leq t \leq b, \|q - \xi(t)\| \leq \alpha\}$.

Definition 5.5. Let f be a map from $\mathbb{R}^n \times \mathbb{R}$ to \mathbb{R}^n . Let $a, b \in \mathbb{R}$, $a \leq b$, and ξ be a continuous map from $[a, b]$ to \mathbb{R}^n . A *variational generator* for f about ξ is a measurable set-valued map $\Lambda : [a, b] \rightarrow \mathbb{R}^{m \times n}$ with compact convex nonempty values such that there exist $k_\Lambda, \bar{\alpha}, \mathbf{k}$ having the following three properties:

1. $k_\Lambda : [a, b] \rightarrow [0, +\infty]$ is integrable and $\sup\{\|L\| : L \in \Lambda(t)\} \leq k_\Lambda(t)$.

2. $\bar{\alpha} > 0$ and $\mathcal{T}^n(\xi, \bar{\alpha}) \subseteq \text{So}(f)$. (Where $\text{So}(f)$ is the source of f .)
3. $\mathbf{k} = \{k^\alpha\}_{0 \leq \alpha \leq \bar{\alpha}}$ is a family of Lebesgue-integrable functions:

$$k^\alpha : [a, b] \rightarrow [0, +\infty], \quad \text{for } 0 \leq \alpha \leq \bar{\alpha},$$

such that

$$\lim_{\alpha \rightarrow 0} \int_a^b k^\alpha(t) dt = 0 \quad (5.21)$$

and

$$\sup\{\inf\{\|\Delta_\xi^f(q, t, L)\| : L \in \Lambda(t)\} : \|q - \xi(t)\| \leq \alpha\} \leq \alpha k^\alpha(t) \quad (5.22)$$

for all $t \in [a, b]$ and all $\alpha \in (0, \bar{\alpha}]$, where

$$\Delta_\xi^f(q, t, L) \stackrel{\text{def}}{=} f(q, t) - f(\xi(t), t) - L \cdot (q - \xi(t)). \quad (5.23)$$

Now I would like to state a special case of the general sufficient condition in [81] for a set to be a GDQ of a map f .

Theorem 5.13 ([81]). *Assume $a, b \in \mathbb{R}$, $a \leq b$, f is locally integrally continuous², and Λ is a variational generator for f along ξ . Then the set $\mathcal{M}_{b,a}(\Lambda)$ is a GDQ of the map Φ^f at $(\xi(a), \xi(b))$ in the direction of \mathbb{R}^n , where $\mathcal{M}_{t,s}(\Lambda)$ is the set defined by*

$$\mathcal{M}_{t,s}(\Lambda) \stackrel{\text{def}}{=} \{M_L(t, s) : L \text{ is a measurable selection of } \Lambda\}$$

and $M_L(t, s)$ satisfies $M_L(t, s) = I_{\mathbb{R}^n} + \int_s^t L(r) \cdot M_L(r, s) dr$ where $I_{\mathbb{R}^n}$ is the identity map on \mathbb{R}^n .

Now I will proceed to prove Theorem 5.10.

²This property is basically that f is measurable, integrable, and bounded by continuous integrable maps. See [81] for details. For our purposes this property will be automatically satisfied because the solutions to a differential inclusion satisfy a version of Gronwall's Lemma, resulting locally in a linear growth rate of the solution.

Proof:

I will use Theorem 5.13 to show that the set-valued Lie bracket is indeed a GDQ of the map Ξ . Regarding the integral continuity of Theorem 5.13, I will not prove that the Ξ is locally integrally continuous here. It is a simple consequence of the fact that each \mathbf{f} is almost everywhere analytic. The rest of this proof will be dedicated to showing that the set-valued Lie Bracket is a variational generator of Ξ .

Assume that we have an MMDA system as in Definition 3.2. If q_* is a point where the system is analytic (i.e., the switching signal σ is constant in a neighborhood of q_*), then the Lie bracket is single valued, is a *GDQ* by Theorem 5.5, and we can apply the classical Chow's theorem to conclude the proof. Therefore, the only case of interest to us is when q_* is a point of discontinuity of σ . At such a point we know that

$$\dot{q} \in \mathbf{f}u_1 + \mathbf{g}u_2 \quad (5.24)$$

where $\mathbf{f} = co\{f_i\}$ and $\mathbf{g} = co\{g_j\}$. Let $\hat{\rho}$ and \hat{V} be as in Equation (5.14). Let K_1 denote an upper bound of both $\|f_i\|$ and $\|g_j\|$ on \hat{V} for all i, j . Such a bound exists since \hat{V} is compact and f_i and g_j are analytic. Let $Diff(h)$ denote all the points q such that a map h is differentiable. Moreover, for maps h_1 and h_2

$$\gamma(\rho) = \sup_{q \in \{q \mid \|q - q_*\| < \rho\}} d([h_1, h_2](q), [h_1, h_2](q_*)) \quad (5.25)$$

such that $q \in Diff(h_1) \cap Diff(h_2)$. The function $\gamma(\rho)$ will play the role of the function k_Λ and ρ will play the role of $\bar{\alpha}$ in Definition 5.5. As before, let f_{ij}^ζ and g_{kl}^ζ be the regularizations at q_* of the transition of \mathbf{f} from f_i to f_j and of \mathbf{g} from g_k to g_l , respectively. We are guaranteed such regularizations exist locally for MMDA systems because they are piecewise analytic and \hat{V} is compact. Then let \mathbf{f}^ζ and \mathbf{g}^ζ be the *sets* of all such regularizations of \mathbf{f} and \mathbf{g} , respectively.

Let K_2 be an upper bound on both $\|Df_i\|$ and $\|Dg_j\|$. Again, such an upper bound exists for $\|Df_i\| \|Dg_j\|$ because f_i and g_j are analytic for all i, j and \hat{V} is

bounded. Let $K = \max\{K_1, K_2\}$. Lastly, let Q^w denote the linear map

$$\begin{aligned} Q^w : \mathbb{R}^n \times \mathbb{R} &\longrightarrow \mathbb{R}^n \\ (v, r) &\longrightarrow v + rw \end{aligned} \tag{5.26}$$

and if W is a set of vectors in \mathbb{R}^n , define \mathcal{Q}^W by

$$\mathcal{Q}^W = \{Q^w | w \in W\}.$$

Now I will proceed to show that $\mathcal{Q}^{[\mathbf{f}, \mathbf{g}]}$ is a variational generator for the map Ξ . We know from [75] that for the smooth maps f_{ij}^ζ and g_{kl}^ζ (defined in Equation (5.20))

$$\begin{aligned} \left\| \psi^{f_{ij}^\zeta, g_{kl}^\zeta}(q, t, s) - q - \int_0^s \int_0^t \left([f_{ij}^\zeta, g_{kl}^\zeta](\Phi^{(\tau-t)f_{ij}^\zeta} \circ \Phi^\sigma g_{kl}^\zeta \circ \Phi^{tf_{ij}^\zeta}(q)) \right) d\tau d\sigma \right\| \\ \leq 2K^3 |s|^2 |t| e^{|s|K} (1 + K|t|e^{|t|K}). \end{aligned}$$

where ψ is as defined in Equation (5.10). For any given p we are trying to estimate the distance

$$\Delta(p, \zeta) \stackrel{def}{=} d([\mathbf{f}^\zeta, \mathbf{g}^\zeta](p), [\mathbf{f}, \mathbf{g}](q_*)) \tag{5.27}$$

where $d(\cdot, \cdot)$ is the distance function defined in Equation (5.18). We will do so by bounding the total difference between the *set* of the regularized vector field's Lie brackets and the set-valued Lie bracket defined at q_* . Rewrite $[f_{ij}^\zeta, g_{kl}^\zeta](p)$ as

$$Dg_{kl}^\zeta(p)f_{ij}^\zeta - Df_{ij}^\zeta g_{kl}^\zeta = \int_{\mathbb{R}^n} \phi(h) Dg_{kl}(p + \zeta h) f_{ij}^\zeta(p) dh - \int_{\mathbb{R}^n} \phi(h) Df_{ij}(p + \zeta h) g_{kl}^\zeta(p) dh$$

where $\phi(h)$ and h are defined in Equation (5.20). Note that D makes sense as an operator here because we are only in a neighborhood of q_* , we are only considering points in this neighborhood that are also in $Diff(\mathbf{f}) \cap Diff(\mathbf{g})$, and f_{ij} and g_{kl} are almost everywhere analytic and are therefore Lebesgue integrable. Rewrite the above equation as

$$Dg_{kl}^\zeta(p)f_{ij}^\zeta - Df_{ij}^\zeta g_{kl}^\zeta = I_1(p) + I_2(p) \tag{5.28}$$

where

$$\begin{aligned}
I_1(p) &= \int_{\mathbb{R}^n} \phi(h) \bar{\omega}(p + \zeta h) dh \\
\bar{\omega}(z) &= Dg_{kl}(z) f_{ij}(z) - Df_{ij}(z) g_{kl}(z) \\
I_2(p) &= \int_{\mathbb{R}^n} \phi(h) Dg_{kl}(p + \zeta h) \left(f_{ij}^\zeta(p) - f_{ij}(p + \zeta h) \right) \\
&\quad - \int_{\mathbb{R}^n} \phi(h) Df_{ij}(p + \zeta h) \left(g_{kl}^\zeta(p) - g_{kl}(p + \zeta h) \right).
\end{aligned}$$

This implies that

$$d(I_1(p), [f_{ij}, g_{kl}](q_*)) \leq \gamma (\|p - q_*\| + \zeta) \quad \forall i, j, k, l.$$

(We know this from Equation 5.25 and the fact that $I_1(p)$ is the average of $[f_{ij}, g_{kl}](z)$ for $f(z)$ and $g(z)$ differentiable with $\|z - q_*\| \leq \gamma (\|p - q_*\| + \zeta)$.) This in turn implies that

$$d(I_1(p), [f, g](q_*)) \leq \gamma (\|p - q_*\| + \zeta). \quad (5.29)$$

Moreover, we know that $\|f_{ij}^\zeta(p) - f_{ij}(p)\| \leq K\zeta$. This along with the Cauchy Schwartz inequality implies that $\|f^\zeta(p) - f(p)\| \leq K\zeta$. Therefore,

$$\|f^\zeta(p) - f(p + \zeta h)\| \leq 2K\zeta$$

which implies

$$\|I_2(p)\| \leq 4K^2\zeta. \quad (5.30)$$

Equations (5.29) and (5.30) imply that we have the following estimate of Δ (where Δ is defined in Equation (5.27):

$$\Delta(p, \zeta) \leq \gamma (\|p - q_*\| + \zeta) + 4K^2\zeta.$$

Let $p = \Phi^{(\tau-t)f^\zeta} \circ \Phi^{\sigma g^\zeta} \circ \Phi^{tf^\zeta}(q)$. This implies that

$$\|p - q\| \leq K(2|t| + |s|)$$

which implies by the Cauchy-Schwartz inequality

$$\|p - q_*\| \leq K(2|t| + |s|) + \|q - q_*\|.$$

Finally, we have

$$d\left([f_{ij}^\zeta, g_{kl}^\zeta](p), [\mathbf{f}, \mathbf{g}](q_*)\right) \leq \gamma(K(2|t| + |s|) + \|q - q_*\| + \zeta).$$

This implies that

$$d\left([\mathbf{f}^\zeta, \mathbf{g}^\zeta](p), [\mathbf{f}, \mathbf{g}](q_*)\right) \leq \gamma(K(2|t| + |s|) + \|q - q_*\| + \zeta).$$

For $s > 0$ and $t > 0$ (actually, only $st > 0$ is necessary), we have

$$\begin{aligned} d\left(\frac{1}{st}\left(\psi^{f_{ij}^\zeta, g_{kl}^\zeta}(q, t, s) - q\right), [\mathbf{f}, \mathbf{g}](q_*)\right) \leq \\ 2K^3|s|e^{|s|K}(1 + K|t|e^{|t|K}) + \gamma(K(2|t| + |s|) + \|q - q_*\| + \zeta) + 4K^2\zeta. \end{aligned}$$

Let $\zeta \rightarrow 0$ and find

$$\begin{aligned} d\left(\frac{1}{st}\left(\psi^{f_{ij}, g_{kl}}(q, t, s) - q\right), [\mathbf{f}, \mathbf{g}](q_*)\right) \leq \\ 2K^3|s|e^{|s|K}(1 + K|t|e^{|t|K}) + \gamma(K(2|t| + |s|) + \|q - q_*\|) \text{ for all } i, j, k, l. \end{aligned}$$

Define

$$\mathcal{K}(r, q) = 2K^3re^{rK}(1 + rKe^{rK}) + \gamma(3rK + \|q - q_*\|).$$

The family of functions $\mathcal{K}(r, q)$ satisfies the requirements of \mathbf{k} in Definition 5.5.

Therefore, we have

$$d\left(\frac{1}{st}\left(\psi^{f_{ij}, g_{kl}}(q, t, s) - q\right), [\mathbf{f}, \mathbf{g}](q_*)\right) \leq \mathcal{K}(\max(|s|, |t|), q) \text{ for all } i, j, k, l. \quad (5.31)$$

Using Ξ from Equation 5.10, we see that Equation 5.31 implies:

$$d\left(\frac{1}{\varepsilon}(\Xi^{\mathbf{f}, \mathbf{g}}(q, \varepsilon) - q), [\mathbf{f}, \mathbf{g}](q_*)\right) \leq \mathcal{K}(\sqrt{\varepsilon}, q)$$

for $\varepsilon \geq 0$ and

$$d\left(\frac{1}{-\varepsilon}(\Xi^{\mathbf{f},\mathbf{g}}(q, \varepsilon) - q), [\mathbf{f}, -\mathbf{g}](q_*)\right) \leq \mathcal{K}(\sqrt{-\varepsilon}, q)$$

for $\varepsilon \leq 0$. Therefore, since $[\mathbf{f}, \mathbf{g}](q_*) = -[\mathbf{f}, -\mathbf{g}]$ we have

$$d\left(\frac{1}{|\varepsilon|}(\Xi^{\mathbf{f},\mathbf{g}}(q, \varepsilon) - q), [\mathbf{f}, -\mathbf{g}](q_*)\right) \leq \mathcal{K}(\sqrt{|\varepsilon|}, q)$$

for all ε sufficiently small. Therefore, for $v \in [\mathbf{f}, \mathbf{g}](q_*)$ we have

$$\inf_{v \in [\mathbf{f}, \mathbf{g}](q_*)} \|\Xi^{\mathbf{f},\mathbf{g}}(q, \varepsilon) - q - \varepsilon v\| = \mathcal{O}(\varepsilon + \|q - q_*\|).$$

So, using Q as defined in Equation 5.26, we get that

$$\inf_{v \in [\mathbf{f}, \mathbf{g}](q_*)} \|\Xi^{\mathbf{f},\mathbf{g}}(q, \varepsilon) - \Xi^{\mathbf{f},\mathbf{g}}(q_*, 0) - Q^v(q - q_*, \varepsilon)\| = \mathcal{O}(\varepsilon + \|q - q_*\|)$$

implying

$$\inf_{M \in \mathcal{Q}^{[\mathbf{f}, \mathbf{g}]}} \|\Xi^{\mathbf{f},\mathbf{g}}(q, \varepsilon) - \Xi^{\mathbf{f},\mathbf{g}}(q_*, 0) - M(q - q_*, \varepsilon)\| = \mathcal{O}(\varepsilon + \|q - q_*\|). \quad (5.32)$$

Equation 5.32 implies that as $\varepsilon \rightarrow 0$ and as $q \rightarrow q_*$,

$$\text{dist}(\Xi^{\mathbf{f},\mathbf{g}}(q, \varepsilon) - \Xi^{\mathbf{f},\mathbf{g}}(q_*, 0), \mathcal{Q}^{[\mathbf{f}, \mathbf{g}]}) \rightarrow 0.$$

Thus, $\mathcal{Q}^{[\mathbf{f}, \mathbf{g}]}$ is a variational generator for Ξ and is, by Theorem 5.13, a GDQ of Ξ . ■

5.4 Summary

Understanding the issue of controllability is often a first step toward understanding how to control a class of nonlinear systems. This chapter studied multiple model systems where the individual plants are driftless affine but switching can change plants over time. We will use this to examine controllability of the Rocky 7 Mars

rover in Chapter 7.

Author	Assumptions	Theorem Conditions
Murphey and Burdick	MMDA switching across regular boundaries	$\bar{\Delta} = \mathbb{R}^n$
Sussmann and Rampazzo	Lipschitz vector fields	$\bar{\Delta} = \mathbb{R}^n$
Murphey and Burdick	MMDA systems	$\bar{\Delta} = \mathbb{R}^n$

Table 5.1: Different Chow's Theorems with the same condition

Lastly we comment on how generic the condition for controllability is. Table 5.1 is a table of conditions for small time local controllability. It gives the authors, the assumption, and the conditions for controllability. Perhaps surprisingly, the conditions are all the same (as long as Δ and $\bar{\Delta}$ are interpreted properly in each case).

Chapter 6

Variation 1: Distributed Manipulation

This was our paradox: no course of action could be determined by a rule, because every course of action can be made out to accord with the rule.

Ludwig Wittgenstein *Philosophical Investigations*

Distributed manipulators typically consist of a large number of similar or identical actuators combined together with a control strategy to create net movement of an object or objects. The goal of most distributed manipulation systems is to allow precise positioning of planar objects from all possible starting configurations. In effect, a distributed manipulator is a “smart conveyor”. They can be used for separating parts and precisely positioning them for the purpose of assembly operations. Distributed manipulation systems offer potential for micro-assembly using MEMS technology. Distributed manipulator actuation methods ranges from air jets and wheels on the macroscale, to microelectromechanical systems (MEMS) and flexible scilia at the microscale. This chapter concerns itself with a broad class of distributed manipulation problems which involve rolling and sliding contacts between the moving object and actuator surfaces. In such cases friction forces and intermittent contact play an important role in the overall system dynamics. Hence, the analysis here is not necessarily intended for applications such as air jets, for exam-

ple. However, this will generally apply when manipulation is generated by moving mechanical contacts. I will use the PDM from Chapter 3 to produce equations of motion which are both first order and implicitly include contact forces of constraint.

I will only consider distributed manipulation systems that consist of (roughly planar) arrays of actuators that can re-position an object by the movements of its array elements (see Figure 6.1). In the future, arrays of this type should be useful for industrial assembly operations where small parts must be robustly transported and precisely positioned. MEMS technology offers attractive means to important small distributed manipulation devices for precisely positioning small parts. To see the relevance of the issues I am going to consider, one need only log onto the [58] Web site at <http://www.mems-exchange.org/> and look at the industrial view of the challenges facing MEMS in the next decade, there are currently three main problems making it difficult for MEMS to become a more main-streamed technology. They are (in order of relevance to this chapter):

1. Modeling MEMS arrays in a way that captures the essential physics while remaining tractable.
2. Simulation techniques for massively parallel systems.
3. Packaging MEMS technology for purposes of shipment and assembly.

Although this chapter does not address the third issue, it addresses some aspects of the first two problems. This chapter considers the design of manipulation control strategies for such distributed systems. I will focus on autonomous controllers that stabilize an object to a precise configuration in $SE(2)$ on the array.

Methods to design distributed manipulation control systems have been proposed in several works, including [12, 26, 30]. A common approach is based on the notion of *programmable vector fields* [9, 22]. In this methodology, one makes the possibly unrealistic assumption that the array's control capability can be idealized as a continuous distribution of forces across the array surface. In this abstraction, the manipulated object moves under the influence of these forces. The control design problem reduces to the selection of a continuous force field distribution that will

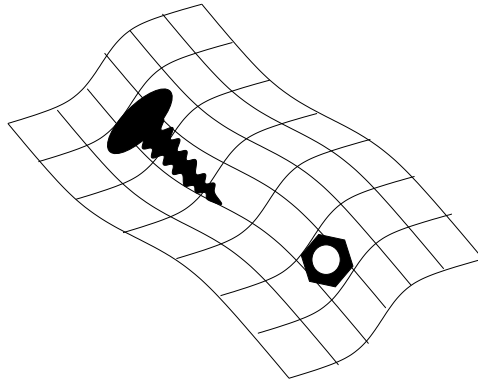


Figure 6.1: Parts on a distributed manipulator

locally transport the object to a prescribed position, and then stabilize it at that configuration. To implement the control strategy on the real array, one must adapt the continuous vector field control to the real (and discrete) actuator array. For a good description of this approach, see [12].

The programmable vector field approach is experimentally known to work in some MEMS-fabricated actuator arrays, where the array elements are “small” and “close” together relative to the size of the object being manipulated [9, 55]. It is additionally well suited to distributed air jets, because the aerodynamics effectively “smooth out” the resulting forces on the object. However, in cases where only a small number of actuators are in contact with the object being manipulated (i.e., the continuous actuation approximation is poor) or the coefficient of friction μ is very high, the continuous approximation has been shown experimentally not to work as well (see Luntz et al. [54]). In these cases, the continuous approximation does not adequately incorporate the physics of the actual array and the object/array interface.

This chapter has three main contributions. First I will show that when one takes into account the discrete nature of real actuator arrays and a fairly general model of the actuator-to-object contact mechanics using the PDM, the control systems designed by the continuous approximation method will be unstable when deployed on the actual array. This is not unexpected, as the programmable vector field

approach is based on the restrictive assumption that the continuous vector field abstraction is a good approximation to the arrays’ actual physical characteristics. This instability result has been previously shown for specific array geometries in Luntz et al. [54]. This thesis generalizes these findings. Section 6.3 shows that such a rotational instability is generic to distributed manipulation when one uses a continuous approximation, and that moreover this instability can be ascribed to the changing contact states between the object and the array. Luntz et al. [49] discussed some of the issues with friction, but here a set-valued analysis approach is used to produce tractable problems while still including effects from the changing contact states. Sections 6.3.2 and 6.3.3 additionally show that when one introduces feedback, then these systems are in principle stabilizable. Section 6.3.4 shows that if one incorporates the contact states, one can design a local control law based on control Lyapunov methods. Section 6.4 considers the case of “full actuation”- when all the actuators can be steered and driven. It gives an extremely simple, scale-able algorithm that is provably globally exponentially stabilizing, thus showing that it is highly desirable to have a fully actuated distributed manipulator. Section 6.5 illustrates how the programmable force field method can be combined with a feedback method to produce globally stabilizing controllers while only having feedback in a neighborhood of the origin. This control system is globally exponentially convergent. The global exponential convergence result depends on estimating the changing contact state, so work by [4, 36] is extended appropriately. These results are illustrated both in simulations and on an experimental test-bed in Section 6.6. Finally, this chapter ends by extending work by [4, 36, 38] in order to provide a way of improving the performance of a distributed manipulator.

6.1 Review of the Programmable Force Fields Approach

The use of programmable vector fields for distributed manipulator control is based on a continuous “force field” abstraction which assumes that at each point on the manipulation surface one can specify the manipulation force at that point. The

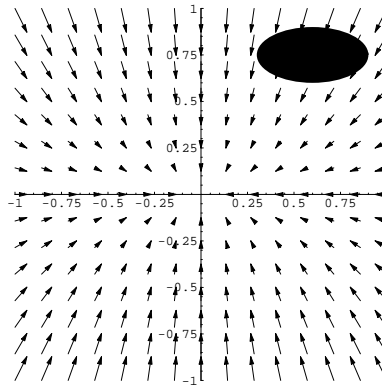


Figure 6.2: Programmable vector field

dynamics of the moving object are obtained by integrating the continuous force field to get a total force on the part. To use the controls on an actual array, where the manipulation forces will be generated at discrete points, one must adapt the continuous approximation to the geometry of a given discrete array. For a good reference, see [12].

The most basic control law comes from the idea of a “squeeze” field. Squeeze fields are in general of the form $F = \{-\alpha x, -\beta y\}$, where α and β are coefficients to be chosen by the control designer. These open loop control laws can stabilize an object to one of several stable equilibria depending on the shape and distribution of mass of the object. A great deal of work has been done to extend this work to more general field capable of stabilizing more general classes of object. See, for instance, Böhringer et al. [11, 12, 13] and Kavraki and Sudsang [79].

The distributed forces can be integrated over the body’s surface to obtain the object’s dynamical response. This process is as follows: assume the part \mathcal{O} can be described by a support characteristic function $\omega(x, y)$ where $\omega(x, y)$ is 1 everywhere on the object surface and 0 otherwise. Moreover, let the part be subject to a force field $f(x, y) : \mathbb{R}^2 \rightarrow \mathbb{R}^2$. Lastly, make the reference frame of \mathcal{O} be at the object’s center of mass, i.e.,

$$\int_{\mathbb{R}^2} \omega(p) dp = 0$$

When the object lies at configuration $q = (x, y, \theta)$ the net force and torque on the

object are

$$F = \int_{\mathbb{R}^2} \omega(p) f(A_\theta p + t) dp \quad (6.1)$$

$$M = \int_{\mathbb{R}^2} \omega(p) A_\theta p \times f(A_\theta p + t) dp \quad (6.2)$$

with $t = (x, y)^T$ and A the 2x2 rotation matrix of angle θ . The condition for equilibrium is $F = M = 0$. Moreover, in the case of many choices programmable vector fields the equilibrium is stable. However, when the actuators are far apart or the coefficient of friction μ is very high, the continuous approximation is known not to work as well, because the objects being moved have dramatically different dynamics depending on the contact state. To use these controls on an actual array, where the manipulation forces will be generated at discrete points, one must adapt the continuous approximation to the given discrete geometry, which will entail including the contact mechanics into the modeling.

Remark 6.1

It should be noted that although the inputs for the programmable force field are forces and the inputs considered later are vector field inputs (velocities), these two are in reality often the same set of inputs because the forces are assumed to be generated by the friction caused by the contact slipping at a given velocity. That is, $F = -\mu N v$ where μ is the coefficient of friction, N is the normal force, and v is the velocity. Therefore, under these assumptions, the input classes are typically equivalent. \diamond

Remark 6.2

Here I should comment on the relationship between the philosophies of the PDM approach and the programmable force field approach. The programmable force field method effectively assumes that there are an infinite number of actuators, that all of the actuators are slipping all the time, and that the physics of con-

tact between the array surface and the object is not important. Hence, the programmable force field method is more appropriate to the analysis and design of gross motions where accuracy is less important and simplicity of analysis and the design problem is appealing. The PDM assumes that there are generally a finite number of discrete contact points, and incorporates Coulomb friction contact physics into the model. However, the PDM can only be well justified for quasi-static systems where the objects move slowly enough that the contact reaction forces dominate the moments of inertia. This will be true in the case of distributed manipulation, where the local behavior of object motion around an equilibrium point is studied. Therefore, the PDM is more appropriate to the analysis and control of local, quasi-static motions, near the equilibrium. These contrasting features inspire the merging of these two techniques in Section 6.5. \diamond

6.2 Modeling the Equilibrium Point of a Distributed Manipulation System

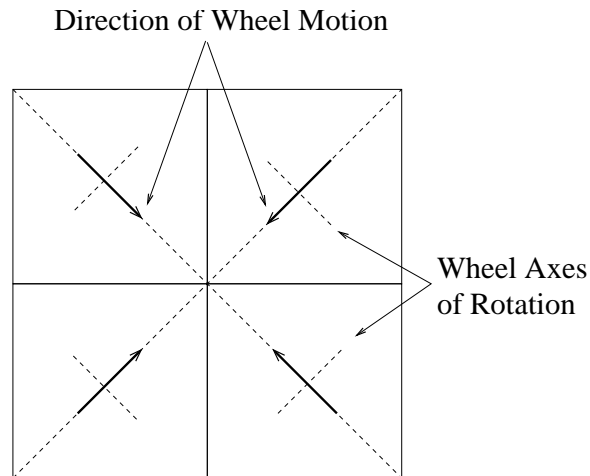


Figure 6.3: Four node array centered at the origin

Here the PDM technique are applied to a specific example. Consider the actuator

array shown in Figure 6.3. It has only four wheels whose rims are oriented towards the origin. Actuation is generated by the contact between the rim and the body. The wheel is assumed to make point contact with the body at all times and it is assumed that the wheels speed u_i is directly controlled. I will use the convention that the i^{th} wheel has a positive input u_i when the top of the wheel is turning towards the the right half plane. For this model it will be shown that if one uses the mechanical model obtained by the PDM, one can get rotational instability in part placement when the passive programmable vector field approach, as described in [10], is applied to this system. Simulations are included in Section 6.2.2. The next section generalizes this result to a broader class of actuator arrays.

The difference between the stability prediction of the continuous approximation and the more exact model rests largely on the fact that the continuous approximation does not take any contact mechanics into account, nor does it account for the fact that most real arrays consist of a finite number of discrete actuators. Of course, as previously remarked, the PDM can only be well justified for quasistatic systems where the objects move slowly enough that the contact reaction forces dominate the moments of inertia. This will be true in the case of distributed manipulation, where the local behavior of object motion around an equilibrium point is studied.

Generally, there is no reason to believe that friction at the contact point will be uniform in all directions of the contact plane. Rather, allow a smooth distribution of coefficient of friction, like that seen in Figure 6.4 (see [33, 34] for a discussion of such friction models). While some materials do have friction of this type, such

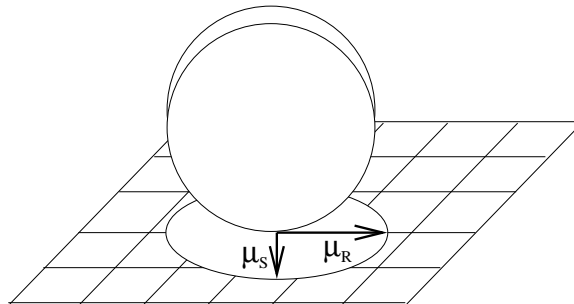


Figure 6.4: A wheel with the vector-dependent friction

anisotropic friction models are more generally useful as a means to approximately model compliance effects and wheel tread effects. For instance, if the wheel shown above was an extremely thin saw blade, then one would expect μ_R (the friction coefficient along the “rim” direction) to be less than μ_S (the friction coefficient along the “side” direction). However, the treads on a tank ensure that μ_R is greater than μ_S . Note that the minimum of the dissipation function will only be nonunique when the ellipse reduces to a circle (i.e., $\mu_S = \mu_R$). Note also that in this case, the same indeterminacy shows up in the Lagrangian mechanics analysis. I should also point out that much of the analysis in this chapter is valid for more general anisotropic friction models in that I primarily utilize the non-uniformity of the frictional constraints.

6.2.1 Equations of Motion

Let us now apply the power dissipation method to this example in Figure 6.3. Let $\Psi : Q \rightarrow TQ$ be a velocity field on $Q = \mathbb{R}^2$. Assume that the equilibrium point of $\Psi(x, y)$ lies at the intersection point of the lines underlying the wheel rims.

With four wheel actuators, there is a potential total of 8 kinematic constraints on the objects motion. However, since the object moves in the plane, at most three of these constraints can be satisfied at any instant—the other constraints are violated via contact slipping. This gives us $\binom{8}{3} = 56$ possible contact states. Using the PDM as the modeling methodology, each has its own first order governing equations. Additionally assume that μ_S and μ_R are uniform across \mathbb{R}^2 and that $|\mu_S - \mu_R|$ is sufficiently small that the center of mass completely determines which constraints are satisfied. That is, assume that the constraints are determined by first computing which actuator is the closest to the center of mass, which actuator is the second closest to the center of mass, and using the constraints from these two actuators to determine the first order governing equations. Given this assumption, only 8 of the 56 contact states ever satisfy the minimum of the power dissipation function on a set of full measure, therefore leaving us with a total of 8 possible contact states.

Assume the u_i are determined by projecting Ψ onto the direction of actuation.

Let

$$g_i = \begin{bmatrix} R(\theta_i) & \begin{bmatrix} x_i \\ y_i \end{bmatrix} \\ 0 & 1 \end{bmatrix}$$

be the homogeneous representation of the element of $SE(2)$ going from the origin to the i^{th} actuator node location and orientation, and $R(\cdot)$ is an element of $SO(2)$.

Then the constraints associated with each actuator are $\Omega_i(q)\dot{q} = 0^1$, where

$$\Omega_i(q) = \begin{bmatrix} \left[\begin{array}{c} Ad_{g_i}^T \begin{bmatrix} 1 \\ 0 \\ 0 \end{bmatrix} \\ Ad_{g_i}^T \begin{bmatrix} 0 \\ 1 \\ 0 \end{bmatrix} \end{array} \right]^T u_i \\ \left[\begin{array}{c} Ad_{g_i}^T \begin{bmatrix} 0 \\ 1 \\ 0 \end{bmatrix} \\ Ad_{g_i}^T \begin{bmatrix} 1 \\ 0 \\ 0 \end{bmatrix} \end{array} \right]^T 0 \end{bmatrix} \quad (6.3)$$

$Ad(\cdot)$ is the adjoint transformation which transforms velocities from one coordinate frame to another (see [68] for details). Note that Ω_i are 2×4 matrices where the top row represents the rolling constraint and the bottom row is the side ways constraint.

To apply the PDM, first note that the minimum only occurs when three of the constraints are satisfied, and that moreover, the constraints satisfied are precisely those which would otherwise dissipate the most energy if they were violated. The contact states that dissipate the least amount of energy are those associated with the potential constraints having the largest three $\alpha_i = N_i \mu_i$. Thus, the constraints whose violation will potentially dissipate the most energy are the ones that are satisfied. Based on these observations, if the center of mass determines the normal forces (based on assumptions about surface uniformity, etc.), and if $\mu(x, y)$ is uniform, then the object's motion satisfies whichever constraints are closest to its center of mass. That is, the particular quadrant in which the center of mass lies determines the first two actively satisfied constraints. The third actively satisfied

¹Note that this is *not* the same Ω as in Chapter 5. It is a set of one forms on TQ .

constraint is one of the two constraints coming from the second closest actuator and is determined by the friction model, i.e., $\mu_S > \mu_R$ or $\mu_S < \mu_R$. Let i be the index of the closet actuator and j be the index of the next closest actuator. When $\mu_S > \mu_R$, the system equations are found by solving for the annihilator of the $\Omega_i(q)$ and the side ways constraint from $\Omega_j(q)$. Assuming unit magnitude input in each actuator, solving each set of constraints, and doing some algebraic simplification yields the following governing equations:

$$\begin{bmatrix} \dot{x} \\ \dot{y} \\ \dot{\theta} \end{bmatrix} = \begin{bmatrix} -\frac{\sqrt{2}}{2} \operatorname{sgn}(x) (\operatorname{sgn}(y^2 - x^2) + 1) \\ \frac{\sqrt{2}}{2} \operatorname{sgn}(y) (\operatorname{sgn}(y^2 - x^2) - 1) \\ -\frac{\sqrt{2}}{2} \operatorname{sgn}(xy^3 - x^3y) \end{bmatrix} \quad (6.4)$$

where $\operatorname{sgn}(x)$ is the sign function found in Example 2.1. If, however, $\mu_S < \mu_R$, the system equations are found by solving for the annihilator of the $\Omega_i(q)$ and the rolling constraint from $\Omega_j(q)$. In this case, the system equations are

$$\begin{bmatrix} \dot{x} \\ \dot{y} \\ \dot{\theta} \end{bmatrix} = \begin{bmatrix} \frac{\sqrt{2}}{2} \operatorname{sgn}(x) (\operatorname{sgn}(y^2 - x^2) - 1) \\ -\frac{\sqrt{2}}{2} \operatorname{sgn}(y) (\operatorname{sgn}(y^2 - x^2) + 1) \\ \frac{\sqrt{2}}{2} \operatorname{sgn}(xy^3 - x^3y) \end{bmatrix} \quad (6.5)$$

6.2.2 Simulations

To illustrate these concepts, this section provides the results of simulations that model a planar distributed manipulation system with actuators located at (i, j) for $i, j \in \{-1, 1\}$. Actuation is provided by unit radius rotating wheels (which rotate along axes orthogonal to the wheel rims depicted in Figure 6.4) with constant friction coefficient μ and point contact between the wheel rims and the manipulated object (a box in this case). The simulations were implemented in *Mathematica*, using its *NDSolve* integrator, modified to allow for differential inclusions. Some extension is necessary in order to avoid the numerical difficulties at switching boundaries ($y = x, y = -x, x = 0, y = 0$ for these simulations). However, this is only a concern for switching boundaries which are stable or attracting, because if the trajectory

intersects the boundary transversely, standard numerical schemes still work. For these simulations, hysteresis is introduced to simulate a discrete system as a hybrid automaton. This produces numerically stable simulations. I should point out, however, that different choices of hysteresis constant h lead to slightly different solutions. The main difficulty is that solutions of differential inclusions are necessarily nonunique, therefore implying that any simulation represents only one solution ϕ to the differential inclusion $\dot{\phi} \in F$.

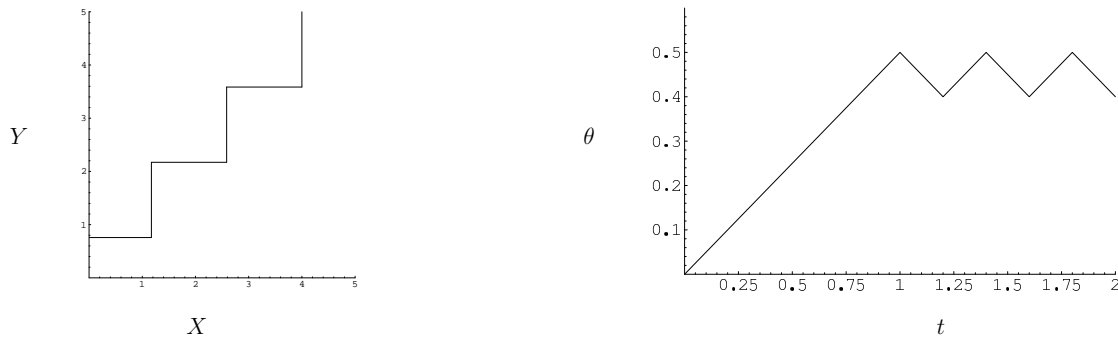


Figure 6.5: X , Y , and θ trajectory of non-feedback system

Figure 6.5 shows the simulation output. Notice that the origin's position is translationally stable, as the switching system equations always satisfy the Lyapunov equation $\frac{\partial V}{\partial q} \dot{q} < 0$ for $q = (x, y)$ and $V = x^2 + y^2$. The simulations are done with a slight hysteresis as the dynamics approach the diagonal $y = x$. Notice that with an initial condition of $\theta_0 = 0$ (the desired θ), θ is unstable and increases linearly until the switching begins and then hovers around a new equilibrium (not the desired $\theta_0 = 0$). That is, the origin is asymptotically stable but the orientation is not.

6.2.3 More General Equations of Motion

This section applies the power dissipation method to the example of an array of actuated wheels in the plane where the location of the i_{th} actuator is located at (x_i, y_i) , has a fixed orientation with respect to the origin of θ_i , and the velocity input at that actuator is u_i . I.e., the i^{th} wheel is spinning at speed u_i . I will show

later in Section 6.3.3 that the instability seen in the previous section arises in the general case as well. The system equations are found by solving for the annihilator of the constraint $\Omega(q)$. If $\mu_S < \mu_R$, and if the two dominating actuators are indexed by i and j , then the first order governing equations derived from the PDM model are

$$\begin{bmatrix} \dot{x} \\ \dot{y} \\ \dot{\theta} \end{bmatrix} = \begin{bmatrix} \frac{u_i[s_j((x_i-x_j)c_i+y_i s_i)+c_i c_j y_j]-u_j y_i}{(x_j-x_i)s_j+(y_i-y_j)c_j} \\ \frac{u_j x_i - u_i[c_i c_j x_i + s_i(x_j s_j + (y_i - y_j)c_j)]}{(x_j-x_i)s_j+(y_i-y_j)c_j} \\ \frac{u_j - u_i \cos(\theta_i - \theta_j)}{(x_i-x_j)s_j+(y_j-y_i)c_j} \end{bmatrix} \quad (6.6)$$

where $c_i = \cos(\theta_i)$, $s_i = \sin(\theta_i)$, etc. It should be noted that here the index notation should be thought of as mapping (i, j) pairs to equations of motion in some neighborhood (not necessarily small) around the i^{th} and j^{th} actuator. The transition between the equations of motion determined by actuators i and j to equations of motion determined by actuators k and l will in general be determined by the location of the center of mass. This in turn leads to the state space being divided up by transition boundaries between different sets of equations of motion. To write this as an MMDA system, rewrite the above system as

$$\begin{bmatrix} \dot{x} \\ \dot{y} \\ \dot{\theta} \end{bmatrix} = f_1 u_1 + f_2 u_2 \quad (6.7)$$

where

$$f_1 \in \left\{ \begin{bmatrix} \frac{-y_i}{(x_j-x_i)s_j+(y_i-y_j)c_j} \\ \frac{-x_i}{(x_j-x_i)s_j+(y_i-y_j)c_j} \\ \frac{1}{(x_i-x_j)s_j+(y_j-y_i)c_j} \end{bmatrix} \right\}$$

$$f_2 \in \left\{ \begin{bmatrix} \frac{s_j((x_i-x_j)c_i+y_i s_i)+c_i c_j y_j}{(x_j-x_i)s_j+(y_i-y_j)c_j} \\ \frac{-c_i c_j x_i - s_i(x_j s_j - (y_i - y_j)c_j)}{(x_j-x_i)s_j+(y_i-y_j)c_j} \\ \frac{-\cos(\theta_i - \theta_j)}{(x_i-x_j)s_j+(y_j-y_i)c_j} \end{bmatrix} \right\}$$

I do not consider the case of $\mu_S > \mu_R$ for reasons I will discuss in Section 6.3.2.

6.3 Local Stability

This section covers the stability and stabilizability of both the specific example considered in Section 6.2.2 and the more general case from Section 6.2.3. In particular, we will see that we can only guarantee Lyapunov stability, not asymptotic stability, for the programmable vector field approach. This will match the intuition behind the simulation in Figure 6.5 that the θ variable is not stabilized by the programmable vector field. It is then shown that if one uses feedback, generalized versions of the example in Section 6.2 are indeed stabilizable to the origin even when the actuators cannot be re-oriented.

6.3.1 XY Stability and θ Instability

In this section it is shown, for the equations of motion in Equation (6.4) and (6.5), that the translational component (x, y) of the object's location in $SE(2)$ is asymptotically stable and that the orientation θ is not asymptotically stable in Equations (6.4) and (6.5). First note that the above system is a differential inclusion of the type found in Chapter 2. To check the (x, y) translational stability of the object's motion, choose $V(x, y) = x^2 + y^2$. Then

$$\begin{aligned}\dot{V} &= \text{co}\{\dot{V}_*, \dot{V}^*\} = \frac{\partial V}{\partial x} \dot{x} + \frac{\partial V}{\partial y} \dot{y} \\ &= x(-\text{sgn}(x)(\text{sgn}(y^2 - x^2) + 1)) + y(\text{sgn}(y)(\text{sgn}(y^2 - x^2) - 1)) \\ &= (y \text{sgn}(y) - x \text{sgn}(x))\text{sgn}(y^2 - x^2) - (x \text{sgn}(x) + y \text{sgn}(y)) \\ &< 0 \quad \forall x, y\end{aligned}$$

We have to check the places where the derivative of V fails to exist, i.e. where $xy = 0$. First we check the case when $x = 0$. Taking the upper derivative as in Equation (2.11), we get

$$\dot{V} = -y \text{sgn}(y)(1 + (\text{sgn}(y))^2)$$

and we know that

$$1 < 1 + (\text{sgn}(y))^2$$

and that for $y \neq 0$

$$-y \text{sgn}(y) = -|y|$$

so

$$\dot{V}^* = \sup_{\xi \in F} \nabla V \xi < 0$$

The case for $y = 0$ is computed similarly.

In the case of $\mu_S < \mu_R$ (Equation (6.5)), we also get $\dot{V}^* < 0$. Moreover, we know from Equations (6.4) and (6.5) that the rotational governing equations do not depend in any way on θ . The angle θ is therefore dependent on the initial conditions only, and is therefore not asymptotically stable. This matches the results in the simulation in Figure 6.5. What we have shown is the following.

Lemma 6.1. *Equation (6.4) and (6.5) are asymptotically stable to the origin in (x, y) and are not asymptotically stable in θ .*

6.3.2 Feedback for Distributed System

Note that the forms of Equations 6.4 and 6.5 are deceptively simple, as these equations assume that all of the actuator inputs assume a constant value. When the inputs are variable, the system equations will have the form

$$\dot{x} = g_{\sigma_1} u_1 + g_{\sigma_2} u_2 + g_{\sigma_3} u_3 + g_{\sigma_4} u_4. \quad (6.8)$$

Equation (6.8) is an MMDA system as in Definition 3.2. The g_i therefore depend discontinuously on the state (x, y) . In the case of $\mu_S > \mu_R$, the system equations are simply of the form $\dot{x} = g_i u_i$ with i corresponding to the index of the quadrant in which the body center of mass currently resides. Therefore the system is not even locally controllable (although it may be globally controllable) meaning that we cannot hope for a simple control law. This has implications from the viewpoint of implementation of a distributed manipulator, in that wheels that favor a no-sliding

constraint along the wheel rim will produce systems easier to control than wheels which are designed to prevent sideways slip. However, if $\mu_S < \mu_R$, we will see in Section 6.3.3 that the system can be stabilized to $(x, y, \theta) = (0, 0, \theta_d)$ where θ_d is some desired orientation value. We will revisit this example to illustrate such a control law in Section 6.3.4.

Remark 6.3

I should point out another interesting characteristic of the governing equations for the model in Equations (6.4) and (6.5). This is because the wheels can only produce translation parallel to the direction they are turning. It is possible to stabilize to the origin while stabilizing the orientation, but it is not possible to stabilize to points within an arbitrarily small neighborhood of the origin. In fact, we can only hope to stabilize to points on the manifolds $x = \pm y$. However, this is acceptable, as the problem we are trying to solve is point stabilization at the origin. Moreover, if one wants to move an object around, for a larger array it is clear that these manifolds would form a connected graph $G \subset \mathbb{R}^2$. It is unclear if a change in geometry would help stabilize to more points in a neighborhood of the origin. \diamond

6.3.3 More General 2-Dimensional Arrays

The stability results of the previous example are not an isolated phenomena, and are generalized in this section. That is, the lack of stability does not necessarily arise from the specific geometry of this example. In this generalization assume that all the actuators are a finite distance apart and make point contact with the object being manipulated. The following theorem indicates that the induced lack of stability of the programmable vector field approach can arise in more general circumstances. The proof of the theorem relies essentially upon the same sorts of calculations as found in Section 6.2.

Theorem 6.2. *Given an elliptic vector velocity field $\Psi(x, y) : \mathbb{R}^2 \rightarrow \mathbb{R}^4$ (where \mathbb{R}^4 is*

the tangent bundle of \mathbb{R}^2), and a discrete planar array geometry indexed by $i, j \in I$ in some neighborhood of the origin, the first order governing equations given by the PDM are asymptotically stable in (x, y) to the origin but not asymptotically stable in θ . Moreover, if $\mu_S < \mu_R$, then such a system is exponentially stabilizable through the use of feedback.

Proof:

To see that the system is not asymptotically stable in θ , it is sufficient to note that $Ad_{g^{-1}}$ in Equation (6.3) depends only on x and y , therefore leaving the θ dynamics with no dependence on θ . This symmetry implies that the system equations are invariant with respect to initial condition in θ ; therefore θ is not stable. To see that the system is stabilizable, assume that the governing equations are determined at time t almost always by two constraints at the actuator i with coordinates (x_i, y_i) and input speed u_i , and one constraint at the actuator j with coordinates (x_j, y_j) and input speed u_j . Moreover assume that $\mu_S < \mu_R$, thereby ensuring a “rolling” constraint is satisfied rather than a “side-slipping” constraint.

The theorem is proved by explicitly showing that the requirements of Theorem 2.3 are satisfied. First choose the Lyapunov function to be $V(q) = \frac{1}{2}\|q\|$. Moreover, choose $V_0 = V_1 = W = V$ (this choice merely takes advantage of the fact that the governing equations are first order). Clearly $V_0 \leq V \leq V_1$. It must be shown that $\dot{V}^* \leq -W$, where \dot{V}^* was defined in Eq. (2.11). First we must compute \dot{V}^* .

Denote $\sin(\cdot)$ by $s(\cdot)$ and $\cos(\cdot)$ by $c(\cdot)$. Recall the governing equations from Eq. (6.6).

$$\dot{q} = \begin{bmatrix} \frac{-(u_j y_i) + u_i (s(\theta_j) (c(\theta_i) (x_i - x_j) + s(\theta_i) y_i) + c(\theta_i) c(\theta_j) y_j)}{s(\theta_j) (-x_i + x_j) + c(\theta_j) (y_i - y_j)} \\ \frac{u_j x_i - u_i (c(\theta_i) c(\theta_j) x_i + s(\theta_i) (s(\theta_j) x_j + c(\theta_j) (y_i - y_j)))}{s(\theta_j) (-x_i + x_j) + c(\theta_j) (y_i - y_j)} \\ \frac{-(c(\theta_i - \theta_j) u_i) + u_j}{s(\theta_j) (x_i - x_j) + c(\theta_j) (-y_i + y_j)} \end{bmatrix}$$

Then, taking $V(x, y, \theta) = \frac{1}{2}\|q\| = \frac{1}{2}(x^2 + y^2 + \theta^2)$ note that in a region where only

one set of governing equations apply (i.e. $\dot{V}^* = \dot{V}$)

$$\begin{aligned}\dot{V} &= x\dot{x} + y\dot{y} + \theta\dot{\theta} \\ &= \frac{u_j (\theta - y x_i + x y_i)}{s(\theta_j) (x_i - x_j) + c(\theta_j) (-y_i + y_j)} \\ &+ \frac{u_i (c(\theta_j) (y s(\theta_i) (y_i - y_j) - c(\theta_i) (\theta - y x_i + x y_j)))}{s(\theta_j) (x_i - x_j) + c(\theta_j) (-y_i + y_j)} \\ &+ \frac{u_i (s(\theta_j) (x c(\theta_i) (-x_i + x_j) - s(\theta_i) (\theta - y x_j + x y_i)))}{s(\theta_j) (x_i - x_j) + c(\theta_j) (-y_i + y_j)}\end{aligned}$$

or

$$\dot{V} = u_i f_i(x) + u_j f_j(x) \quad (6.9)$$

Note that this is split into two coefficients of u_i and u_j , which in turn implies that if one has full knowledge of the state, then one can always choose the inputs so as to make $\dot{V}^* = \dot{V} \leq 0$. Moreover, \dot{V} can be made to be always nonzero through a proper choice of inputs. Due to the form of Eq.(6.9), inputs u_i and u_j can always be chosen so that

$$\dot{V} \leq -V.$$

We have to check on the boundary between two different contact states. On the boundary

$$\dot{V}^* = \sup\left\{\frac{\partial V}{\partial q} \dot{q}_i, \frac{\partial V}{\partial q} \dot{q}_j\right\}$$

where

$$\frac{\partial V}{\partial q} \dot{q}_i = u_{i_1} f_{i_1} + u_{i_2} f_{i_2}$$

$$\frac{\partial V}{\partial q} \dot{q}_j = u_{j_1} f_{j_1} + u_{j_2} f_{j_2}$$

subject to the constraint that $u_{j_1} = u_{i_2}$. Substituting and comparing,

$$\dot{V}^* = \sup\{u_{i_1} f_{i_1} + u_{i_2} f_{i_2}, u_{i_2} f_{j_1} + u_{j_2} f_{j_2}\}$$

thus implying that despite the constraint both can be made arbitrarily negative, thus ensuring that

$$\dot{V}^* \leq -V.$$

Hence, the system is locally exponentially stabilizable. Moreover, one can explicitly write down a control law once one is given a Lyapunov function that is the desired metric on $SE(2)$ and whose vanishing point is the desired equilibrium. Again, taking $V(x, y, \theta) = \frac{1}{2}\|q\| = \frac{1}{2}(x^2 + y^2 + \theta^2)$, one can in every region that is not a boundary solve the equation

$$\dot{V} = \frac{\partial V}{\partial q} \dot{q} = -k\|q\|^2$$

for u_i and u_j . Then

$$u_i = \frac{u_j^{num}}{u_j^{den}} \quad (6.10)$$

where

$$u_j^{num} = u_j (\theta - y x_i + x y_i) + k (\theta^2 + x^2 + y^2) (s(\theta_j) (x_i - x_j) + c(\theta_j) (-y_i + y_j))$$

and

$$\begin{aligned} u_j^{den} = & s(\theta_j) (x c(\theta_i) (x_i - x_j) + s(\theta_i) (\theta - y x_j + x y_i)) \\ & + c(\theta_j) (y s(\theta_i) (-y_i + y_j) + c(\theta_i) (\theta - y x_i + x y_j)) \end{aligned}$$

where u_j can be chosen arbitrarily. Suppose that the system state lies on a boundary between a state where u_j and u_k are the two dominating inputs and a state where u_j and u_k are the dominating actuators. Then one computes the control law on the boundary and gets

$$u_j = \frac{u_j^{num}}{u_j^{den}} \quad (6.11)$$

$$\begin{aligned}
u_j^{num} &= (-1 + \delta) u_k (\theta - y x_i + x y_i) + k (\theta^2 + x^2 + y^2) (s(\theta_j) (-x_i + x_j) + c(\theta_j) (y_i - y_j)) \\
&\quad + \delta u_i (s(\theta_j) (x c(\theta_i) (x_i - x_j) + s(\theta_i) (\theta - y x_j + x y_i)) \\
&\quad + c(\theta_j) (y s(\theta_i) (-y_i + y_j) + c(\theta_i) (\theta - y x_i + x y_j))) \\
u_j^{den} &= \delta (\theta - y x_i + x y_i) + (-1 + \delta) s(\theta_j) (x c(\theta_i) (x_i - x_j) + s(\theta_i) (\theta - y x_j + x y_i)) \\
&\quad + (-1 + \delta) c(\theta_j) (y s(\theta_i) (-y_i + y_j) + c(\theta_i) (\theta - y x_i + x y_j)) \\
&\quad + \delta (\theta - y x_i + x y_i) + (-1 + \delta) s(\theta_j) (x c(\theta_i) (x_i - x_j) + s(\theta_i) (\theta - y x_j + x y_i)) \\
&\quad + (-1 + \delta) c(\theta_j) (y s(\theta_i) (-y_i + y_j) + c(\theta_i) (\theta - y x_i + x y_j))
\end{aligned}$$

where u_i and u_k are set and $\delta \in [0, 1]$ parameterizes the differential inclusion. The important point here is that one *can* choose a set of inputs that will satisfy the Lyapunov theorem in Chapter 2. Therefore, the origin is exponentially stable. ■

A possible difficulty with this result is that the stabilizing control switches discretely as the contact state switches, which suggests the need for a way of estimating the contact state. However, it certainly may be possible to choose control laws such that the resulting system will be stable without this estimation—the previous arguments do not consider this. In fact, the control laws computed based on the ideas in the preceding section perform quite well, suggesting that a more general proof is possible. The $\mu_S < \mu_R$ assumption only has an obvious physical interpretation for wheel-like contacts, and I do not yet have a formulation for generic contacts. The case $\mu_S > \mu_R$ may be stabilizable, but not in as straight forward a fashion. This is for largely the same reason that it may be globally controllable, but is not locally controllable, as discussed in Section 6.3.2.

Remark 6.4 Weakly Stabilizable vs. Strongly Stabilizable

Notice that the control law computed in Equation (6.11) depends on the parameter δ . This implies that on the boundaries between contact states the system is only *weakly stabilizable* in the sense defined in Chapter 2. That is, for every selection of the differential inclusion, there exists a control that expo-

nentially stabilizes the system to the origin. However, one can often estimate δ based on the geometry of the contact state boundaries. See Utkin [83] for details of this. A static estimation of $\delta = 0.5$ works well for the example in Section 6.2 both in simulation and in the experiment. Moreover, these boundaries only constitute a set of measure 0 in the state space, and as we will see in the example done in the next section, one can often choose inputs that will make these boundaries *strongly stabilizable*, but I cannot yet show that it is true in the generic case. To treat cases when the system cannot be made strongly stabilizable and a static estimation of δ will not work, in Section 6.7, I will extend work by Hespanha [38] to show that online estimation of δ can provide stability provided certain assumption on how fast the contact state is allowed to change.

◇

6.3.4 Simulations

To these ideas, apply the method to a situation near the boundary $x = y$ for $x > 0$ and then apply it near the boundary $y = 0$ for $x > 0$. Restricting attention to this region provides all the salient features of the theory while keeping the problem tractable. A description of this control law as it was implemented experimentally can be found in Appendix A in Tables A.2 and A.3. Rescaling all the u_i in Equation (6.8) by $\frac{1}{\sqrt{2}}$, the governing equations in this boundary region $y = 0, x > 0$ are

$$\dot{q} = \begin{bmatrix} -u_1 - u_4 \\ -u_1 + u_4 \\ co\{u_1, u_4\} \end{bmatrix} \quad (6.12)$$

Do a control Lyapunov design using $V = \frac{1}{2}\|(x, y, \theta)\|^2$. This means that $\dot{V} = \frac{\partial V}{\partial q}\dot{q} = x(-u_1 + u_4) + y(-u_1 - u_4) + \theta(co\{-u_1, u_4\})$. Rewrite $co\{-u_1, u_4\}$ as $\delta(-u_1) + (1 - \delta)u_4$ thereby parameterizing all selections of $co\{-u_1, u_4\}$ by δ . Solving the equation

$\dot{V} = \frac{\partial V}{\partial q} \dot{q} = -k\|q\|^2$ (with $k > 0$), we see that a choice of

$$\begin{aligned} u_1 &= \frac{-k\theta((1-\delta)\theta+x-y)+k\|(x,y,\theta)\|^2}{\delta\theta+x+y} \\ u_4 &= -k\theta \end{aligned} \quad (6.13)$$

makes $\dot{V} = -k\|q\|^2$. Therefore the system is exponentially stabilized. This example should illustrate some of the weaknesses of the theory described in Section 6.3.3. Since this is only a weakly stable solution, the estimation of δ is necessary. In numerical simulations one knows that $\delta = \frac{1}{2}$, and the simulation works well. However, in a real system δ would have to be estimated on-line. Section 6.7 extends work in [38] to the case of distributed manipulation so that the feedback law will not be sensitive to variations in δ , and therefore not as sensitive to effects of chattering, etcetera.

Consider the case when $x = y, x > 0$. In this case the governing equations in this boundary region are

$$\dot{q} = \begin{bmatrix} co\{-u_1 - u_4, -u_1 + u_2\} \\ co\{-u_1 + u_4, -u_1 - u_2\} \\ co\{u_2, -u_4\} \end{bmatrix}. \quad (6.14)$$

This situation may seem more hopeless than the one in Equation 6.12. However, as we will see in a moment, this is not the case. In fact, this differential inclusion is strongly stabilizable. Again do a control Lyapunov design using $V = \frac{1}{2}\|(x, y, \theta)\|^2$. The choice of

$$\begin{aligned} u_1 &= \frac{-((-1+d)v_2+d v_4)(th+x-y)+k(th^2+x^2+y^2)}{x+y} \\ u_2 &= -k\theta \\ u_4 &= k\theta \end{aligned} \quad (6.15)$$

makes $\dot{V} = -k\|q\|^2$. Moreover, this choice of $u_2 = -u_4 = -k\theta$ makes Equ-

tion (6.15) reduce to

$$\begin{aligned} u_1 &= \frac{-(-k\theta(th+x-y))+k(th^2+x^2+y^2)}{x+y} \\ u_2 &= -k\theta \\ u_4 &= k\theta \end{aligned} \tag{6.16}$$

which has no dependency on δ . Therefore this differential inclusion is strongly stabilizable.

Figure 6.6, shows the simulation results when this system is controlled using this feedback law. Notice that the translational stability of the location of the moving frame origin is maintained, while the rotational dynamics are stabilized to $\theta = 0$ due to the properties of the proposed feedback law.

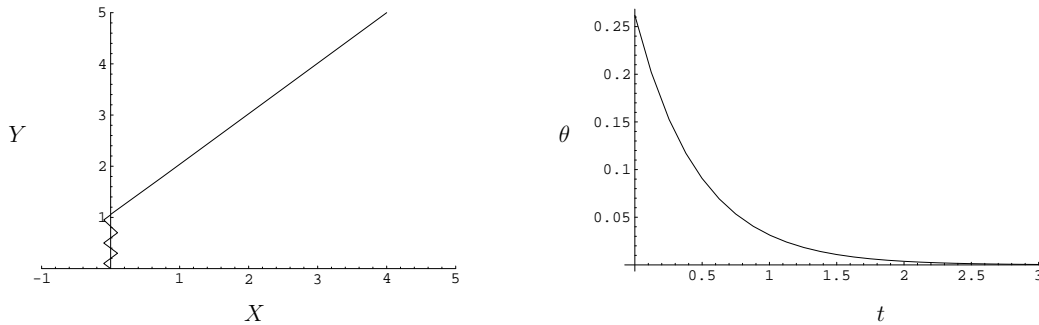


Figure 6.6: X , Y , and θ trajectory of feedback system

6.4 Aside: Fully-Actuated Distributed Manipulation

This section describes in detail how a globally stabilizing *smooth* controller can be constructed. This approach requires that the distributed manipulator be fully actuated - i.e., at each actuator location the actuator can be oriented in any direction, and produce a velocity in that direction of arbitrary magnitude. The former is the important part while the latter can be made more realistic by using saturation functions. This consideration allows us to ensure that *none* of the wheels slip. Others

have considered this problem, particularly in [52, 53, 49]. However, their approach differs radically from the one found here. First, they use components of the open loop theory (using radial fields and rotation fields) to stabilize the system. This involves switching and/or superimposing these fields, leading to significant analytical challenges. The approach here instead takes advantage of the structure of rigid body mechanics and uses techniques from [68] to create control laws.

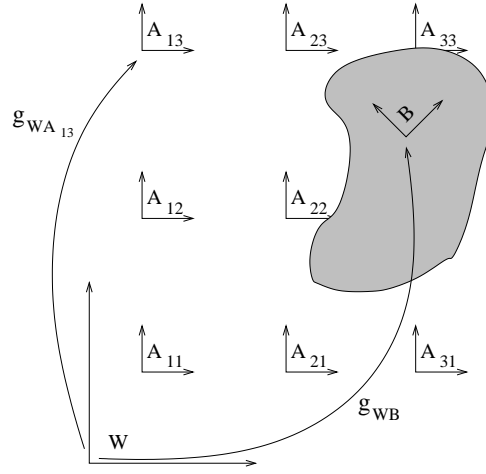


Figure 6.7: Rigid body velocities

Consider Figure 6.7. In this figure we see an abstraction of the 9 cell experimental system. (Details of this system can be found in Appendix A). There is the world frame (denoted by W), the body frame (denoted by B) attached to the moving object, and an actuator frame (denoted by A_{ij} for an actuator located at (x_i, y_j)) which has fixed orientation with respect to the world frame. The rigid body transformation from the world frame to the body frame is denoted by g_{WB} and the rigid body transformation from the world frame to the actuator frame is denoted by $g_{WA_{ij}}$. Recall that the g_{ab} are defined by

$$g_{ab} = \begin{bmatrix} R(\theta) & \begin{bmatrix} x_{ab} \\ y_{ab} \end{bmatrix} \\ 0 & 1 \end{bmatrix}$$

where $R(\theta)$ describes the relative orientation of frame b with respect to frame a , and x_{ab} and y_{ab} are the translations going from frame a to frame b . Notice that for any body frame motion, there is an equivalent motion in the actuator frame. In particular, we know that the relative velocity $V_{body} = (\dot{x}_{body}, \dot{y}_{body}, \dot{\theta}_{body})$ of a point above actuator A_{ij} on the body is:

$$Ad_{g_{W A_{ij}}} V_{body}$$

where in $SE(2)$ the Adjoint operator Ad_g is defined by

$$Ad_g = \begin{bmatrix} R(\theta) & \begin{pmatrix} y_{ab} \\ -x_{ab} \end{pmatrix} \\ 0 & 1 \end{bmatrix}$$

This implies we can take the following approach as a control strategy. Suppose we are given a Lyapunov function on the $SE(2)$, denoted suggestively by $V(\cdot)$. Take a “control Lyapunov” approach to the problem by defining the target dynamics to be

$$\dot{q} = -\frac{\partial V(q)}{\partial q}$$

where V is a Lyapunov function yet to be defined. This system is trivially exponentially stable. The velocity \dot{q} is mapped to the actuators in order to get a feedback law. Choose the Lyapunov function to be $V(x, y, \theta) = k_1 x^2 + k_2 y^2 + k_3 \theta^2$ for $k_i > 0$. The Adjoint operator mapping velocities from W to the A_{ij} for actuator frames oriented the same as the world frame is:

$$Ad_{g_{W A_{ij}}} = \begin{bmatrix} Id & \begin{pmatrix} y_j \\ -x_i \end{pmatrix} \\ 0 & 1 \end{bmatrix}$$

Transforming the velocity into the actuator frame yields $Ad_{g_{W A_{ij}}} \cdot (-\frac{\partial V(q)}{\partial q})$. Sub-

stituting in for $\frac{\partial V(q)}{\partial q}$, the actuator velocities should be

$$\begin{bmatrix} k_3 y_i (\theta - \theta_d) - k_1 (x - x_d) \\ -k_3 x_i (\theta - \theta_d) - k_2 (y - y_d) \\ -k_3 \theta \end{bmatrix}$$

where x_d, y_d, θ_d are the desired values and x, y, θ are the state feedback values. To transform this into wheel velocities and wheel orientations for the particular example found here, calculate the magnitude and direction of the (x, y) velocity. This gives for each actuator:

$$\theta_{ij} = \tan^{-1} \left(\frac{-k_3 x_i (\theta - \theta_d) - k_2 (y - y_d)}{k_3 y_i (\theta - \theta_d) - k_1 (x - x_d)} \right) \quad (6.17)$$

and

$$v_{ij} = \sqrt{(-k_3 x_i (\theta - \theta_d) - k_2 (y - y_d))^2 + (k_3 y_i (\theta - \theta_d) - k_1 (x - x_d))^2} \quad (6.18)$$

where θ_{ij} is the orientation of the (i, j) actuator and v_{ij} is the wheel velocity of that actuator. So, given all the actuator locations, one computes Equations (6.17) and (6.18) for each actuator, and the feedback law is complete. This control law is impressive for two reasons. First, it is easy to implement, and scales nicely with the number of actuators. Second, it works extremely well on the experiment (see Section 6.6). However, it is not a control law one could easily heuristically guess, giving credence to the value of using differential geometric methods in control design. Moreover, this control lends itself very well to control problems beyond point stabilization. In particular, trajectory tracking can be accomplished with little to no modification.

Lastly, note that there is no point in simulating these equations, since the equa-

tions of motion are defined to be

$$\dot{q} = \begin{bmatrix} -k_1x \\ -k_2y \\ -k_3\theta \end{bmatrix}.$$

However, experimental results in Section 6.6 illustrate that this method works extremely well. In fact, it seems to be a natural choice of feedback law in the case of full state feedback and full actuation partially because it is empirically very robust and easy to implement. However, in the case where one does not have full actuation, one must ask how one can achieve global stability since Theorem 6.2 is a local result. Control strategies must be developed that govern gross motions as well as terminal stabilization. To realize this goal, Section 6.5 addresses this issue by extending LaSalle’s invariance principle to the case of differential inclusions. This result is then used to combine the programmable vector field approach with the feedback strategies found in Theorem 6.2.

6.5 Global Stability

Here the philosophies of [79, 12] and the work in previous sections are “blended” using a variation of the classical LaSalle Invariance Principle (see [42]). That is, the programmable vector field approach is used to govern the gross motions of the object far away from the equilibrium point, and local stabilizing feedback law from the previous section in the vicinity of the equilibrium configuration. The intuition behind this result, and its application to the problem at hand, is that if one can move a package from one point a in the plane to another point b (an equilibrium point), and if one has feedback in a neighborhood of point b , the package can be allowed to spin freely along its path to b , and one can wait to control the package’s orientation after it has come sufficiently close to b . Consider Fig. 6.8. If a is in the upper right-hand corner, then it is clear that even with switching between contact states, a package starting at a will eventually arrive in the *feedback region* \mathcal{M} in the

middle of Fig. 6.8. In fact, Theorem 6.2 implies just that, since translation motions (but not rotational motions) are stable under the programmable vector field model, even when discrete contacts are taken into account. From a practical point of view this means that as long as one has no performance goals for the orientation θ outside of \mathcal{M} , one does not need feedback outside of \mathcal{M} .

6.5.1 A LaSalle Result

The goal of this section is to formally prove these intuitive notions. However, because of the multiple model aspect of the governing equations, an extension of LaSalle's theorem must be found. I should note that the basic difference between the classical

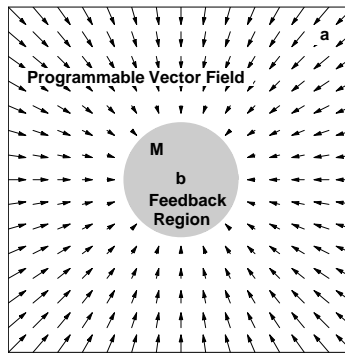


Figure 6.8: A LASALLE invariance theorem

version of the LaSalle theorem and the one found here is that here we must consider systems governed by differential inclusions. In such systems, the idea of a “flow” does not include uniqueness. That is, rather than having a result for *the* unique flow $\phi(t)$, it must be valid for the flow $\phi(t)$, in the sense of the definition in Chapter 5, satisfying $\dot{\phi} \in F(t, x)$. Indeed, this is the underlying theme to much of the study of stability of differential inclusions.

Theorem 6.3. *Let \mathcal{M} be the “feedback region,” a compact simply connected subset of \mathbb{R}^2 . Let $V(x)$ be a Lyapunov function on \mathcal{M} and let $F(x, t)$ be a convex set-valued map. Let $\phi_t(x_0)$ denote a flow that satisfies $\dot{x} \in F(x, t)$, starting from x_0 . Let \mathcal{M} be a positively invariant compact set under all flows $\phi_t(p)$ satisfying the differential inclusion $\dot{x} \in F(x, t)$ (\mathcal{M} is positively invariant if $\dot{V}^*(x) \leq 0$ for all $x \in \mathcal{M}$, where*

\dot{V}^* is defined in Equation (2.11)). Let

$$\begin{aligned} E &= \{x \in \mathcal{M} \mid 0 \in \dot{V}(x)\} \\ N &= \left\{ \bigcup \phi(t, x_0) \mid x_0 \in E \text{ and } \phi(t) \in E \ \forall t > 0 \right\} \end{aligned}$$

Then, for all $x \in \mathcal{M}$, $\phi(t, x) \rightarrow N$ as $t \rightarrow \infty$.

That is, E is the set on which the Lyapunov function is zero, and N is the union of all trajectories that start in E and remain in E for all $t > 0$.

Proof:

This proof is roughly patterned on the proof of LaSalle's Invariance Theorem found in [86]. First recall that the ω -limit point of a differential inclusion (or differential equation) and a point $p \in \mathbb{R}^n$ is defined as a point $q \in \mathbb{R}^n$ where for all solutions $\phi_t(p)$ to the differential inclusion $\dot{x} \in F(x, t) \exists t_1, \dots, t_i$ with $i \uparrow \infty$ such that $\phi(t_i) \rightarrow q$ as $i \uparrow \infty$. The ω -limit set is the collection of such points, and is denoted $\omega(p)$.

It must be shown that $\dot{V} = 0$ on $\omega(p)$ ($\forall p \in \mathcal{M}$). Assume q is an ω -limit point of the differential inclusion, then set $V(q) = c_q$. We will show that V is constant on $\omega(p)$. First we will need the following fact about ω -limit sets.

Lemma 6.4. $\omega(p)$ is invariant under the flow of F .

Proof:

Let $q \in \omega(p)$ and $q_s = \phi_s(q)$. We first must consider if the map $\phi_s(\cdot)$ exists for all s . First, note that since \mathcal{M} is compact, we have existence of $\phi_s(\cdot)$ for $s \in (0, \infty)$. (This is a natural extension of the classical result for ODE's - see [27, pages 77-86]) Now we show that it is true for $s \in (-\infty, 0)$. Using the fact that the limit of any uniformly convergent sequence of solutions to a differential inclusion is also a solution (see Lemma 1 in [27, page 76]), we can choose a sequence $\{t_i\}$ with $t_i \rightarrow \infty$ as $i \uparrow \infty$ such that $\phi_{t_i}(p) \rightarrow q$ as $i \uparrow \infty$

(this is by definition of $\omega(p)$). Then using the fact that $\phi_s(\phi_{t_i}) = \phi_{s+t_i}(a.e.)$ as one takes the limit $i \uparrow \infty$, we get that $\phi_s(q)$ exists for $s \in (-\infty, 0)$.

Now that we have the existence of the map $\phi_s(\cdot)$ for all s , we can choose a sequence t_1, \dots, t_i with $i \uparrow \infty$ such that $\phi_{t_i} \rightarrow q$ as $t \rightarrow \infty$. Then the map $\phi_{t_i+s}(p) = \phi_s(\phi_{t_i}(p))$ converges to q_s as $i \uparrow \infty$. This implies that $q_s \in \omega(p)$ and $\omega(p)$ is therefore invariant. ■

Lemma 6.4 implies that $c_q = \inf\{V(\phi_t(x)) | t \geq 0\}$ because $\dot{V}^* \leq 0$ everywhere in \mathcal{M} . Thus, $V(\phi_t(x)) = c_q$, so $0 \in \dot{V}^*$ on $\omega(p)$. Therefore $\omega(p) \subset E$. Again, because of the above fact that $\omega(p)$ is invariant, $\omega(p) \subset N$. This leads us to the fact that $\phi_t(x) \rightarrow N$ as $t \rightarrow \infty$, the desired result. ■

Now to apply this to the case of distributed manipulation, one must only show that a distributed manipulator will satisfy the requirements and assumptions of Theorem 6.3. This will lead to the following Corollary of Theorem 6.3. Assume the distributed system can be represented by an array of actuators a_{ij} with the coordinate location of (x_i, y_j) and assume that the PDM model solution depends only on the center of mass (equivalently, that the coefficient of friction is uniform). For us, \mathcal{M} will be the feedback region of the distributed manipulator, that is, the area in which one has some sort of state feedback available.

Theorem 6.5. *Given a discrete planar array geometry, an elliptic vector velocity field $\Psi(x, y) : \mathbb{R}^2 \rightarrow \mathbb{R}^4$ outside of $\mathcal{M} = B_\epsilon \times S_1$ for some $\epsilon > 0$, and a locally stabilizing feedback law (such as the one in Theorem 6.2) the solution to the governing equations given by the PDM is globally stable.*

Proof:

Assume that the desired equilibrium point is always in \mathcal{M} . This implies that since $\mathcal{M} \subset SE(2)$, then $\mathcal{M} = B_\epsilon \times S_1$ where B_ϵ is the ϵ -ball in \mathbb{R}^2 , and \mathcal{M} is therefore compact. Therefore the first part of Theorem 6.3 is supplied. \mathcal{M} is positively invariant by Theorem 6.2 using an elliptic vector field. Moreover, for a choice of

$V = \|q\|^2$, E consists solely of the origin. This implies that the origin is stable. In fact, asymptotically stable, because \mathcal{M} is reached in finite time, and once inside \mathcal{M} the origin is asymptotically stable by Theorem 6.2. ■

The following corollary indicates that the induced instability of the programmable vector field approach can be corrected with a local feedback law, and that moreover the performance can be made exponential.

Corollary 6.6. *Given a discrete planar array geometry, an elliptic vector velocity field $\Psi(x, y) : \mathbb{R}^2 \rightarrow \mathbb{R}^4$ outside of $\mathcal{M} = B_\epsilon \times S_1$ for some $\epsilon > 0$, and $\mu_S < \mu_R$, the solution to the governing equations given by the PDM is exponentially stabilizable.*

Proof:

First, note that Theorem 6.2 and Section 6.4 already showed that both the under-actuated and fully actuated systems are locally exponentially stabilizable. It will be shown that exponential stability can be maintained outside of \mathcal{M} . Corollary 6.2 shows that the origin is globally stable. All we need to show is that there is an exponential $k_3\|q\|e^{-st}$ which provides an upper bound on \dot{V}^* . From Section 6.3.3 we know that outside \mathcal{M} the x and y coordinates can be exponentially stabilized, but the θ coordinate is only neutrally stable. Therefore, the maximum value of $\|x, y, \theta\|$ is $d(\partial\mathcal{M}, 0) + \pi^2$, where $d(\cdot, 0)$ is the maximum distance from the origin to the boundary of a set. Setting $k_3 = d(\partial\mathcal{M}, 0) + \pi^2$ it is clear that outside of \mathcal{M} the solutions converge exponentially to \mathcal{M} , and inside \mathcal{M} we have already shown that the origin is exponentially stable. Therefore the origin is globally exponentially stable. ■

6.5.2 Simulations

To illustrate these concepts, this section provides the results of a simulation that model a planar distributed manipulation system with actuators located at (i, j) for $i, j \in \mathbb{N}$. Actuation is provided by unit radius rotating wheels (which rotate

along axes orthogonal to the wheel rims depicted in Fig. 6.9) with constant friction coefficient μ and point contact between the wheel rims and the manipulated object (a box in this case). The feedback region, \mathcal{M} , lies in the interior of a circle of radius 4 (in the length units used by the simulation, see Fig. 6.9), and the only four actuators inside \mathcal{M} are at $(\pm 1, \pm 1)$. Outside of \mathcal{M} , the actuators are located at $(\pm i, \pm j)$ for $i, j \geq 2$. The four actuators inside the circle represent the four node system studied in Section 6.2. The simulated task involves moving a unit mass box from $\{3, 10, \frac{\pi}{4}\}$ to the origin in \mathbb{R}^2 . The final configuration's orientation is stabilized to $\theta = 0$, where θ is measured between the box's long axis and the x axis of \mathbb{R}^2 . The experimental test-bed is used to demonstrate the ideas in this and the previous section. These experiments can be found in Section 6.6.

The simulation was implemented in *Mathematica*, using its *NDSolve* integrator, modified to allow for differential inclusions. Some modification is necessary in order to avoid the numerical difficulties at switching boundaries ($y = x, y = -x, x = 0, y = 0$ for this simulation). However, this is only a concern for switching boundaries which are stable or attracting, because if the trajectory intersects the boundary transversely, standard numerical schemes still work. For this simulation, the switching boundaries (which are stable) are allowed to have the averaged, projected dynamics. This, like the method of introducing hysteresis to simulate a discrete system as a hybrid automaton, produces numerically stable simulations. I should point out, however, that the choice of the averaged solution is only one possible choice satisfying the differential inclusion. That is, if one has a boundary N and vector fields g_{σ_1} on one side of the boundary and g_{σ_2} on the other, the choice of $\dot{q} = \frac{g_{\sigma_1} + g_{\sigma_2}}{2}$ is just one choice satisfying $\dot{q} \in F = \text{co}\{g_{\sigma_1}, g_{\sigma_2}\}$. Again, the difficulty is that solutions of differential inclusions are necessarily nonunique, therefore implying that any simulation represents only one solution ϕ to the differential inclusion $\dot{\phi} \in F$.

Outside \mathcal{M} , the programmable vector field is simply $\{\dot{x}, \dot{y}\} = \{-x, -y\}$. Inside \mathcal{M} the feedback law derived in Section 6.3.4 is used to stabilize the box to the origin. Snapshots of the box's position are shown at integer time units $t = 1, \dots, 12$. The

actual box's boundary is larger than the one shown in the figure. This was done so that the simulation could be visualized more easily.

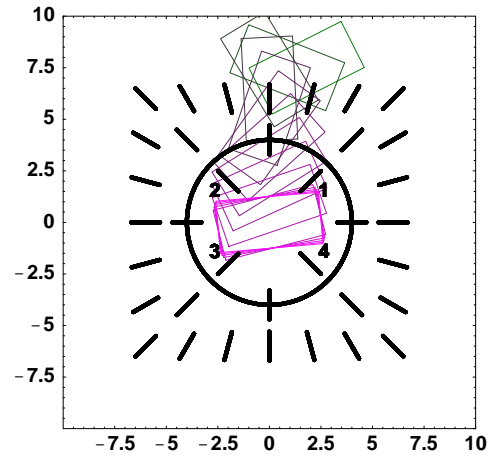


Figure 6.9: A box being transported to $\{x, y, \theta\} = \{0, 0, 0\}$ from $\{3, 10, \frac{\pi}{4}\}$

6.6 Experiments

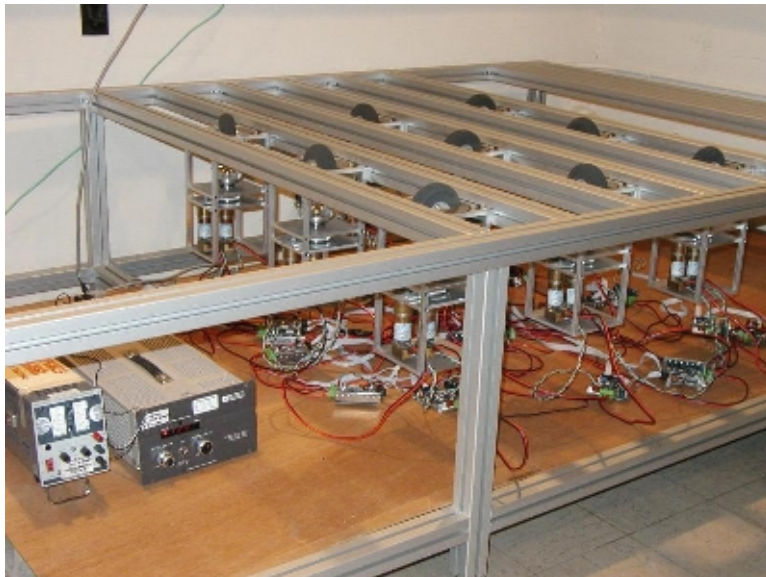


Figure 6.10: Experimental setup

An experimental apparatus has been developed at Caltech for testing some of the theories in this thesis. A photograph can be seen in Figure 6.10. This experiment has 9 steer-able wheels which can be controlled from a centralized computer. The system uses visual feedback through a black and white monochrome camera. For the manipulated object a piece of plexiglass is used. Details of the experimental apparatus can be found in Appendix A. Moreover, movies of these and other experiments can be found at <http://robotics.caltech.edu/>. The plot of each experiment includes the x , y , and θ trajectories as functions of time and a plot of the (x, y) trajectory in the plane. The following experiments all have relatively little output error because are using visual feedback is being used. However, there is approximately a 0.5 cm error in the translational directions and an error of 0.05 rad in the estimated orientation. As the theory only considers point stabilization, these are the only experiments included here. However, I should point out that the experimental setup is appropriate for doing trajectory tracking and other more challenging problems.

6.6.1 Programmable Vector Field

As in the simulations, first an experiment using the open-loop control structure based on programmable vector field (in Böhringer et al [12]) is performed. As expected, the object's orientation is not stable. In fact, small perturbations in the angle of the actuators can cause drift in the orientation. Notice, however, that the x and y coordinates converge to the origin. This experiment used an initial state of approximately $(x_0, y_0, \theta_0) = (0.25 \text{ m}, -0.2 \text{ m}, -1.5 \text{ rad})$, and the final position was approximately $(x_f, y_f, \theta_f) = (0.01 \text{ m}, 0.01 \text{ m}, -1.5 \text{ rad})$.

6.6.2 Local Nonsmooth Feedback

Figure 6.12 shows an experiment using only four cells to emulate the example in Section 6.2. In this experiment, the feedback controller from Section 6.3.4 is used. Since the (x, y) origin is precisely where it is difficult to stabilize an object's orientation, an initial condition with a very high initial θ error value and very small (x, y) error values was given. That is, the goal was to re-orient the object while

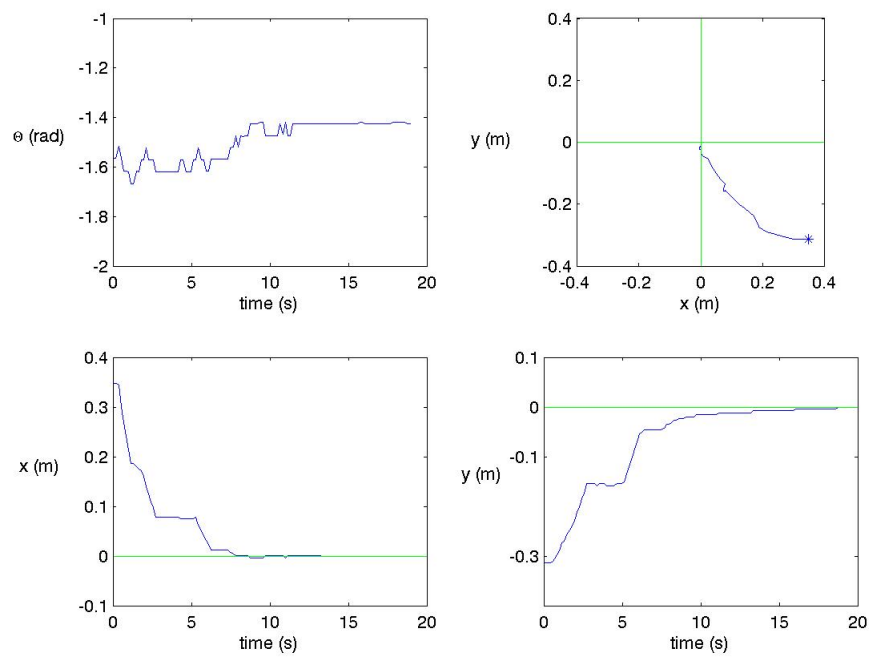


Figure 6.11: Programmable vector field experiment

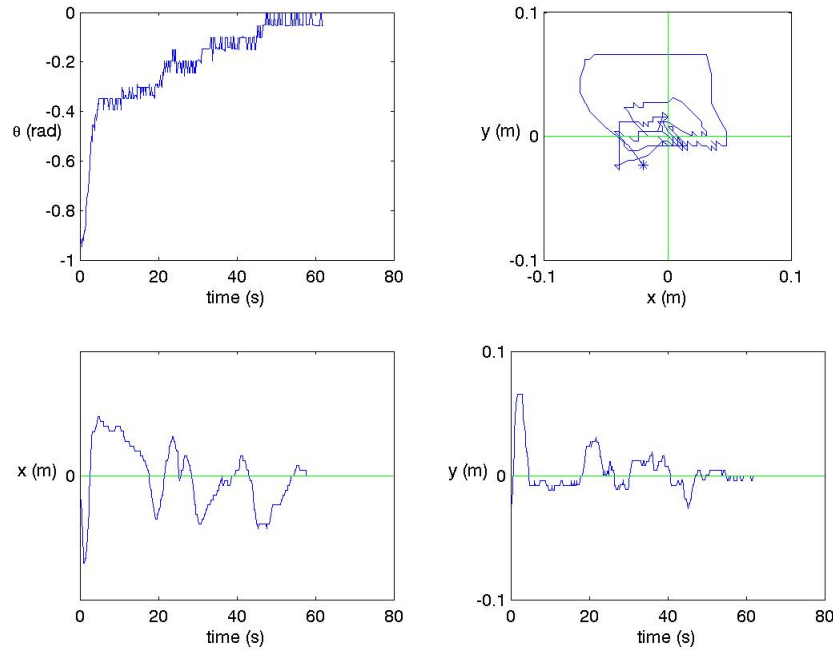


Figure 6.12: Under-actuated feedback control

basically maintaining its position. Notice that the controller design first destabilizes the (x, y) origin because θ is large, and thereby avoids the indeterminacy that occurs at the origin. A complete description of all 16 states of this controller can be found in Appendix A in Tables A.2 and A.3. This experiment used an initial state of approximately $(x_0, y_0, \theta_0) = (-0.15 \text{ m}, -0.2 \text{ m}, -0.9 \text{ rad})$, and the final position was approximately $(x_f, y_f, \theta_f) = (0.01 \text{ m}, 0.01 \text{ m}, 0.05 \text{ rad})$ (the angle cannot currently be resolved any further at this point because of camera pixelization error).

6.6.3 Fully Actuated

Figure 6.13, shows the experimental results when this system is controlled using the feedback law described in the Section 6.4. Notice that the translational stability of the origin is maintained, while the rotational dynamics are stabilized to $\theta = 0$ due to the feedback law. The important point to notice is the smoothness of the the trajectory. This experiment used an initial state of approximately

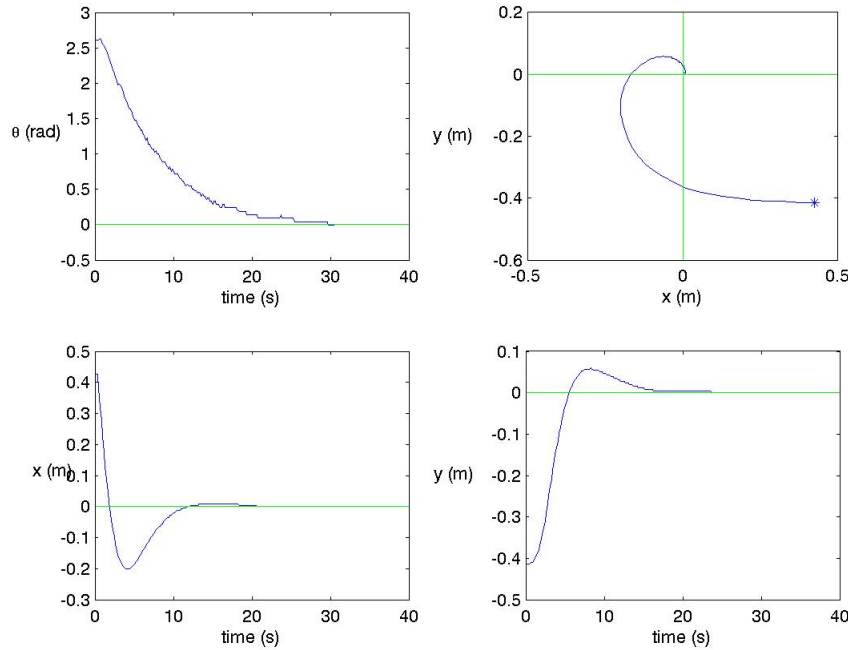


Figure 6.13: Fully-actuated feedback control

$(x_0, y_0, \theta_0) = (0.4 \text{ m}, -0.4 \text{ m}, 2.6 \text{ rad})$, and the final position was approximately $(x_f, y_f, \theta_f) = (0.01 \text{ m}, 0.01 \text{ m}, 0.05 \text{ rad})$. This experiment clearly indicates that when a distributed array is fully actuated, the feedback law in Equation (6.18) will work extremely well. More importantly it is computationally very simple, and the number of computations required to compute it goes up linearly in the number of actuators because it only depends on the current state, not what other actuators are doing.

6.6.4 Global Invariance

Figure 6.14 shows an experiment using the programmable vector field outside a radius of 0.3 m from the origin. Inside this radius it uses the fully actuated feedback. As expected, the performance of this feedback law is quite good. It uses the simplicity and open loop nature of the programmable vector field to drive the state into the circle shown in the figure, and then it uses feedback locally

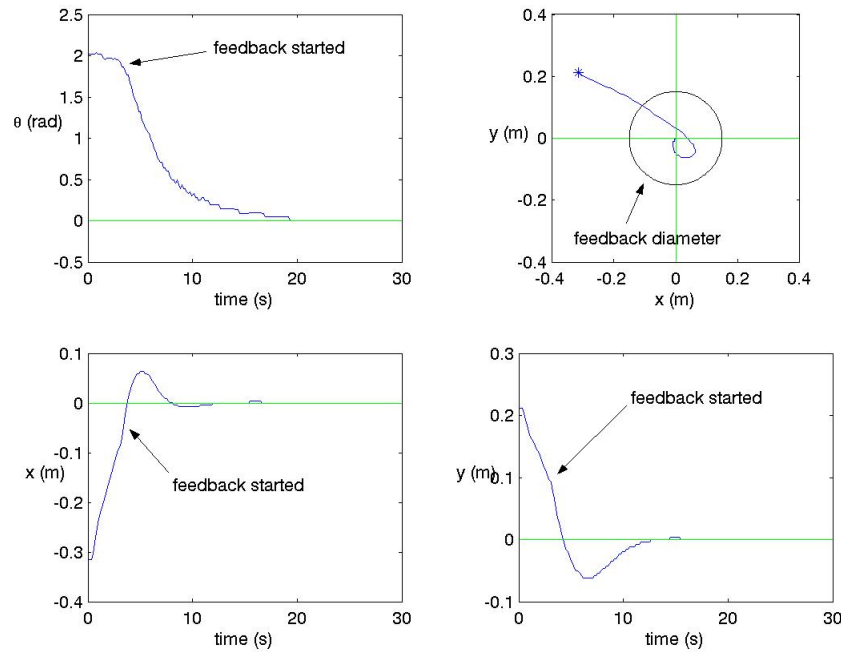


Figure 6.14: Combining the programmable vector field with local feedback

to stabilize the system. This experiment used an initial state of approximately $(x_0, y_0, \theta_0) = (-0.4 \text{ m}, 0.3 \text{ m}, 2.2 \text{ rad})$, and the final position was approximately $(x_f, y_f, \theta_f) = (0.01 \text{ m}, 0.01 \text{ m}, 0.05 \text{ rad})$.

6.7 Methods for Estimating Contact States

Notice in Figure 6.12 that the speed at which the trajectories converge to zero is not terribly good. In order to improve this, here this section adds another technique relevant to distributed manipulation and describe a method of stabilizing distributed systems based on supervised control. After illustrating the challenges in the under-actuated case of distributed manipulation, this section presents a more broadly applicable control strategy which promises to be very useful. First, I will describe some basic results from the theory of switched systems that directly applies to distributed manipulation. The basic idea is that if there is a family (finite or pos-

sibly countably infinite) of plants P_σ indexed by σ , then one can choose controllers appropriate to each P_σ and orchestrate a “switching” between these controllers such that the resulting system is stable. This is traditionally an adaptive control technique where σ is constant but unknown, but here I will show that given certain conditions on the type of “disturbance” switching allowed to occur in an MMDA system, many of the results in [36, 4] still apply. In particular, I will show that for a family of plants P_σ and associated controllers \mathcal{C}_σ the total system is stable even if the environment causes the system to switch between plants, provided it does so sufficiently slowly. Moreover, even given a sufficiently small, nonzero lag time τ_l between the environmental signal determining the plant and the supervisor signal determining the controller, the system remains stable. This section is intended to correct some of the practical problems with the locally exponentially stabilizing controllers found in Section 6.3.2, in that it incorporates estimating the contact state, and therefore eliminates the need for estimating δ in Equation (6.11), it does so at the expense of only allowing certain classes of environmental switching, namely those that are bounded above by a sufficiently slow linear switching function.

6.7.1 Background - Scale-Independent Hysteresis Switching

Consider the figure in Figure 6.15. Here let us first review some of the basic ideas in switching signal control theory. (Most of what is here can be found in a more complete form in Hespanha et al. [38, 37].)

In attempting to place the foundations for a unified framework to treat stabilization of overconstrained systems, first consider some results from adaptive control theory. Ultimately, we will consider a variation on the work done in Hespanha et al. [36, 4]. In that work, linear plants were considered and assumed to belong to some finite or possibly infinite family of plants (the multiple model plant found in the figure). Additionally, the assumption is made that the transfer function describing the input output relationship for a given system belongs to the set

$$\bigcup_{p \in \mathcal{P}} \mathcal{F}(p)$$

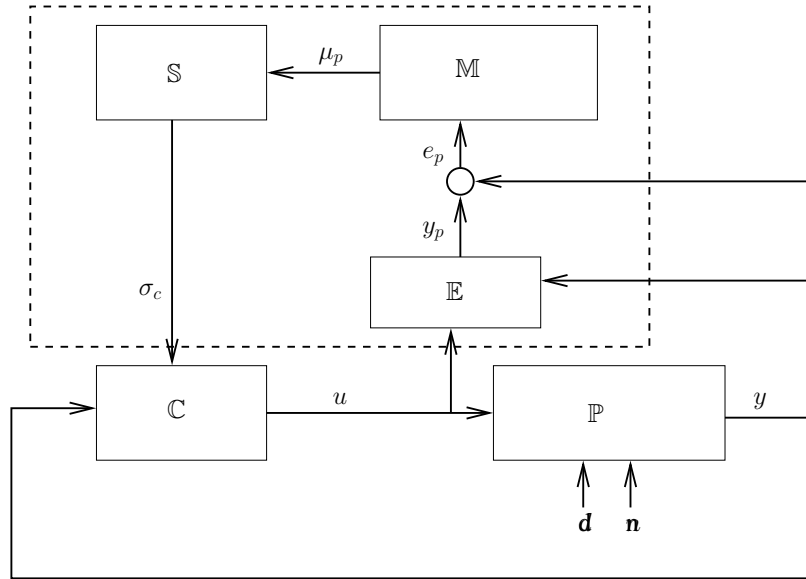


Figure 6.15: A supervisory control system

where p is a parameter taking values in some index (or continuum) set \mathcal{P} and \mathcal{F} is a transfer function. In this setting, each one of these p represents a possible kinematic state of the distributed manipulator (or other group linear mechanical system), and denote by p^* the *actual* process at any given time. Therefore, in the case of a distributed manipulator with 4 actuators, $|\mathcal{P}| = 56$, as pointed out in Section 6.2. Denote the set of possible admissible plants by \mathbb{P} . In the case of linear dynamical systems, associated with each plant P_p coming from \mathbb{P} there is a matrix A_p describing the dynamics and a known stabilizing controller C_q . Denote the set of these controllers by \mathbb{C} . To determine which model in \mathbb{P} most closely “matches” the *actual* process, the input-output relationships for all the plants in \mathbb{P} will need to be estimated. Hence, the need for the *estimator*, denoted by \mathbb{E} , which will generate errors between the predicted output for each plant and the actual output of the process. These errors will then be fed into the *monitoring signal generator*, denoted

by \mathbb{M} , which will provide monotone increasing signals μ_p determined by

$$\begin{aligned}\dot{W} &= -2\lambda W + \begin{bmatrix} x_{\mathbb{E}} \\ y \end{bmatrix} \begin{bmatrix} x_{\mathbb{E}} \\ y \end{bmatrix}^T, & W(0) \geq 0 \\ \mu_p &:= (c_p - 1)W(c_p - 1)^T + \epsilon_\mu, & p \in \mathcal{P}\end{aligned}\tag{6.19}$$

where $W(t)$ is a symmetric non-negative-definite $k \times k$ matrix with $k = \dim(x_{\mathbb{E}}) + 1$, $x_{\mathbb{E}}$ is the state of the estimator, ϵ_μ is a parameter determined by the monitoring signal designer, and c_p is the output one form determining y (from Figure 6.15) from $y = c_p x_{\mathbb{E}}$. The monitoring signal will be fed into the *switching logic*, denoted by \mathbb{S} , which will then determine by means of a *switching signal*, σ_c , which controller to use to control the process. Call the triple $(\mathbb{S}, \mathbb{M}, \mathbb{E})$ the *supervisor*. Depending on the particular construction of the supervisor, many things can be proved about the stability, robustness, and performance of such a system. I will present some of the results key to the analysis in a moment.

Note how the switching signal generator operates. Consider, as in [36], a *scale-independent hysteresis switching logic*. Let h be a positive constant set by the supervisor. The idea is that after initializing $\sigma_c = q$ for $q \in \mathcal{P}$, the system evolves and at every time step \mathbb{S} compares $(1 + h)\mu_p$ to μ_q (where μ_p and μ_q are defined in Equation (6.19)). If there exists a p such that $(1 + h)\mu_p \leq \mu_q$, then the supervisor sets $\sigma_c = p$, otherwise it leaves it unchanged. The advantage to this choice is that it gets rid of chattering. The disadvantage is that in the interim time one can potentially have an unstable plant/controller pair, a subject of the next section.

The following theorem states that if one switches between stable linear systems sufficiently slowly, the resulting dynamics are also stable. For the proof, see [38]. This result is used by showing that for a sufficiently high hysteresis constant, one can always make a supervisor stable. For us, the switching will arise in more than one context, which will be discussed shortly. First, let us define some terms. For a switching signal σ , let $N_\sigma(t, \tau)$ denote the number of discontinuities of σ on the open interval (t, τ) . Moreover, let $S_{ave}[\tau_{AD}, N_0]$ be the set of all switching signals for which $N_\sigma(t, \tau) \leq N_0 + \frac{\tau-t}{\tau_{AD}}$ where N_0 is called the *chatter bound* and τ_{AD} is

called the *average dwell time*.

Theorem 6.7 (Hespanha and Morse [38]). *Given a compact set of $n \times n$ matrices $\mathcal{A} : \{A_p : p \in \mathcal{P}\}$ and a positive constant λ_0 such that $A_p + \lambda_0 I$ is asymptotically stable for each $p \in \mathcal{P}$, then, for any $\lambda \in [0, \lambda_0)$, there is a finite constant τ_{AD}^* such that*

$$\dot{x} = A_{\sigma} x$$

is uniformly exponentially stable over $\mathcal{S}_{ave}[\tau_{AD}, N_0]$ with stability margin λ , for any average dwell time $\tau_{AD} \geq \tau_{AD}^$ and any chatter bound $N_0 > 0$.*

I can now discuss the stability of a supervisor ($\mathbb{S}, \mathbb{M}, \mathbb{E}$) plant (\mathbb{C}, \mathbb{P}) pair. The goal is to extend some of the results found in Hespanha et al. to the case of distributed manipulation where an external signal is causing switching. To do this, one of the more important theorems proved by Hespanha et al will be discussed shortly. Then a variation of this will be proved in the next section. In it, the case of no noise, no disturbances, and no unmodeled dynamics is considered. In this case, the process will asymptotically approach one of the plants in \mathbb{P} . Consequently, not only is the resulting system stable, but switching stops in finite time. Formally:

Theorem 6.8 (Hespanha and Morse [38]). *Suppose that the noise and disturbance signals are zero and there are no unmodeled dynamics, and set $\epsilon_{\mu} = 0$. Then all the signals in the supervisory control system remain bounded for every set of initial conditions such that $W(0) > 0$. Moreover, the switching stops in finite time, and we have $y(t) \rightarrow 0$ as $t \rightarrow \infty$.*

If there are noise and disturbance signals but still no unmodeled dynamics, then the result is still as good as one can hope—that is, in general the output becomes small over time as long as the disturbances remain small, and if the disturbances go to 0 as y goes to 0, then the system is still asymptotically stable. However, if there are additionally unmodeled dynamics, then only a semi-global statement can be made. Details can be found in [38].

There are advantages and disadvantages to this approach to control. One of the major advantages to this approach is the simplicity of control design. That

Advantages	Disadvantages
Only design controllers for individual A_σ	Requires many control designs
Orchestrating the switching is easy	Switching must be “slow” (see Assumption 6.1 on page 125)
Easy to prove things about the algorithms	Difficulties in including continuum
Avoids “chattering”	Difficult to provide balance between environmental switching and controller switching while maintaining stability

Table 6.1: Advantages and disadvantages of supervisory control

is, for each plant one can choose a controller from classical control theory, and then use the analysis found here to show that the orchestrated switching retains the stability properties. Moreover, orchestrating this switching is relatively easy, for it is based on the hysteresis constant in the switching signal generator and the monitoring signal generator only. This approach also avoids “chattering”, a phenomenon often associated with discontinuous control laws (such as those coming from sliding mode control—see [83]). Disadvantages include that the designer must come up with many control designs for the problem (as opposed to the programmable vector field approach which reduces the design problem to the design of *one* desirable field, for instance). Switching must be “slow,” and this method is really intended for a finite number of elements in \mathcal{P} . Fortunately, the PDM gives a finite number of kinematic states. The largest disadvantage is that there is a balance to be found between how fast one switch the control signal to reduce time delay and how slow switching must be in order to maintain stability. This will be discussed shortly.

6.7.2 Applications to Distributed Manipulation

Now return to the case of distributed manipulation. We already know from Section 6.2 that distributed manipulators can be modeled as MMDA systems. Consider each kinematically compatible dynamic state to be one possible plant governing the equations of motion, and that the system “jumps” between these kinematic states based on the configuration, normal forces, and dissipation forces. Based on the ideas in Section 6.7.1, one can hope to be able to design a controller for each kinematic state, and then use the monitoring signal to check which kinematic state the system is in at a given time and use the switching logic to generate the controllers. Notice that there are *two* discrete signals being created in the system. First, there is the environmental signal, σ_e , which is effectively a disturbance, being generated in \mathbb{D} , the environmental signal generator. We have no direct access to this signal, and must therefore estimate it online. The second signal, σ_c , is being generated by \mathbb{S} , the switching logic, in exactly the same way that it was in Section 6.7.1.

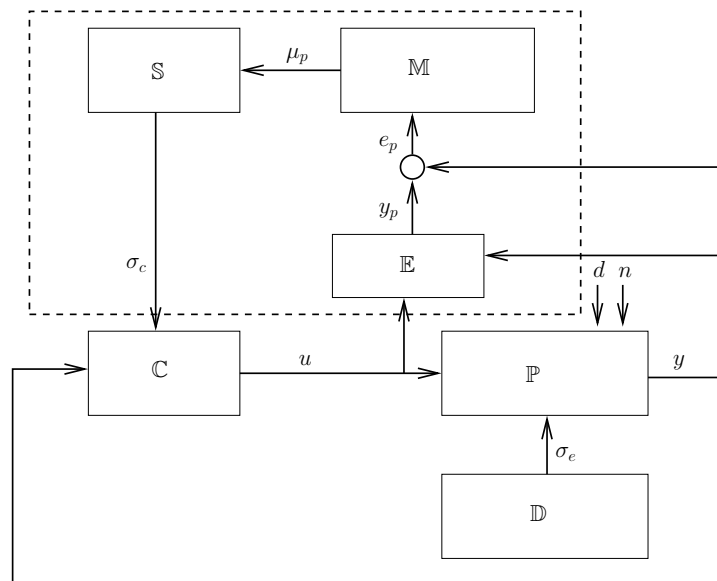


Figure 6.16: A supervisory control system

Consider the block diagram in Fig 6.16. Not surprisingly, it is quite similar to the one found in Fig 6.15. Only here there is an environmental signal generator \mathbb{D}

creating σ_e . Now to give some other notation. Denote by τ_d the upper bound on time-delay (created by the hysteresis in the switching logic). Denote by $N_{\sigma_e}(t_0, t)$ the number of switches σ_e experiences during time $[t_0, t)$.

Now let us move on to the key assumption that will be made during this section, and comment that it is one that can only marginally be defended. Assume, in order to do the subsequent analysis, that the environmental switching is “slow on the average,” in the technical sense found in Assumption 6.1. One could ask: is there any reason to expect an arbitrary environmental signal σ_e to have N_{σ_e} bounded above by an affine linear function? In general, the answer is no, but for quasistatic systems scaling down the inputs leads to a corresponding slowing down in the dynamics. Therefore any dependence that the switching has on the configuration can be made slow. Moreover, friction often creates hysteresis, thereby creating slow switching in a similar fashion to the hysteresis found in the switching logic. Nevertheless, the following theorems present a way of *classifying* systems. That is, for systems with a characteristic average dwell time, one can say that they are or are not stabilizable given certain dwell times and stability margins.

Assumption 6.1. *Assume σ_e switching is “slow on the average,” i.e.,*

$$N_{\sigma_e}(t, \tau) \leq N_0 + \frac{t - \tau}{\tau_{AD}}$$

where $N_0 > 0$ is called the “chatter bound” and τ_{AD} is called the “average dwell time.”

Two more concepts are needed before the proofs of analogs of the theorems found in Section 6.7.1 can be presented. First, the concept of *perfectly adapted* is needed, which means that the supervisor knows what the actual kinematic state is at any given time. Secondly, a measure of how well it does so is needed: in particular, on a given time interval what percentage of time the supervisor signal σ_c matches the environmental signal σ_e is needed.

Definition 6.1. We say a supervisor \mathbb{S} is *perfectly adapted* if

$$\lim_{h \rightarrow 0} \sigma_c(h) = \sigma_e$$

where h is the hysteresis constant.

Definition 6.2. We say that \mathbb{S} is ν *adapted* on an interval (t_i, t_j) if

$$\int_{t_i}^{t_j} |\sigma_c - \sigma_e| dt = \nu$$

Notice that ν adapted is not the same as perfectly adapted even when $\nu = 0$. That is, a supervisor \mathbb{S} can be perfectly adapted with $\nu \neq 0$.

Consider the case when there are no disturbances, no noise, no unmodeled dynamics, and the system is perfectly adapted with $\nu = 0$. Then we have a system that by Assumption 6.1 switches slowly enough to satisfy the requirements in Theorem 6.7. Therefore, if all the individual systems are asymptotically (exponentially) stable, then the resulting system

$$\dot{x} = A_{\sigma_e, \sigma_c} x \tag{6.20}$$

is asymptotically (exponentially) stable. We therefore have:

Corollary 6.9. *Assume there are no disturbances, no noise, and no unmodeled dynamics. Assume Assumption 6.1, \mathbb{S} is perfectly adapted, and $\nu = 0$. Then the resulting switched system is stable.*

Remark 6.5

I should make a remark here on the applicability of this theory to distributed manipulation. In the fully actuated case covered in Section 6.4, we saw that a nonlinear controller was globally stabilizing. Notice, however, that in the previous sections the challenges were all in cases of underactuation. In the case of the example in Section 6.2, this meant that wheels cannot be re-oriented. In these cases, the governing equations for each possible contact state are linear.

Hence, linear switching systems such as those in Equation (6.20) are appropriate models to study. \diamond

Theorem 6.7 can only apply to cases where there is no delay between the environment switching and the controller switching. This is due to the fact that any given controller C_p is only designed for the plant P_p , and there is therefore no guarantee that other combinations (C_p, P_q) for $q \neq p$ will be stable. Therefore, we need to come up with a parallel of Theorem 6.7 to prove that with sufficiently small time delays such a system is stable. It should not be surprising that we are balancing the relationship between the hysteresis constant h and the average dwell time. We need the hysteresis constant to be small, on the one hand, to reduce the time delay and therefore the time the system is in a potentially unstable mode. On the other hand, we need to keep h sufficiently large in order to keep switching from destabilizing the system. Therefore, we are requiring the system (and, most significantly, σ_e) to satisfy a nontrivial condition. However, as discussed earlier, the fact that we are dealing with quasistatic systems will help us to “slow down” the switching to any desirable level. First, we need the following theorem which states that as long as such a balance is achieved between the unstable and stable switching modes, then the resulting system is stable. I should point out that this result is not necessary in [36] because it implicitly assumes that, given (C_i, P_i) controller/plant pairs, each C_i stabilizes *every* P_j . This is because the goal of that work is to obtain better performance through the adaptive control scheme.

Theorem 6.10. *Given two compact set of $n \times n$ matrices $\mathcal{A} : \{A_p : p \in \mathcal{P}\}$, $\mathcal{A}' : \{A'_q : q \in \mathcal{P}\}$ and a positive constant λ_0 such that $A_p - \lambda_0 I$ is asymptotically stable for each $p \in \mathcal{P}$, then, for any $\lambda \in [0, \lambda_0)$, there is a finite constant τ_{AD}^* and a finite constant d_σ such that if t_i and t_{i+1} are switching times for the switching signal σ :*

$$\dot{x} = \begin{cases} A'_q x & \text{on } [t_i, t_i + d_\sigma) \\ A_p x & \text{on } [t_i + d_\sigma, t_{i+1}) \end{cases}$$

is uniformly exponentially stable over $\mathcal{S}_{ave}[\tau_{AD}, N_0]$ with stability margin λ , for any

average dwell time $\tau_{AD} \geq \tau_{AD}^*$ and any chatter bound $0 < N_0 < 1$.

Proof:

Given a family of stable plants indexed by $p \in \mathcal{P}$ with matrix representations A_p with $A_p - \lambda_0 I$ asymptotically stable and another set of plants indexed by $q \in \mathcal{Q}$ with matrix representations A'_q (potentially unstable), we know the following two things:

1. As in [38], we know there exist Lyapunov functions V_p associated with each plant such that

- (a) for all p

$$\dot{V}_p = \frac{\partial V_p}{\partial x} A_p x \leq 2\lambda_0 V_p \quad (6.21)$$

- (b)

$$\alpha(\|x\|) \leq V_p(x) \leq \bar{\alpha}(\|x\|) \quad (6.22)$$

for class \mathcal{K}_∞ functions α and $\bar{\alpha}$. (Denote by \mathcal{K} the set of all continuous function $\alpha : [0, \infty) \rightarrow [0, \infty)$ that are zero at zero, strictly increasing, and continuous, and by \mathcal{K}_∞ the subset of functions in \mathcal{K} that are unbounded.)

- (c) there exists a $\mu \geq 1$ such that

$$V_{p_i}(x) \leq \mu V_{p_j}(x) \quad (6.23)$$

for all $x \in \mathbb{R}$ $p_i, p_j \in \mathcal{P}$

2. Each A'_q , since they are compact (and despite being potentially unstable), has a maximum eigenvalue which will be called $\lambda_{A'_q}$. Moreover, since \mathcal{Q} is a finite set, there is a maximum among these $\lambda_{A'_q}$, call it $\lambda_{A'}$. Therefore, the time derivative of any of the Lyapunov functions V_p $p \in \mathcal{P}$ along trajectories of A'_q satisfy:

$$\dot{V}_p = \frac{\partial V_p}{\partial x} A'_q x \leq 2\lambda_{A'} V_p \quad (6.24)$$

This is the idea that how quickly solutions blow up for linear systems can be bounded. This fact will be important later in this proof. I should also note that the set \mathcal{Q} is substantially larger than the set \mathcal{P} —for us $p \in \mathcal{P}$ represent the matching of plants with their respective stabilizing controllers, whereas $q \in \mathcal{Q}$ represent the matching of plants with *any* other controller.

Fix τ_{AD}^e , the average dwell time for the signal $\sigma_e(t)$. First it will be proven that for a given dwell time, the Lyapunov functions V_p decrease along trajectories of G for d_σ sufficiently small. Then it will be shown that if the switching from σ_e (which determines τ_{AD}^e) is sufficiently slow, the resulting linear switched system is stable. Let

$$\{t_0, t_1, t_2, \dots, t_{N_{\sigma_e}(t_0, T)-1}, T\}$$

be the switching times for σ_e . On an interval $[t_i, t_{i+1})$ let d_σ denote the time delay between σ_e switching and σ_c switching. Then choose d_σ such that

$$0 < d_\sigma < \frac{\lambda - \lambda_0}{\lambda_{A'} - \lambda_0} (t_{i+1} - t_i)$$

this implies that

$$\lambda_0(t_{i+1} - t_i - d_\sigma) + \lambda_{A'} d_\sigma < \lambda(t_{i+1} - t_i)$$

which in turn implies that

$$V_p(x(t_{i+1})) < e^{\lambda(t_{i+1}-t_i)} V_p(x(t_i)) \quad (6.25)$$

Moreover, this is true on any interval, and, because of Assumption 6.1, we can deduce the following: if on the time intervals $[t_{i+1} - t_i)$ we have that

$$t_{i+1} - t_i < \tau_{AD}^e (1 - N_0)$$

then

$$N_0 + \frac{t_{i+1} - t_i}{\tau_{AD}^e} < 1$$

(because $0 < N_0 < 1$) and $N_{\sigma_e}(t, \tau)$ only takes values in the positive integers, so $N_{\sigma_e}(t, \tau) = 0$ on any interval shorter than that. Therefore there is a lower bound on $|t_{i+1} - t_i|$. This implies there exists a lower bound on the d_σ (called d_*) required to ensure that all the V_p decrease along the trajectories described above.

If d_* is the lower bound, then Equation 6.25 holds for all $p \in P$ $q \in Q$.

Following the philosophy laid out in [38], denote by $V_{\sigma(t)}$ the Lyapunov function V_p at time t for $\sigma(t) = p$ and set

$$v(t) := e^{-2\lambda_0 t} V_{\sigma(t)}(x(t))$$

(noticing that $\lambda_0 < 0$ implies that $-2\lambda_0 t$ will be positive). We know that $v(t)$ is piecewise continuous since $\sigma(t)$ is piecewise continuous, and it is in particular strictly continuous on $[t_i, t_{i+1})$. Therefore, we know that

$$\lim_{t \rightarrow t_{i+1}} V_p(x(t)) \leq e^{\lambda(t_{i+1} - t_i)} V_p(x(t_i))$$

from Equation (6.25). This implies

$$\begin{aligned} \lim_{t \rightarrow t_{i+1}} v(t) &= \lim_{t \rightarrow t_{i+1}} e^{-2\lambda_0 t} V_{\sigma(t)}(x(t)) \leq e^{-2\lambda_0 t_i} e^{\lambda(t_{i+1} - t_i)} V_{\sigma(t_i)}(x(t_i)) = v(t_i) \\ &\Rightarrow \lim_{t \rightarrow t_{i+1}} v(t) \leq v(t_i). \end{aligned}$$

By Equation (6.23), we know that

$$v(t_{i+1}) = e^{-2\lambda_0 t_{i+1}} V_{\sigma_e(t_{i+1})} \leq \mu e^{-2\lambda_0 t_{i+1}} V_{\sigma(t_i)}$$

so

$$v(t_{i+1}) \leq \mu v(t_i) \quad \forall i \in \{0, 1, \dots, N_{\sigma_e(t)}(t_0, T) - 1\} \quad (6.26)$$

Iterating the above quantity from $i = 0$ to $i = N_{\sigma_e(t)}(t_0, T) - 1$, we get

$$v(t_{N_{\sigma_e(t)}(t_0, T)}) \leq \mu^{N_{\sigma_e(t)}(t_0, T)} v(t_0).$$

Using a limiting argument like that used to arrive at Equation 6.25, we know that

$$V_{\sigma_e(T)}(x(T)) \leq \mu^{N_{\sigma_e}(t_0, T)} e^{-2\lambda_0(T-t_0)} V_{\sigma_e(t_0)}(x(t_0))$$

therefore

$$V_{\sigma_e(T)}(x(T)) \leq e^{-2\lambda_0(T-t_0) + N_{\sigma_e}(t_0, T) \log \mu} V_{\sigma_e(t_0)}(x(t_0)).$$

Thus, by Equation 6.26 we get

$$\|x(T)\| \leq \alpha \left(e^{-2\lambda_0(T-t_0) + N_{\sigma_e}(t_0, T) \log \mu} \bar{\alpha}(\|x(t_0)\|) \right).$$

To get a stability margin of λ_d , we need to satisfy:

$$-\lambda(T-t_0) + \frac{1}{2} N_{\sigma_e}(t_0, T) \log \mu < k - \lambda_d(T-t_0)$$

for $k > 0$. Choose d_σ such that the stability margin from Equation 6.25 satisfies $\lambda \in (\lambda_d, \lambda_0)$. Now solve for $N_{\sigma_e}(t_0, T)$ and get the following relationship:

$N_{\sigma_e}(t_0, T)$ satisfies $N_0 := \frac{2k}{\log \mu}$ and $\tau_{AD}^e := \frac{\log \mu}{2(\lambda - \lambda_d)}$. Therefore, using λ from above, we get the following relationship between τ_{AD}^e and d_σ .

$$\tau_{AD}^e > \frac{\log \mu}{2 \left(\frac{\lambda_0(t_{i+1}-t_i-d_\sigma) + \lambda_{A'} d_\sigma}{t_{i+1}-t_i} - \lambda_d \right)} \quad (6.27)$$

Therefore, when Equation 6.27 is satisfied, the switching system is exponentially stable. ■

Consider the situation where \mathbb{P} is exactly one of the admissible plants. That is, there are no disturbances, no noise, and no unmodeled dynamics. Allow the environment to switch with average dwell time τ_{AD}^e and show that for a sufficiently “fast” supervisor (\mathbb{S} , \mathbb{E} , \mathbb{M}) the resulting system is still stable. The following result is a corollary to Theorem 6.10

Corollary 6.11. *Assume that there is no noise ($n = 0$), no disturbances ($d = 0$), and no unmodeled dynamics ($\delta = 0$). Assume that \mathbb{S} is perfectly adapted, and is*

moreover ν adapted for some constant ν . Let $\epsilon_\mu = 0$, and let Assumption 6.1 hold. Then all the signals in the supervisory control system remain bounded for every set of initial conditions such that $W(0) > 0$. Moreover, $\exists \tau_{AD}^e$ and $h > 0$ such that $N_{\sigma_c}(t_0, t) \leq k(t - t_0)$ and we have $y(t) \rightarrow 0$ as $t \rightarrow \infty$.

Proof:

First of all, the proof of the boundedness of signals is exactly the same as that found in [38], so I will not reiterate it here. I will only show the stability of the resulting system. Let the times $\{t_1, t_2, \dots, t_m, \dots\}$ be switching times for σ_e coming from \mathbb{D} . Consider the interval $[t_i, t_{i+1})$. We know that $\sigma_e = k$ on $[t_i, t_{i+1})$. Therefore, if \mathbb{S} is perfectly adapted, $\sigma_c = k$ on $[t_h, t_{i+1})$ for some t_h such that $t_i < t_h < t_{i+1}$.

Denote by A_i all combinations of plants P_i with their respective stabilizing controllers C_i . Denote by $A'_{i,j}$ all combinations of plants P_i with any other controller A'_j not designed to stabilize the plant P_i . We know that with h sufficiently small, the maximum lag time d_σ between σ_e switching and σ_c switching can be made arbitrarily small. By Theorem 6.10, then, if τ_{AD}^e is sufficiently large, the resulting switched system is stable. ■

Corollary 6.11 indicates that if the contact states change slowly enough and feedback is fast enough, then the system can be controlled by estimating the contact state online. This means that one does not have to concern oneself with the friction model to establish where switching occurs, as was done previously in Section 6.3.4 in order to derive a control law. Instead, the contact states can change arbitrarily, so long as they do so sufficiently slowly on the average.

6.8 Summary

The work presented in this chapter provides a fundamentally different approach to the control of distributed manipulation. Work done by others, particularly the use of programmable vector fields, has traditionally assumed that all the actuators

in a distributed array were operating at sufficiently high velocities that they were all slipping all the time. This causes significant stress on both the object being manipulated and the actuators themselves. (Indeed, I discovered this when I implemented the programmable vector field on the test-bed and within three runs of the experiment broke nearly half of the cells.) The methods presented assume that if the actuators are moving at sufficiently slow velocities some, but not necessarily all, actuators are always in contact with the moving body. This requires less energy for a given motion and moreover induces smaller forces on the object and actuators. Moreover, the methods presented here succeeded in designing feedback controllers that stabilize an object to a point on a distributed array. It is possible to prove performance bounds on how long it takes an object to reach the goal configuration by showing that exponential convergence can be guaranteed. Most importantly, this was done without explicitly modeling friction, which subsequently leads to relatively simple control laws, improving the likelihood that these control laws can be scaled up to high numbers of actuators.

Chapter 7

Variation 2: Overconstrained Wheeled Vehicles

Doubt is not a pleasant mental state, but certainty is a ridiculous one.

Voltaire

This chapter examines an application of the controllability theory in Chapter 5 to the case of MMDA systems where the individual models are essentially nonlinear. (Essentially nonlinear systems are those that have uncontrollable linearizations.) I will primarily focus on an example for the following reasons. First, the concepts from Chapter 5 are more easily illustrated in this nonlinear setting in the context of an example. Moreover, the example I am going to treat, the Mars Rover, is itself an important engineering application, and this chapter contributes to understanding how to design an appropriate control structure.

7.1 The Rocky 7 Mars Sojourner

Most mobile robots use wheels since they provide one of the simplest means for mobility. Wheels impose nonholonomic constraints on a vehicle's motion, and thus the subject of control and motion planning for nonholonomic wheeled vehicles has been widely pursued [8, 70, 69, 82]. Most wheeled robots operate in relatively benign

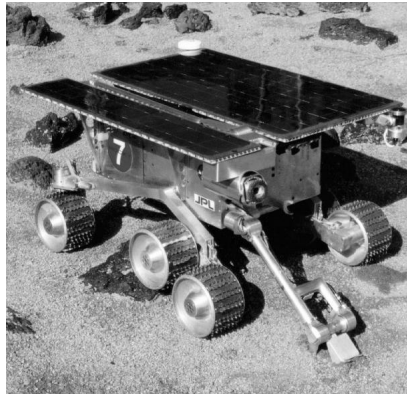


Figure 7.1: Photo of Rocky 7 mars rover prototype

man-made environments. In unstructured terrain where there are many obstacles, legged robots may be used [78], although then one is faced with challenges that are associated with balance. Therefore, the simplicity of a wheeled robot makes it an appealing alternative to legged robots even in somewhat rough terrains.

In order to operate in moderately rough terrains without resorting to the inherent complexity of legged system design, “overconstrained” wheeled vehicle designs have been proposed. The most famous example of such a vehicle is the Sojourner robot deployed during the Mars Pathfinder mission. Figure 7.1 shows the “Rocky 7,” a prototype for future Mars rover vehicles whose suspension and wheel kinematics are basically identical to the Sojourner vehicle. The Rocky 7 employs six wheels, with both front wheels independently steered and all six wheels independently driven, making it an eight-dimensional control space. The rear wheels on each side are coupled through a “bogey” linkage mechanism that helps the vehicle negotiate obstacles that are up to 1.5 times the wheels’ diameter. Below I will show that standard nonholonomic motion planning and control theories cannot be applied to this vehicle. Moreover, its contact state changes based solely on the terrain, which means that the motion planning algorithm must take these contact changes into account.

To understand the key issues that are addressed in this chapter, consider a highly simplified model of the Rocky 7 vehicle (Figure 7.2(b)). In this simplified model

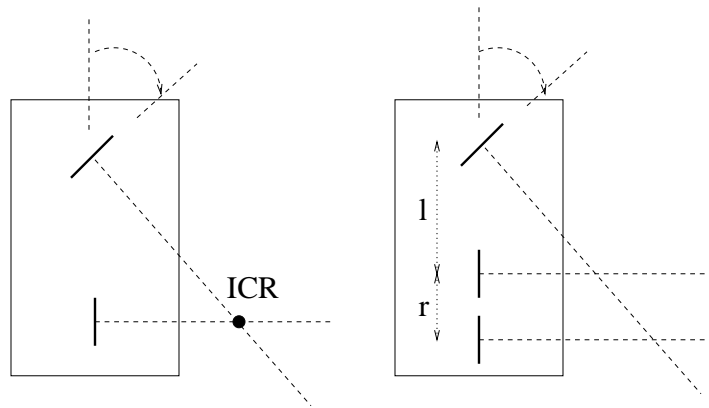


Figure 7.2: (a) kinematic car; (b) simplified Rocky 7.

vehicle, the Simplified Rocky 7, hereafter referred to as SR7, operates on flat terrain. To realize the model of Figure 7.2, each pair of Rocky 7 wheels is conceptually “collapsed” into a single wheel, in a manner similar to that of conventional models of the classical kinematic car (Figure 7.2(a)). Furthermore, assume that only the front wheel is actuated. While highly simplified, this model captures many of the essential features and challenges of overconstrained wheeled vehicles. Obviously, the fact that Rocky 7 operates in non-planar terrain and has additional wheel actuation will pose further complexities.

The motion any every planar body can be characterized at each instant by its Instantaneous Center of Rotation (ICR). In the classical kinematic car model (Figure 7.2(a)), the assumption that the wheels do not slip defines an instantaneous center of rotation at the intersection of the lines that are collinear with the two wheel axes. Note that the presence of an additional wheel leads to an overconstraint and *kinematic constraints alone can not be used to determine the ICR of the SR7 vehicle* in Figure 7.2(b).

Unfortunately, current nonholonomic motion planning techniques implicitly require that the Instantaneous Center of Rotation (ICR) be known so that the state equations are well defined before the geometry can be exploited. On the other hand, intuition would suggest that the control algorithm for parallel parking a car should also work to produce similar motion on a six wheeled vehicle (such as a large truck

or a simplified model of the Rocky 7 as seen in Figure 7.2 with two parallel axes near the back). The dynamics of such a vehicle are overconstrained because both back wheel axes prevent the automobile wheels from sliding sideways, which means there are two parallel constraints. In order to satisfy these constraints, the vehicle must always drive straight forward, and if the front wheel is turned, the vehicle must stay still. Therefore, even in the kinematic case, finding the equations of motion governing the system is a nontrivial task.

One might argue that the “extra” wheels in the systems of Figures 7.1 and 7.2(b) can be practically ignored. After all, 18-wheeled trucks have similar overconstrained geometries. However, we seek dexterous maneuvering of such robots far beyond that which is required for 18-wheelers. For example, future Mars rover mission scenarios call for a manipulator arm with only 2 or 3 degrees of freedom (see Figure 7.1 for an example) to collect rock samples and emplace sensors. Arbitrary displacements of the arm’s end-effector will require the vehicle to make non-trivial local sideways motions so as to compensate for the arm’s kinematic deficiency.

As represented by Mars exploration opportunities, overconstrained vehicles are a potentially important class of mobile robots. It is ultimately desirable to develop theories and algorithms that parallel those for nonholonomic mobile robots. While the mechanics of overconstrained vehicles have previously been considered [84], no systematic control and motion planning theory exists. This chapter makes some first steps in this direction. The question of how to model such systems for the purpose of motion planning is first addressed. The power dissipation model is used to develop the governing equations, whose structure has been shown to be that of an MMDA system. To simplify the problem, the number of contact states is reduced by “matching” as many of the inputs as possible so as to minimize the number of contacts that must slip when the vehicle is moving. This process is similar to the case $u_1 = u_2$ for the planar bicycle in Chapter 3 (see page 28). This is followed by applying the controllability test of Chapter 5 to answer the question of whether the Rocky 7 is controllable or not. Then a variation on this model is considered which allows for two steerable wheels. The implications of

these two examples are somewhat surprising, because controllability depends on how one reduces the input state. I will give details of this in Section 7.3. The key point is that choices made by the control designer can lead to the resulting problem satisfying or not satisfying the sufficient conditions for controllability given in Chapter 5. After addressing controllability, motion primitives for vehicles with changing contact states are considered. These methods are heuristic, but give insight into how the motion planning problem for such vehicles will eventually be solved.

7.2 A Simpler Rocky 7—The Kinematic Car

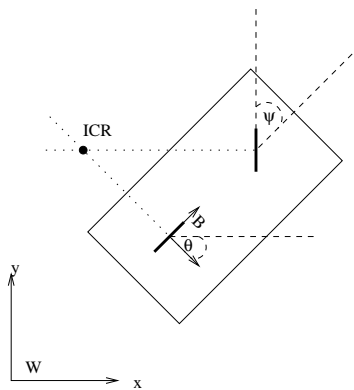


Figure 7.3: The kinematic car

The kinematic car as shown in Figure 7.3 has been studied extensively as an example of a system with nonholonomic constraints. It is used here as an example of how to apply Chow's theorem (Theorem 2.2) to a smooth nonholonomic system. It has been shown by Murray et al. [70] that sinusoidal inputs at integral frequencies will produce Lie bracket motions associated with parallel parking and that global stabilization can be obtained using feedback.

Assume that the car is driven by the front wheels and that the wheels roll without

slipping. The constraints associated with zero wheel slip are

$$\begin{bmatrix} \sin(\theta + \psi) & -\cos(\theta + \psi) & -l \cos(\psi) & 0 & 0 \\ \sin(\theta) & -\cos(\theta) & 0 & 0 & 0 \\ \cos(\theta + \psi) & -\sin(\theta + \psi) & -l \sin(\psi) & R & 0 \end{bmatrix} \begin{bmatrix} \dot{x} \\ \dot{y} \\ \dot{\theta} \\ \dot{\phi} \\ \dot{\psi} \end{bmatrix} = 0.$$

where R is the radius of the front wheels, x and y are the coordinates of the body frame B , θ is the angle between the B frame and the W frame, ϕ is the front wheel angle, and ψ is the angle between the front wheels and the B frame. First find g_1 and g_2 that annihilate these constraints, and then take their Lie brackets to find the distribution

$$g_1 = \begin{bmatrix} \cos(\theta) \\ \sin(\theta) \\ \frac{1}{l} \tan(\psi) \\ 0 \end{bmatrix} \quad g_2 = \begin{bmatrix} 0 \\ 0 \\ 0 \\ 1 \end{bmatrix}$$

$$g_3 = [g_1, g_2] = \begin{bmatrix} 0 \\ 0 \\ -\frac{1}{l \cos^2(\psi)} \\ 0 \end{bmatrix} \quad g_4 = [g_1, g_3] = \begin{bmatrix} -\frac{\sin(\theta)}{l \cos^2(\psi)} \\ \frac{\cos(\theta)}{l \cos^2(\psi)} \\ 0 \\ 0 \end{bmatrix}$$

so $\bar{\Delta} = \text{span}\{g_1, g_2, g_3, g_4\} = \mathbb{R}^4$, which implies that the system is locally controllable. Stabilization for the kinematic car, and other nonholonomic systems like it, has been studied extensively in the literature (see [35, 82]).

7.3 Simplifying the Rocky 7

Here the relatively simple version of the Rocky 7 (found in Fig. 7.4) is considered and the result of Section 5.2.1 is applied. This system is “overconstrained” because not all of nonholonomic kinematic wheel constraints can be simultaneously satis-

fied. Consequently, as stated previously, the vehicle’s motion cannot be determined directly from kinematic constraints (i.e., it’s governing equations of motion cannot be put in the form $\dot{q} = \sum_i g_i(q)u_i$ with the g_i smooth). At least one of the non-powered wheels must be slipping at all times, except when the vehicle moves straight ahead. Hence, classical nonholonomic control theories do not apply to this vehicle. Therefore, the power dissipation methodology from Chapter 3 is used for obtaining equations of motion. Since one or more of the contact points must always be in a slipping state due to the overconstrained geometry, the power dissipation approach states that the vehicle’s motion at any instant is the one that minimizes \mathcal{D} , the power lost to slip. It was already shown that the minimum of the power dissipation function yields governing equations that are MMDA systems (Definition 3.2). See Section 4.1 for some details of such a reduction in the smooth case. See Section 4.2 for details on the reduction in the MMDA case. This basically makes use of the fact that the PDM always chooses states that satisfy $D_{con} = D_{kin}$.

Section 7.3.1 discusses the full input space for a six-wheeled, fully actuated system. As we will see, such a system is quite complex, which leads us to do an input state reduction to two inputs which I discuss in Section 7.3.2. In Section 7.3.3, as an example of how poor choices can be made in such a reduction, I attempt to gain more actuation by allowing both front wheels to be independently steerable and then show that such a system does not satisfy the sufficient conditions for controllability.

7.3.1 Six Wheels and Two Steerable Wheels

First consider a full kinematic model of the Rocky 7 Sojourner robot. It has two steerable front wheels (inputs u_1, u_2) and all six of its wheels are driven (inputs u_3, \dots, u_8). Assume that the vehicle is on flat ground with only variations in the coefficient of friction altering the contact state. Idealize the steering of the wheels as a rotation about a vertical axis. In this model, there are a total of 12 nonholonomic constraints on the system, with each wheel contributing a “no side-ways slip” constraint and a “no rolling” constraint. Clearly, not all of these constraints can

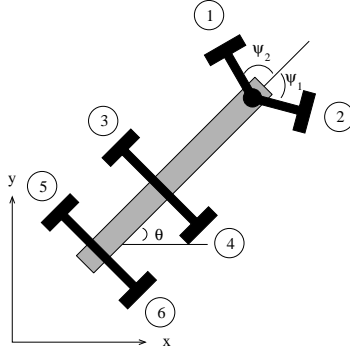


Figure 7.4: 6 driven wheels, 2 steerable wheels

be simultaneously satisfied except in nongeneric cases: 1) the two rear axles are parallel, and therefore can only accommodate forward motion without slipping, and 2) there is no a priori reason to believe that the inputs u_i will produce mutually compatible velocities. Thus, the system is overconstrained. Applying the PDM to this system, one gets

$$\binom{12}{3} = \frac{12!}{9!3!} = 220$$

kinematic states. That is, there are 220 different combinations of slipping motions. This number is daunting both from a complexity and from practical standpoint.

To make progress tractable on the analysis front, reduce the number of inputs by introducing “matching” constraints. Observe that for any choice of u_1 and u_3 one can choose the other u_i inputs to be kinematically compatible with the motion produced by u_1 and u_3 . Therefore, reduce the dimension of the input space by requiring the following to hold:

$$\begin{aligned} u_6 &= Ad_{g_{63}}^{[2]} u_3 \\ u_7 &= Ad_{g_{73}}^{[2]} u_3 \\ u_8 &= Ad_{g_{83}}^{[2]} u_3 \\ u_5 &= Ad_{g_{53}}^{[2]} u_3 \\ u_4 &= Ad_{g_{43}}^{[2]} u_3 \\ u_2 &= Ad_{g_{12}}^{[2]} u_1 \end{aligned} \tag{7.1}$$

where $Ad_{g_{ij}}^{[k]}$ is the k^{th} component of the Adjoint operator of the rigid body trans-

formation going from frame i (associated with the point where the input u_i acts on the system) to frame j . Practically speaking, these constraints force the two front wheels to steer together and the remaining wheels to have a compatible motion. Therefore, u_1 and u_3 completely determine all other control inputs. One can think of this system as being driven by two “virtual” inputs, v_1 and v_2 so as to get an underactuated vehicle. This determines the model in Section 7.3.2. This technique is basically an ad-hoc reduction in the shape space instead of the traditional group space reduction.

7.3.2 Reduction 1

Here I take the reduction as posed in the previous section. In this example, the front wheel is driven u_1 and steered by u_2 , while u_3 and u_4 drive the middle and back wheels respectively. Setting $u_3 = u_1$ and $u_4 = u_1$ produces the desired reduction in Equation (7.1). Additionally, the front wheel is always assumed to be in contact with the ground¹.

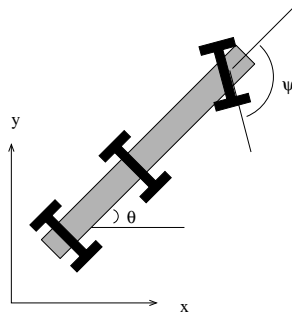


Figure 7.5: 1 driven and steered wheel, 2 passive wheels

Assume that this is driven by the front wheels and that the wheels roll without

¹I realize this is a strong assumption, but without it the Rocky 7 is trivially uncontrollable and not locally stabilizable because it can only move forwards and backwards. Future work will include finding a more global framework so that this condition is not necessary

slipping. The constraints associated with zero wheel slip are

$$\Omega(q)\dot{q} = \begin{bmatrix} \omega_1 \\ \omega_2 \\ \omega_3 \\ \omega_4 \end{bmatrix} \begin{bmatrix} \dot{x} \\ \dot{y} \\ \dot{\theta} \\ \dot{\phi} \\ \dot{\psi} \end{bmatrix} = \begin{bmatrix} \sin(\theta + \psi) & -\cos(\theta + \psi) & -l \cos(\psi) & 0 & 0 \\ \cos(\theta + \psi) & -\sin(\theta + \psi) & -l \sin(\psi) & R & 0 \\ \sin(\theta) & -\cos(\theta) & 0 & 0 & 0 \\ \sin(\theta) & -\cos(\theta) & r & 0 & 0 \end{bmatrix} \begin{bmatrix} \dot{x} \\ \dot{y} \\ \dot{\theta} \\ \dot{\phi} \\ \dot{\psi} \end{bmatrix} = 0.$$

where R is the radius of the front wheels, x and y are the coordinates of the body frame B , θ is the angle between the B frame (located at the center of the middle axle) and the W (world) frame, ϕ is the front wheel angle, and ψ is the angle between the front wheels and the B frame. The constraints $(\omega_1, \omega_2, \omega_3, \omega_4)$ are the front wheel rolling, front wheel side ways slipping, middle wheel side ways slipping, and back wheel side ways slipping. It is easy to check that for $\psi \neq 0$ this only has a solution of $\dot{q} = 0$. Moreover, if $\dot{\phi} \neq 0$ it has no solution when $\psi \neq 0$.

Using the power dissipation approach, we know that the minimum of \mathcal{D} must occur when either the middle or back wheel slips (because the front wheel is assumed to always be in contact with the ground). This means that the constraint associated with either ω_3 or ω_4 must not be satisfied. This leaves us with two possible sets of constraints:

$$\Omega_1 \dot{q} = \begin{bmatrix} \omega_1 \\ \omega_2 \\ \omega_3 \end{bmatrix} \begin{bmatrix} \dot{x} \\ \dot{y} \\ \dot{\theta} \\ \dot{\phi} \\ \dot{\psi} \end{bmatrix} = 0 \quad \text{and} \quad \Omega_2 \dot{q} = \begin{bmatrix} \omega_1 \\ \omega_2 \\ \omega_4 \end{bmatrix} \begin{bmatrix} \dot{x} \\ \dot{y} \\ \dot{\theta} \\ \dot{\phi} \\ \dot{\psi} \end{bmatrix} = 0$$

The \dot{q} that annihilate these constraints are the possible governing equations in both cases. If the vehicle configuration is $q = [x, y, \theta, \psi]^T$ and the controls u_1 and u_2 are associated with the drive and steering velocities respectively, the vehicle's

governing equations of motion are

$$\dot{q} = g_{\sigma_1}(q)u_1 + g_3(q)u_2 \quad \sigma_1 : (q, t) \rightarrow \{a, b\}$$

$$g_a = \begin{bmatrix} \cos(\psi) \cos(\theta) \\ \cos(\psi) \sin(\theta) \\ \frac{1}{l} \sin(\psi) \\ 0 \end{bmatrix} \quad g_b = \begin{bmatrix} \cos(\theta) \cos(\psi) - \frac{r \sin(\theta) \sin(\psi)}{l+r} \\ \cos(\psi) \sin(\theta) + \frac{r \cos(\theta) \sin(\psi)}{l+r} \\ \frac{1}{l+r} \sin(\psi) \\ 0 \end{bmatrix} \quad g_3 = \begin{bmatrix} 0 \\ 0 \\ 0 \\ 1 \end{bmatrix}$$

The function which determines the switching boundaries is

$$\Psi(q) = \left(\frac{F_1 \mu_1}{F_2 \mu_2} \right)^2 \left(\frac{l-r}{r} \right)^2 - 1$$

where F_i are the normal forces above the middle axis and back axis, and the μ_i are the coefficients of friction at the two rear wheel contacts. When $\Psi(q) > 0$, $\sigma_1 = a$; when $\Psi(q) < 0$, $\sigma_1 = b$. Therefore switching is determined by $q \in Q$ such that $\Psi(q) = 0$. Intuitively, variations in wheel-ground friction and vehicle weight distribution can cause alternations in the choice of the slipping wheel.

Controllability is determined by the rank of the distribution:

$$\Delta = \{g_3, g_{\sigma_1}, [g_3, g_{\sigma_1}], [[g_3, g_{\sigma_1}], g_{\sigma_1}]\} \quad (7.2)$$

Computing accordingly, we get $[g_{\sigma_1}, g_3] =$

$$co \left\{ \begin{bmatrix} \cos(\theta) \sin(\psi) \\ \sin(\theta) \sin(\psi) \\ -\frac{\cos(\psi)}{l} \\ 0 \end{bmatrix}, \begin{bmatrix} \frac{r \cos(\psi) \sin(\theta)}{l+r} + \cos(\theta) \sin(\psi) \\ -\frac{r \cos(\theta) \cos(\psi)}{l+r} + \sin(\theta) \sin(\psi) \\ -\left(\frac{\cos(\psi)}{l+r}\right) \\ 0 \end{bmatrix} \right\}$$

and

$$[g_{\sigma_1}, [g_{\sigma_1}, g_3]] = co \left\{ \begin{bmatrix} \frac{-1}{l} \sin(\theta) \\ \frac{1}{l} \cos(\theta) \\ 0 \\ 0 \end{bmatrix}, \begin{bmatrix} \frac{-1}{l+r} \sin(\theta) \\ \frac{1}{l+r} \cos(\theta) \\ 0 \\ 0 \end{bmatrix} \right\}$$

Now, using the algebraic equivalent for $co\{\cdot, \cdot\}$, we can evaluate the determinant of Equation 7.2:

$$\begin{aligned} & \det [g_3, co\{g_{1a}, g_{1b}\}, [g_3, co\{g_{1a}, g_{1b}\}], [[g_3, co\{g_{1a}, g_{1b}\}], co\{g_{1a}, g_{1b}\}]] \\ &= \det [g_3, co\{g_{1a}, g_{1b}\}, co\{[g_3, g_{1a}], [g_3, g_{1b}]\}, \\ & \quad co\{[g_{1a}, [g_{1a}, g_3]], [g_{1b}, [g_{1b}, g_3]]\}] \\ &= \det [g_3, \delta_1 g_{1a} + (1 - \delta_1) g_{1b}, \delta_2 [g_3, g_{1a}] + (1 - \delta_2) [g_3, g_{1b}], \\ & \quad \delta_3 [g_{1a}, [g_{1a}, g_3]] + (1 - \delta_3) [g_{1b}, [g_{1b}, g_3]]] \end{aligned}$$

where $\delta_i \in [0, 1]$ for $i = 1, 2, 3$. The determinant is

$$\frac{(l + r\delta_3)(2l + r(\delta_1 + \delta_2) + r(\delta_2 - \delta_1) \cos(2\psi))}{2l^2(l + r)^2}$$

which equals 0 only if $\delta_3 < 0$ and these values are not admissible. Hence, the vehicle is always STLC, as expected. Physically, this result implies that the vehicle remains locally controllable even as the status of slipping wheel alters unexpectedly.

7.3.3 Reduction 2

It is clearly necessary that all of the individual models in an MMDA system be controllable in order for the condition in Theorem 5.2 to be satisfied. Now one may ask if it is sufficient that all of the individual models in an MMDA system be controllable. If it is, then one need only concern oneself with the analysis of the individual smooth models. The answer to this question, perhaps surprisingly, is no. This example illustrates the reason.

Consider a vehicle with the same two front steerable wheels as the Rocky 7, but with only one back wheel for simplicity (Fig. 7.6). This choice, though seemingly reasonable, will cause the resulting system to fail the controllability test. For sim-

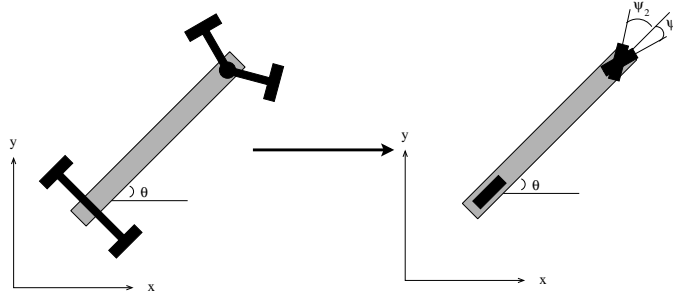


Figure 7.6: 2 driven and steered wheels, 1 passive wheel

licity assume that the two front wheels are collapsed down along their respective axes so that they both are connected to the body at the same point (see Figure 7.6). We will see that this vehicle is *only* controllable when $\psi_1 = \psi_2$, or when it is indistinguishable from a kinematic car. An analysis of this system using the PDM shows that there are two distinct kinematic states for this vehicle (i.e., two different permutations of wheel slip). In each case the governing equations of motion are equivalent to the equations of motion for a kinematic car, i.e.,

$$\dot{q} = g_{\sigma_1}(q)u_1 + g_3(q)u_2 \quad \sigma_1 : (q, t) \rightarrow \{a, b\}$$

where

$$g_a = \begin{bmatrix} \cos \psi_1 \cos \theta \\ \cos \psi_1 \sin \theta \\ \sin \psi_1 \\ 0 \end{bmatrix} \quad g_b = \begin{bmatrix} \cos \psi_2 \cos \theta \\ \cos \psi_2 \sin \theta \\ \sin \psi_2 \\ 0 \end{bmatrix} \quad g_3 = \begin{bmatrix} 0 \\ 0 \\ 0 \\ 1 \end{bmatrix}$$

Restricting attention to brackets which are nonzero for the individual models, controllability is determined by the rank of:

$$(g_3, g_{\sigma_1}, [g_3, g_{\sigma_1}], [[g_3, g_{\sigma_1}], g_{\sigma_1}])$$

We then have

$$[g_3, g_{\sigma_1}] = co \left\{ \begin{array}{l} \left[\begin{array}{c} \cos \psi_1 \sin \theta \\ \cos \psi_1 \cos \theta \\ -\cos \psi_1 \\ 0 \end{array} \right], \left[\begin{array}{c} \cos \psi_2 \sin \theta \\ \cos \psi_2 \cos \theta \\ -\cos \psi_2 \\ 0 \end{array} \right] \end{array} \right\}$$

and

$$[[g_3, g_{\sigma_1}], g_{\sigma_1}] = \begin{bmatrix} -\sin \theta \\ \cos \theta \\ 0 \\ 0 \end{bmatrix}$$

Evaluating the determinant as before, let us now determine if there exists a selection of the differential inclusion such that this is not full rank, i.e., does there exist δ_1, δ_2 such that

$$\det [g_3, \delta_1 g_{1a} + (1 - \delta_1)g_{1b}, \delta_2 [g_3, g_{1a}] + (1 - \delta_2)[g_3, g_{1b}], \\ \delta_3 [g_{1a}, [g_{1a}, g_3]] + (1 - \delta_3)[g_{1b}, [g_{1b}, g_3]]] = 0$$

Computing, the above determinant equals

$$\delta_1 + \delta_2 - 2\delta_1\delta_2 - 1 + (\delta_1 + \delta_2 - 2\delta_1\delta_2) \cos(\psi_1 - \psi_2).$$

Now, if

$$\chi(\delta_1, \delta_2) \stackrel{def}{=} \frac{1}{\delta_1 + \delta_2 - 2\delta_1\delta_2} - 1$$

the controllability condition depends on whether there exists δ_i such that $\chi(\delta_1, \delta_2) \in [-1, 1]$. Clearly there do exist such δ_i ; just choose $\delta_1 = 0$ and $\delta_2 = 1$ giving $\chi = 0$. However, one may ask if making $|\psi_1 - \psi_2|$ sufficiently small makes the system controllable. Doing so changes the requirement to $\chi \in [-\varepsilon, \varepsilon]$, which again has a solution for the same choice of δ_i . Therefore, controllability of this vehicle design sensitive to switching. That is, although on the one hand it is desirable to get extra actuation by controlling ψ_1 and ψ_2 independently, on the other hand it is

desirable to have a model that can be shown to be controllable.

Now, what if the selections of $[g_{\sigma_1}, g_3]$ and $[[g_{\sigma_1}, g_3], g_3]$ are coupled in some way? Consider the situation where, if we again parameterize the selections of $[g_{\sigma_1}, g_3]$ by $\delta_1 \in [0, 1]$ and the selections of $[[g_{\sigma_1}, g_3], g_3]$ by $\delta_2 \in [0, 1]$, we have $\delta_2 = h(\delta_1)$. For example, take h to be the identity. Then

$$\chi(\delta_1, \delta_2) = \frac{1}{2\delta_1 - 2\delta_1^2} - 1$$

which only has a solution in $[-1, 1]$ for $\delta_1 = \frac{1}{2}$. Therefore, if we allow a slightly weaker notion of controllability by only requiring that the system be controllable almost always, this system is controllable. However, given the choice between a weaker notion of controllability and the standard one, it is preferable to show the standard one.

7.4 Motion Primitives

This section describes some simple motion planning techniques for overconstrained wheeled vehicles. As stated, classical controllability results and nonholonomic motion planning ideas can easily be extended to the case of controlled switching. The case of uncontrolled switching is more complicated, as seen in the simulation of Fig. 7.7. In this simulation, the SR7 drives with constant steering wheel speed and angle. With no switching, the vehicle's center would describe a circular motion of constant radius. However, in this simulation the vehicle passes over terrain regions with different friction coefficients, resulting in switching in the dynamics. The path's noncircular geometry clearly indicates that switching can introduce considerable error. This simulation shows why standard nonholonomic techniques are not directly applicable. This unpredictable switching behavior may make the open loop motion planning problem seem insurmountable, and suggests that feedback is an appropriate strategy in this case. However, some heuristic techniques are available.

In nonholonomic systems, motion in the linearly uncontrollable directions is created by coupled periodic inputs (or "Lie bracket motions"). This knowledge

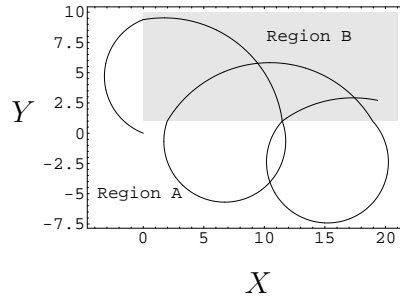


Figure 7.7: SR7 with constant wheel angle and speed

guided the extension of the classical Lie bracket to the switched case. With this extension, it appears true that many (though probably not all) of the open loop local motion planning concepts from the classical nonholonomic literature can be adapted to the overconstrained situation.

7.4.1 Aside: Controlled Switching

Here let us make a momentary aside to the underactuated vehicle discussed above in Section 5.1. The fixed wheel kinematic car (FWKC) discussed is controllable when switching is taken into account. Hence, arbitrary motions will generally require controlling the switching σ . Motion in the linearly uncontrollable direction is obtained by creating a flow along g_1 , inducing a switch (by “waving” the manipulator arm) so that the system continues to flow along g_2 , inducing another switch to flow along $-g_1$ (by arm motion and wheel rotation reversal), and switching again to induce flow along $-g_2$. These actions are taken over time intervals of $t = 0.25$. At time $t = 1$, we see in Fig. 7.8 that net displacement has been produced.

In general, one can adapt the approach suggested in [70] to this situation, with discrete switches replacing the role of some sinusoidal inputs. In summary, the algorithm is: a) turning until the desired value of θ is achieved b) move forward until $\langle (x_d - x), [\cos(\theta), \sin(\theta)] \rangle = 0$ (i.e., the car is parallel with the desired goal), c) compute the time needed for the car to pass through the desired point, d) stop

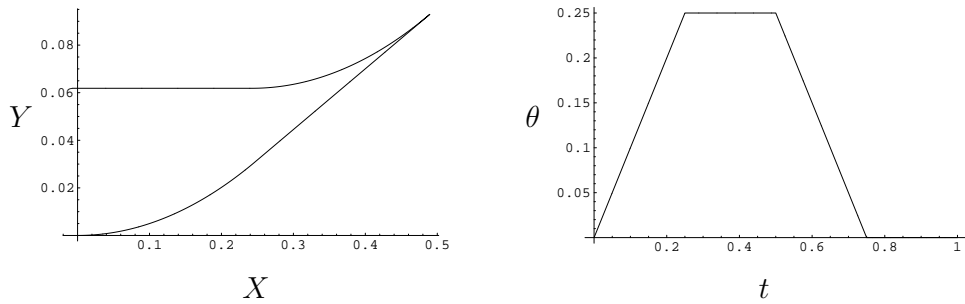


Figure 7.8: (a) X and Y variables; (b) θ variables of the FWKC bracket-like motion.

at the desired goal point (θ will have already returned to its original value). This simple algorithm was used to drive the FWKC from the origin to the point (2,2) in Fig. 7.9.

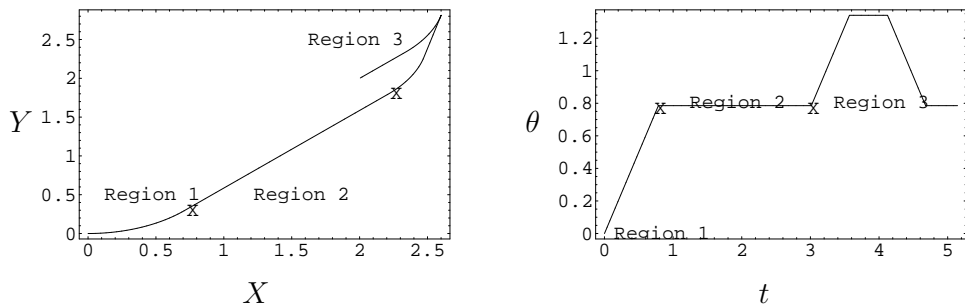


Figure 7.9: a) X and Y variables of Simulation 1 b) θ variable of Simulation 1

7.4.2 Uncontrolled Switching

In the uncontrolled switching case, the primary difficulty shifts from control of an otherwise underactuated mechanism to the errors associated with switching between models of the MMDA system. The algorithmic approach proposed is similar to the controlled switching case. However, it is still rather ad hoc. While we wish to use the Lie bracket motion to arrive at the final state, the actual Lie bracket is $[f, \gamma] = \delta[f, g_1] + (1 - \delta)[f, g_2]$, where δ is unknown. However, there is a natural

choice of δ . If we know something about the environment's properties, δ is chosen to be the percentage of time that the vehicle is expected to be in state 1: $\delta = 0.5$ corresponds to equal possibility of being in one state or another. I heuristically chose to base the Lie bracket motion on the vector field $g = \delta[f, g_1] + (1 - \delta)[f, g_2]$. Consider Figure 7.10. This Lie bracket motion was produced using sinusoids at integrally related frequencies based on the assumption that $\delta = .5$. Error enters, particularly in the orientation, due to the discontinuities in contact state. This result illustrates that for motion planning purposes, one must use some form of feedback.

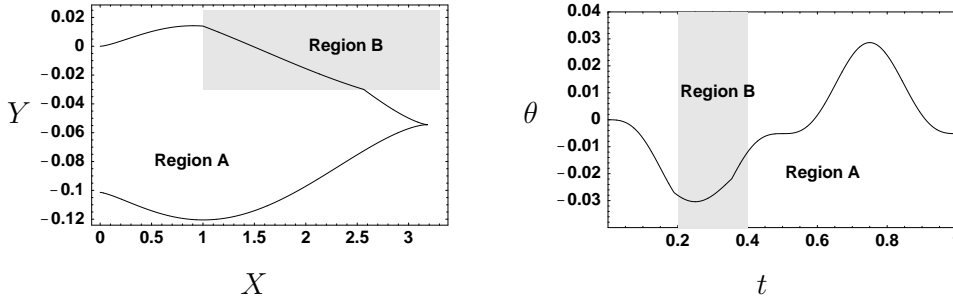


Figure 7.10: a) X and Y coordinates of a Lie Bracket Motion of Rocky 7 b) θ motion

Traditionally, the use of sinusoids has arisen as the solution to the optimal control problem of how to reposition a nonholonomic system like the kinematic car in its Lie bracket direction while minimizing $J = \int_0^T \|u\|^2 dt$ [17, 68, 76]. Likewise, one can introduce an optimal control framework here where the cost function is chosen to minimize a weighted cost function of power and of error due to switching. To achieve this result, choose

$$J = \int_0^T a_1 \|u\|^2 + a_2 \|\varphi\|^2 dt \quad (7.3)$$

for $a_i > 0$ instead of $J = \int_0^T \|u\|^2 dt$ as in Refs. [17, 68, 76]. Here φ is the angle between g_1 and g_2 defined by the Euclidian metric on TQ (although certainly other

choices of metric may be made on TQ). I.e.,

$$\varphi = \cos^{-1} \left(\frac{\langle g_1, g_2 \rangle}{\|g_1\|^2 \|g_2\|^2} \right) \quad (7.4)$$

Equation 7.4 $\varphi \approx \psi$ to third order in q , making

$$J = \int_0^T a_1 \|u\|^2 + a_2 \|\psi\|^2 dt \quad (7.5)$$

a natural choice of cost function. Interestingly, this cost function is the same as in Refs. [68, 76], except that $\|\cdot\|$ is now relative to the choice of metric. Intuitively, this choice of cost function encapsulates the fact that the more one is willing to keep the wheels pointing close to straight forward (and therefore is willing to sacrifice speed in the Lie bracket direction) the more one can reduce error. In the simulation in Fig. 7.11, this method comes very close to the goal state of $[4, 4, \frac{\pi}{4}]^T$ in only two iterations.

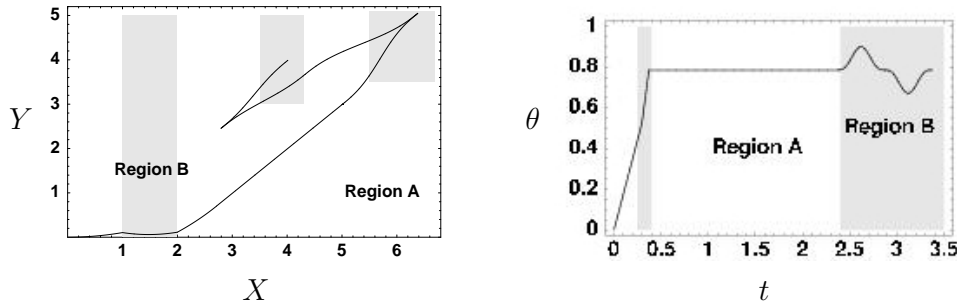


Figure 7.11: a) X and Y Coordinates for Simulation 2 b) θ for Simulation 2

However, I should point out that this method is not formal at all. I do not assert that this algorithm is necessarily any better than any other algorithm, only that it allows us use some of the classical ideas in motion planning for smooth nonholonomic system in approaching the problem for vehicles such as the Mars rover. In the future, work on stabilization for the vehicles will include extensions not only of the time-varying feedback laws derived in [82] but will additionally include extensions of the

work by [4, 35, 36] to the case of this class of nonlinear systems.

7.5 Summary

Understanding the issue of controllability is often a first step toward understanding how to control a class of nonlinear systems. Chapter 5 developed controllability results for MMDA systems that can be viewed as extensions of Chow's classical controllability theorem. This chapter examined in detail the controllability of a simple model of the Rocky 7 Mars Sojourner. Variations of this model studied in Section 7.3.3 illustrate that controllability of the individual models that make up an MMDA system is *not* sufficient to guarantee controllability of the overall MMDA system. Although preliminary methods for open loop motion planning of such systems can be found in Section 7.4, the potential importance of the vehicles discussed in Section 7.3 in future planetary exploration missions indicates the need for more in-depth analysis of stabilization. Future work will investigate algorithms for stabilizing the multiple model systems of Definition 3.2. In particular, I will use the formalism of *GDQs* developed in Sussmann [81] to adapt the supervisor-based algorithms discussed in Section 6.7 to this nonlinear setting.

Chapter 8

Finale: Conclusions

I can take any amount of criticism, so long as it is unqualified praise.

Noel P. Coward

In this thesis I have presented a number of results relevant to the analysis of driftless overconstrained mechanical systems. At one extreme of the theory/experiment spectrum, extremely general conditions for controllability of a driftless overconstrained multi model system were produced. At the other extreme, systematic control strategies were developed for distributed manipulation that when applied to a distributed manipulation test-bed produced concrete control laws which worked well. Somewhere in the middle of this spectrum contributions to the foundations of stability analysis for nonlinear overconstrained systems were made. These contributions extend classical results from the control literature, including notions of controllability and kinematic reducibility, control Lyapunov functions, and methods for steering nonholonomic systems to this new domain. The notion of generalized differentials in particular plays a large role throughout this thesis. These results are described in Section 8.1. Many of these results raise as many questions as they answer, which leads to a list of future research in Section 8.2.

8.1 Summary

In Chapter 3 I reviewed the power dissipation methodology for finding tractable governing equations for overconstrained mechanical systems. Formal properties of these equations were then developed, and they were shown to be generically discontinuous or multi model. The advantage of the PDM is that it yields relatively tractable equations, whereby techniques from nonsmooth analysis can be used to understand stability issues.

In Chapters 4 and 5 I treated some of the more formal characteristics of multiple model driftless affine systems. These types of systems result from the power dissipation methodology. First conditions for kinematic reducibility of overconstrained systems were developed: individual models (equivalently, contact state kinematics) must be kinematically reducible. However, this does not hold true for controllability. That is, it is not true that a multiple model driftless affine system, which has all of its individual models controllable, will necessarily be controllable. I did, however, prove a sufficient condition for such controllability to hold.

Regarding distributed manipulation, it was found in Chapter 6, again using the power dissipation method, that the rotational dynamics of systems governed by programmable vector field controllers are not asymptotically stable. Moreover, a feedback law that stabilizes the system was found. This feedback law is smooth if the distributed system is fully actuated, and nonsmooth if it is not. I was additionally able to prove that distributed manipulators can be globally exponentially stabilized to a point by “patching” together open loop programmable vector field strategies and the closed loop strategies. Hence, there is no reason to have to incorporate the costly addition of feedback throughout the path followed by the object. Moreover, the power dissipation method gives significant insight into evaluation of design philosophies, in this case leading us to believe that contact designs with $\mu_S < \mu_R$ are superior to those with $\mu_S > \mu_R$. These results were additionally verified on an experimental test-bed.

Understanding the issue of controllability is often a first step toward understanding how to control a class of nonlinear systems. In Chapter 7, I showed that standard

nonholonomic motion planning and control theories cannot be directly applied to the important class of overconstrained wheeled vehicles. Some initial steps towards a motion planning were outlined and preliminary results for control of such vehicles were given. The extension of Chow's theorem proven in Chapter 5 was used to show conditions under which vehicles like the Mars rover are controllable. Moreover, variations of the rover were used to illustrate that controllability of the individual models that make up a multiple model driftless affine system is *not* sufficient to guarantee controllability of the overall multiple model driftless affine system.

8.2 Future

Vehicles, MEMS arrays, automated parts feeding, robotic fish, and a variety of other mechanical devices include nonsmooth effects in their dynamics, typically due to friction or dissipation. As there is no systematic way to treat these systems, we must either sacrifice accuracy by idealizing them as smooth systems or sacrifice performance by slowing them down enough so that the nonsmooth terms can be neglected. Given the widespread occurrence of such systems, a unified approach to control of these systems would have wide ranging benefits. In the broadest sense, future goals focus on developing such a unified scheme. This will begin in the short term with extensions to topics in this thesis.

Theory

There are a number of theoretical questions that need to be answered relative to the theoretical aspects of this work. Among them are many natural extensions from the geometry of smooth control systems to nonsmooth control systems. For instance, as a converse condition to the controllability theorem in Chapter 5, what version of the Frobenius theorem holds for nonsmooth systems? It is clear that if all the vectors making up the inclusion $\dot{x} \in F(x, t) = co(g_i)$ are equally integrable, i.e., they have the same integral manifold, then the inclusion F is integrable. However, there should be a version of Frobenius theorem appropriate to the case where the

distribution is closed for all the individual models of a multiple model driftless affine system. A related question, and perhaps more fundamental, is whether or not we can extend the controllability criterion in Chapter 5 to more general differential inclusions. The result given in this thesis relied heavily on the differential inclusions we were considering to be almost everywhere not only single-valued, but differentiable as well. Another question is how do we extend Brockett's [16] requirement for stabilizability? This will rest on the dependency of homotopy on the differentiability of the maps under consideration. I anticipate the theory of GDQs should give insight into this problem, but exactly the way these results will play out is unclear. Another interesting problem is to ask how we can take advantage of analyticity in the case of differential inclusions. For instance, as we define them, multiple model driftless affine systems are analytic almost everywhere, so even if the differential inclusion is a closed convex set of vector fields, it is one for which the derivatives of all its component vector fields reveal all of the local behavior. One could hope that the sufficient condition for controllability given in Chapter 5 is also necessary. As [44] points out, it is unclear how to extend control laws designed for a $(\mathcal{U}, \overline{\mathcal{U}})$ reducible system on Q to TQ . Certainly future work will include this in both the smooth and nonsmooth case. Lastly, one can ask what is the relationship between GDQs and robust control. In particular, is there a way of stating robust stabilizability criteria in terms of controllability of the set-valued map that includes the disturbances and uncertainties. Such a relationship could lead the way to intrinsic representations of robustness since GDQs are well defined on manifolds. Moreover, it could help us make more progress towards nonlinear versions of the small gain theorem, as well as other fundamental results in robust control.

Distributed Actuation

Distributed actuation offers many challenges in the next few years. These questions range from relatively easy questions to extremely difficult. Naturally, even at the relatively easy end, there are still interesting questions to answer. For instance, computing the Lagrangian formulation including contact states to see if any addi-

tional structure can be gleaned for the purposes of control design could potentially lead to controllers with better performance.

An equally interesting question is to determine a way to eliminate the practical need for *visual* feedback. For instance, one could use binary sensors that are active if the object is above them and inactive if it is below them. How fine a grid of such sensors, for a given object, is needed to uniquely identify its location and orientation? Perhaps more realistically, how fine a grid is required to identify these with some error ϵ ? Moreover, are there “behaviors” that would allow better estimation of the current location and orientation? For instance, it is easy to imagine that a combination of open loop plans for global maneuvers could allow a computer to discern the orientation of an object, but not without doing non-globally optimal trajectories. Hence, it is possible that distributed manipulation may be a good example of the trade off between information gathering through limited sensors and optimal controls given full state feedback. More work must be done on trajectory tracking, both theoretically and experimentally. On the physics side, how do we deal with more general environmental switching dependencies. The models used in this thesis all rely on the switching depending solely on the location of the center of mass. However, one would imagine that outside the domain of a very carefully set up experiment, additional dependencies will arise. In a somewhat similar vein, at what point does the open loop control strategy developed by Böhringer and Kavraki begin to be appropriate? For instance, can we make a “limit” like statement such as: “as the number of actuators on a compact set goes to ∞ , the error due to the programmable vector field approach will approach 0.” Such a result would be very useful in determining if a closed loop control structure is necessary for controlling a given object on a given set of actuators. From a controls perspective, how can we take advantage of discrete symmetries for distributed actuation. It is clear from the control designs given in Chapter 6 that many of the control laws are symmetric around the origin, and therefore we should use this symmetry to reduce the number of explicit controls we need to write down. However, we have not developed any systematic formal methods for doing so. Lastly, more experimentation must be done

on a more realistic MEMS level.

Underactuated but Overconstrained Systems

Systems such as the Mars rover offer many opportunities for future research. They illustrate the trade-off between static stability and easy of control. The results presented in Chapter 7 represent only the most basic advances in understanding a complete set of methods for such vehicles. Moreover, many choices still have to be made at a relatively high level. For instance, is there any reason to believe that time-varying feedback has any particular advantage of discontinuous feedback for such systems? How do we prove global stability for nonlinear over constrained systems? Can we extend work of [57] on stabilization of smooth nonholonomic systems to these systems to improve performance? Another example of an underactuated system is that of a robotic fish. It is well known that the control vector fields describing such a fish are only Lipschitz continuous at zero velocity (see [60]). Future work should include applying the work in [75] and in Chapter 5 to see under what conditions, if any, the robotic fish is locally controllable. For instance, one of the problems that This will perhaps lead to insights regarding what type of control strategies are reasonable and what types are not.

Control of Systems with Friction

Friction and intermittent contact represent a major challenge to the control community. This work only superficially treated friction models. Many previous methods have involved approximating the discontinuities produced by friction with differentiable ones, and then using the differentiability properties of those approximations. This thesis offers some of the basic analytical techniques necessary to treat nonsmooth systems, in particular nonsmooth systems arising from friction. However, much work needs to be done in order to treat systems with friction in a coherent, systematic, and rigorous fashion.

Appendix A

Coda: Experimental Setup

You are only as good as your last demo.

Howie Choset

This appendix describes an experimental distributed manipulation system, as well as the nonsmooth algorithm described in Section 6.3.3. Section A.1 briefly describes some other experimental distributed manipulation systems and how the Caltech system is related to theirs. Section A.2 describes both the mechanical design of the system, as well as the vision system that monitors the object's position. This section additionally provides an overview of the software used to run the experiment. Section A.3 fully describes the algorithm used in Section 6.3.3 and that was implemented in the experiment shown in Figure 6.12. I will end this appendix with a comment on the superposition principle for systems with contact forces in Section A.4.

A.1 Previous Experimental Setups

The experimental setup is related to that in used in Luntz et al. [50, 51, 48, 54]. Their setup consists of a planar table with an array of adjacent cells mounted on a table. Each cell consists of two wheels whose rotation axes are perpendicular. A

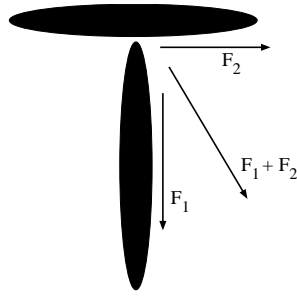


Figure A.1: Force Superposition

common assumption made in the field of distributed manipulation is that of force superposition. Consider Figure A.1 depicting two wheels that are perpendicular to each other, exerting forces on an invisible object resting on them. The superposition principle assumes that if we know the forces F_1 and F_2 , we can superimpose them to get a desired force F_{1+2} . This is the assumption made on the experiment used by Luntz et al [50, 51, 48, 54]. Their system uses a light sensor at each cell. Therefore it is known whether the object is above a given cell or not¹. It has been used as a test-bed in numerous experiments in distributed manipulation. As we will see, the experimental apparatus used in this thesis has a number of key advantages.

A.2 Fully Actuated Distributed Manipulator (FADM)

The distributed manipulator used for the experiments is pictured in Figure A.2. The design is a modular one based on a basic cell design. The Fully Actuated Distributed Manipulation (FADM) system has a total of 10 cells. Each cell contains two actuators. One actuator orients the wheel axis, while the other actuator drives the wheel rotation (see Figure A.5). These cells can be repositioned easily into different configurations - Figure A.6 has the FADM system in an 8 cell configuration which emulates the setup used in [50, 51, 48, 54] and described in the previous section. Both orientation and the wheel velocity are driven by Pittman brushless 12V motors which are connected to JR-Kerr Pic-Servo-3PH motor controller boards.

¹This experiment will change to a vision-based feedback system soon.

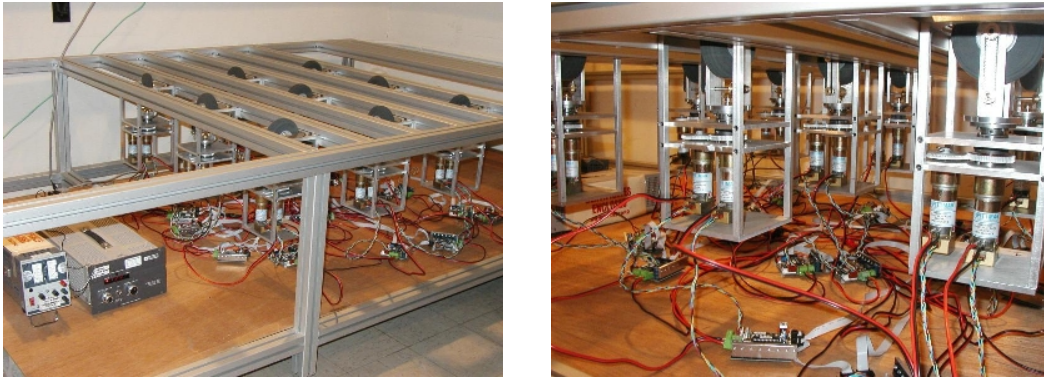


Figure A.2: Front and Underside of the FADM System

All 20 motor boards are connected through a daisy chain to a central computer through one of its serial ports. The motors are all powered by a variable regulated power supply rated up to 14 amps. The motor controller boards are powered by a separate power supply rated up to 3 amps. (The motor controller boards by themselves use around 100-140 mA each).

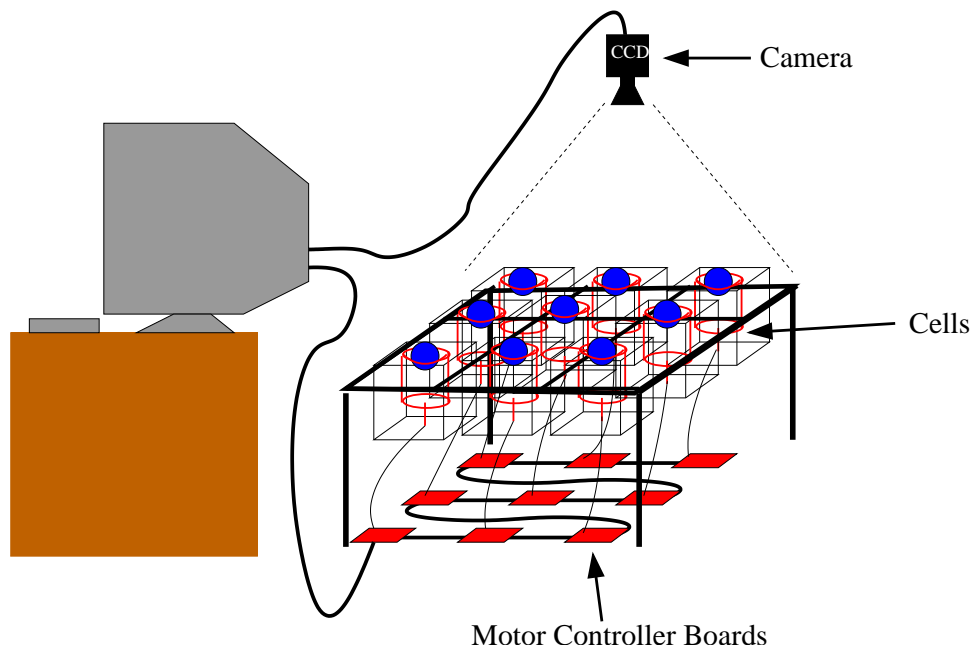


Figure A.3: Cartoon of Experiment

The cells themselves have a four-inch radius wheel made of soft foam rubber to

accentuate the friction reaction force. These wheels were chosen because they have the proper friction distribution described in Section 6.2.

A Sony XC-73 monochrome CCD camera with a Cosmocar C60607 6 mm lens is used for the vision system. Images are captured by an Imagenation PXC-200 framegrabber card. For feedback, feature tracking software (written in C) developed at Caltech in the Computational Vision Laboratory of Pietro Perona is used (see [31]). The software was adapted to select a right triangle (seen in Figure A.6) and track its motion so as to obtain coordinates of the moving body. This software code is integrated with motor control software through the motor boards. Because of the long communication delays required to send control signals to all motor controller boards, it is only possible to realize about six to seven iterations per second. Therefore, our feedback only has a time resolution of about 6 Hz. Moreover, we have implemented almost no low level controls to account for aliasing, actuator saturation, etcetera. Efforts are under way to improve the code so as to enable both faster iterations and more robust performance.

A.3 Algorithm for Nonsmooth Feedback

This section gives the algorithm used in the underactuated distributed manipulation experiment found in Chapter 6. Consider Figure A.4. Here is a four cell region like that seen in Figure 6.3. It is divided up into 16 regions, labeled **I–VIII** and $0–2\pi$ in increments of $\frac{\pi}{4}$. The roman numerals stand for the open areas in which one contact state holds and the π regions are the boundaries between contact states. Depending on where the object is, the algorithm chooses a different appropriate control law. This is schematically depicted in Table A.4. In each one of these regions a control law calculated from the Lyapunov function $k(x^2 + y^2 + \theta^2)$ is shown, where k is some constant to be chosen during implementation. These control laws can be found in Tables A.2 and A.3.

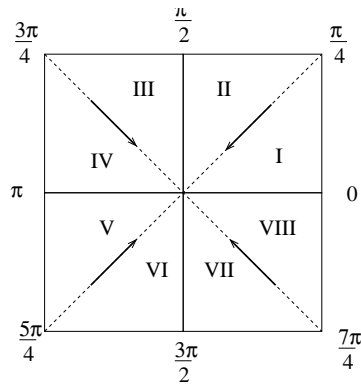


Figure A.4: Algorithm for Nonsmooth Feedback

A.4 A Comment on Superposition of Forces

An underlying assumption throughout this thesis is that the mechanics of contact between an object and the manipulation surface matter - one can not assume them away. Now consider Figure 6.13. In this experiment steerable wheels and a smooth control algorithm were used to control the object being manipulated. Excellent performance was realized. Now consider Figure A.8, which shows results of the following experiment. In this experiment *the same* algorithm is used under the superposition assumption while using a set up like that seen in Figure A.6. The results were terrible. The object never comes close to the desired equilibrium. Therefore, the superposition principle is not a good approximation when dealing with actuators that have significant contact mechanics. The reason this algorithm does not work is that the superposition principle does not take into account the reaction forces due to sliding across the wheel. Consider Figure A.1 again. Suppose that $F_1 = 0$ and F_2 is some nominal force. The superposition principle assumes that F_2 would be the only contributing force in that situation, despite the fact that is known to be false. At high enough speeds this is a good approximation, but at low speeds the contact constraint forces must be taken into consideration.

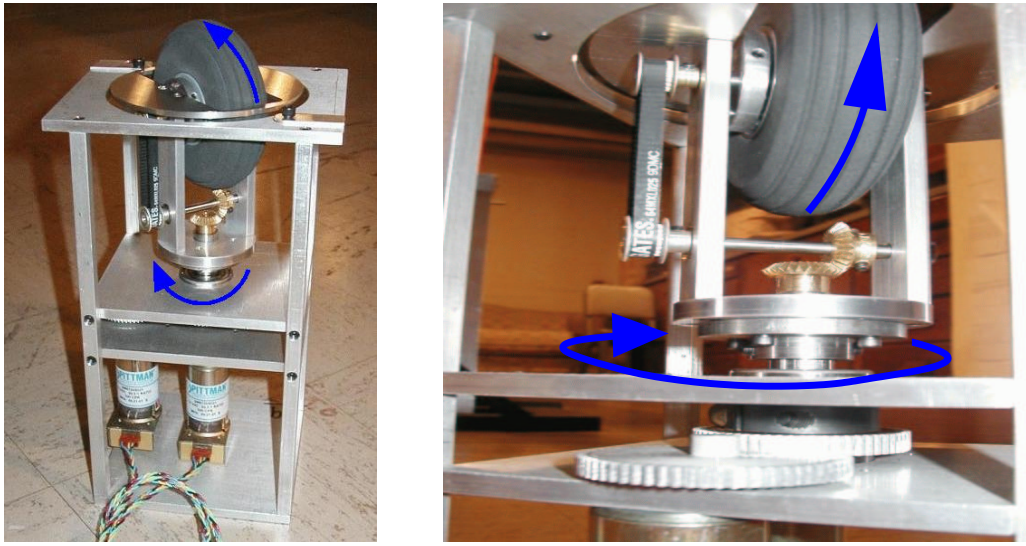


Figure A.5: Pictures of one of the Cells - The cells have two motors mounted to them, each controlling a different axis of motion (marked in blue) of the cell. For a sense of scale, the wheels are four inches in diameter.

if $x > e$ $y > e$		elseif $x < -e$ $y > e$
if $ x > y + e$		if $ x < y - e$
then I		then VII
elseif $ x < y - e$		elseif $ x > y + e$
then II		then VIII
else $\text{PI}/4$		else $7\text{PI}/4$
elseif $x < -e$ $y > e$		elseif $x > e$
if $ x < y - e$		then 0
then III		elseif $x < -e$
elseif $ x > y + e$		then PI
then IV		elseif $y > e$
else $3\text{PI}/4$		then $\text{PI}/2$
elseif $x < -e$ $y > e$		elseif $y < -e$
if $ x > y + e$		then $3\text{PI}/2$
then V		else ORIGIN
elseif $ x < y - e$		
then VI		
else $5\text{PI}/4$		

Table A.1: Nonsmooth control law

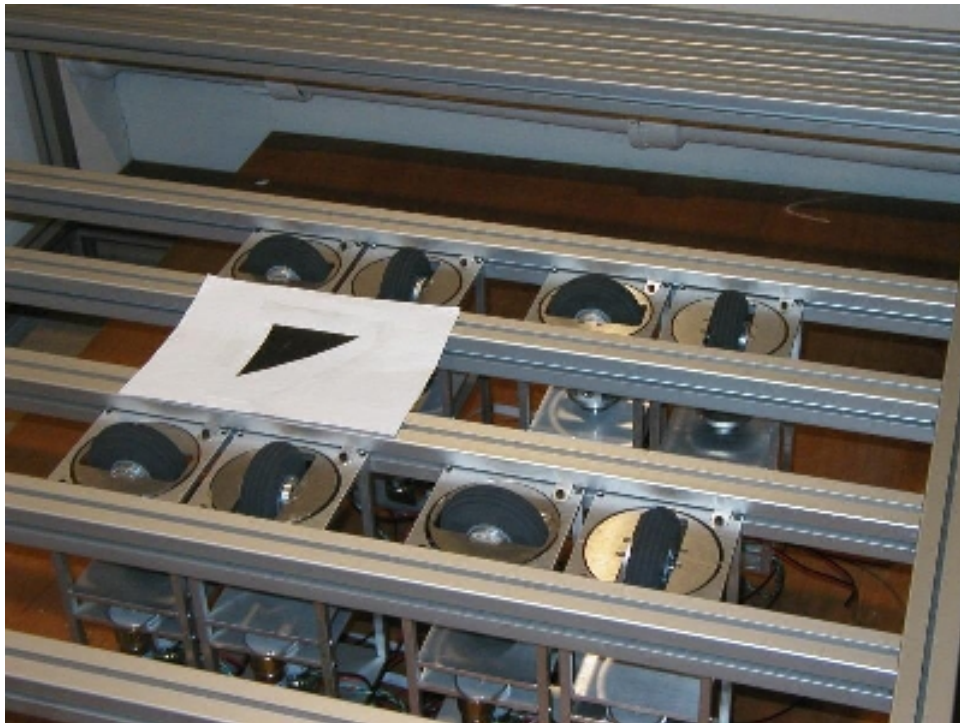


Figure A.6: 8 cell configuration of FADM system—the cells mount into a table which makes it easy to reconfigure them into new arrays. A piece of plexiglass is used as the manipulated object (so that an observer can see what the cells are doing underneath) and a black triangle is used to acquire the location of the plexiglass.

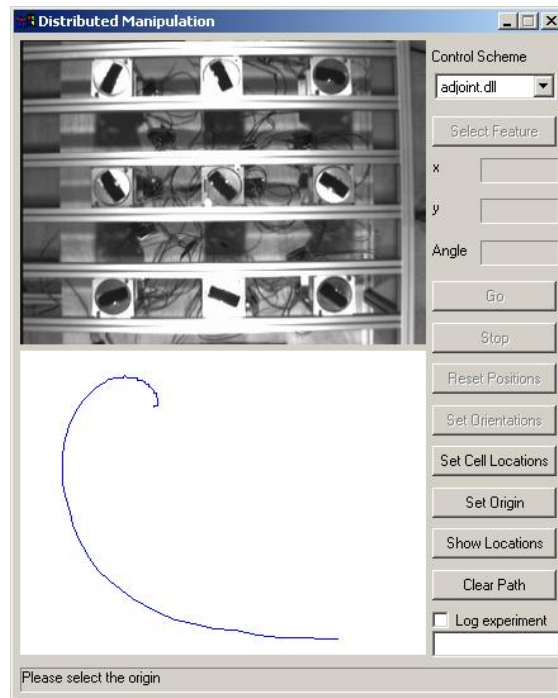


Figure A.7: FADM Computer Interface: The interface has a continuously updated screen that shows the user both the video output and where the algorithm is estimating the triangle (which is used for feedback) is located. Below the video is the estimated path of the object as it moves. On the right-hand side the user can choose the control scheme and select features in the video. For instance, the user can tell the program the initial location of the cells and the triangle being used for feedback.

Region	Control Law	Region	Control Law
I	$u_1 \frac{-(u_4(\theta+x-y))+k(\theta^2+x^2+y^2)}{x+y}$ $u_2 k\theta$ $u_3 \frac{-(u_4(\theta+x-y))+k(\theta^2+x^2+y^2)}{x+y}$ $u_4 k\theta$	II	$u_1 \frac{u_2(\theta+x-y)+k(\theta^2+x^2+y^2)}{x+y}$ $u_2 -k\theta$ $u_3 \frac{u_2(\theta+x-y)+k(\theta^2+x^2+y^2)}{x+y}$ $u_4 -k\theta$
III	$u_1 k\theta$ $u_2 \frac{u_1(\theta+x+y)-k(\theta^2+x^2+y^2)}{x-y}$ $u_3 k\theta$ $u_4 \frac{u_1(\theta+x+y)-k(\theta^2+x^2+y^2)}{x-y}$	IV	$u_1 -k\theta$ $u_2 -\frac{u_3(\theta+x+y)+k(\theta^2+x^2+y^2)}{x-y}$ $u_3 -k\theta$ $u_4 -\frac{u_3(\theta+x+y)+k(\theta^2+x^2+y^2)}{x-y}$
V	$u_1 \frac{u_2(\theta-x+y)-k(\theta^2+x^2+y^2)}{x+y}$ $u_2 k\theta$ $u_3 \frac{u_2(\theta-x+y)-k(\theta^2+x^2+y^2)}{x+y}$ $u_4 k\theta$	VI	$u_1 -\frac{u_4(\theta-x+y)+k(\theta^2+x^2+y^2)}{x+y}$ $u_2 -k\theta$ $u_3 -\frac{u_4(\theta-x+y)+k(\theta^2+x^2+y^2)}{x+y}$ $u_4 -k\theta$
VII	$u_1 k\theta$ u_2 $u_3 k\theta$ $u_4 \frac{u_3(-\theta+x+y)+k(\theta^2+x^2+y^2)}{x-y}$	VIII	$u_1 -k\theta$ $u_2 \frac{u_1(\theta-x-y)+k(\theta^2+x^2+y^2)}{x-y}$ $u_3 -k\theta$ $u_4 \frac{u_1(\theta-x-y)+k(\theta^2+x^2+y^2)}{x-y}$

Table A.2: List of control laws for regions I-VIII

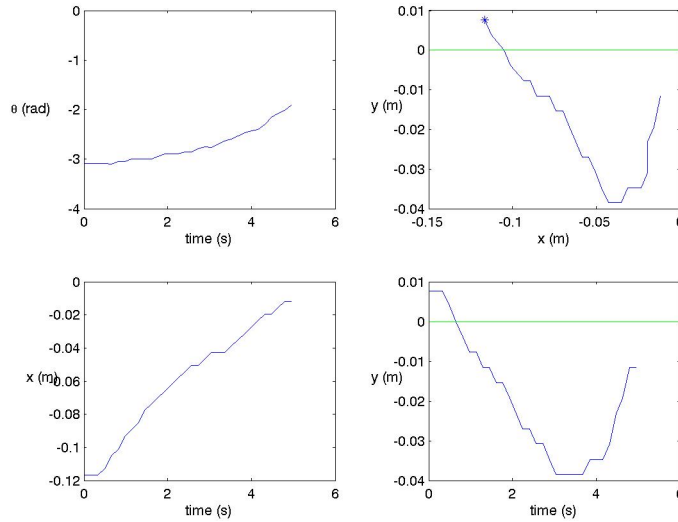


Figure A.8: Superposition experiment

Region	Control Law	Region	Control Law
$\mathbf{0}$	$u_1 \quad k\theta$ $u_2 \quad \frac{-u_1((-1+\delta)\theta+x+y)+k(\theta^2+x^2+y^2)}{\delta\theta+x-y}$ $u_3 \quad -k\theta$ $u_4 \quad \frac{-u_1((-1+\delta)\theta+x+y)+k(\theta^2+x^2+y^2)}{\delta\theta+x-y}$	$\pi/4$	$u_1 \quad \frac{-(-u_2+\delta(u_2+u_4))(\theta+x-y)+k(\theta^2+x^2+y^2)}{x+y}$ $u_2 \quad -k\theta$ $u_3 \quad \frac{-(-u_2+\delta(u_2+u_4))(\theta+x-y)+k(\theta^2+x^2+y^2)}{x+y}$ $u_4 \quad k\theta$
$\pi/2$	$u_1 \quad \frac{u_2(\delta\theta+x-y)+k(\theta^2+x^2+y^2)}{(1-\delta)\theta+x+y}$ $u_2 \quad -k\theta$ $u_3 \quad \frac{u_2(\delta\theta+x-y)+k(\theta^2+x^2+y^2)}{(1-\delta)\theta+x+y}$ $u_4 \quad k\theta$	$3\pi/4$	$u_1 \quad k\theta$ $u_2 \quad \frac{(-u_3+\delta(u_1+u_3))(\theta+x+y)-k(\theta^2+x^2+y^2)}{x-y}$ $u_3 \quad -k\theta$ $u_4 \quad \frac{(-u_3+\delta(u_1+u_3))(\theta+x+y)-k(\theta^2+x^2+y^2)}{x-y}$
π	$u_1 \quad k\theta$ $u_2 \quad -\frac{u_3(\delta\theta+x+y)+k(\theta^2+x^2+y^2)}{(-1+\delta)\theta+x-y}$ $u_3 \quad -k\theta$ $u_4 \quad -\frac{u_3(\delta\theta+x+y)+k(\theta^2+x^2+y^2)}{(-1+\delta)\theta+x-y}$	$5\pi/4$	$u_1 \quad \frac{(-u_4+\delta(u_2+u_4))(\theta-x+y)-k(\theta^2+x^2+y^2)}{x+y}$ $u_2 \quad -k\theta$ $u_3 \quad \frac{(-u_4+\delta(u_2+u_4))(\theta-x+y)-k(\theta^2+x^2+y^2)}{x+y}$ $u_4 \quad k\theta$
$3\pi/2$	$u_1 \quad -\frac{u_4(\delta\theta-x+y)+k(\theta^2+x^2+y^2)}{(-1+\delta)\theta+x+y}$ $u_2 \quad -k\theta$ $u_3 \quad -\frac{u_4(\delta\theta-x+y)+k(\theta^2+x^2+y^2)}{(-1+\delta)\theta+x+y}$ $u_4 \quad k\theta$	$7\pi/4$	$u_1 \quad k\theta$ $u_2 \quad \frac{-(-u_1+\delta(u_1+u_3))(\theta-x-y)+k(\theta^2+x^2+y^2)}{x-y}$ $u_3 \quad -k\theta$ $u_4 \quad \frac{-(-u_1+\delta(u_1+u_3))(\theta-x-y)+k(\theta^2+x^2+y^2)}{x-y}$

Table A.3: List of control laws for regions $\mathbf{0} - \frac{7\pi}{4}$

A Note on Notation

This note attempts to introduce a systematic and consistent formalism. However, I should note that my attempts to do so have been thwarted over time by both the overwhelming number of things needing notation in this thesis, the number of relatively disjoint theories all with their own notations, and this author's inability to create a suitable way to combine them. Therefore, the reader may notice that the notation used in this thesis differs considerably even from some of the articles on which this thesis is based. Nevertheless, I try to adapt as standard a notation as possible. I encourage the reader to use the symbol index below. In general, I will denote sets by upper case letters (A and Ω), and elements of said sets by lower case letters (a, ω). I will deviate from this only when I need to distinguish between subsets as a domain (say $A \subset \Omega$) and a subset of a function space (i.e. a set-valued map $\mathbf{f} : A \rightarrow B$). In general I will attempt to use the convention of making set-valued maps bold face (\mathbf{f}, \mathbf{g}). Sadly, even this convention does not always seem consistent, because I will refer to the flow of a differential inclusion $\dot{x} \in \mathbf{f}(t, x)$ by $\Phi^{\mathbf{f}}$ and in the case \mathbf{f} is single valued (i.e. $\mathbf{f} = f$) I will refer to it as Φ^f . The problem is that in both cases the map Φ is a set valued map from \mathbb{R} to Q . So, rather than break even further from traditional convention, I accept lack of perfection in consistency.

As much as possible, I will use the convention of stating theorems, lemmas, and corollaries in the form **Theorem 1.1 (Author [year])** so that the references will be clear. The only exception to this will be the classical results found in the introduction where sources and references are already made explicit, and, of course, the results which are new in this thesis.

General Notation

\mathbb{R}	The real numbers	12
\mathbb{Q}	The rational numbers	12
\mathbb{N}	The natural numbers	12
<i>a.e.</i>	almost everywhere	20
<i>a.a.</i>	almost always	19
C^k	Differentiable k times	12
$[\cdot, \cdot]$	The Lie bracket	12
$\langle \cdot, \cdot \rangle$	The symmetric product	43
TQ	The tangent space to a configuration manifold	12
Q	A configuration manifold	12
Δ_q	Vector field distribution at a point q	13
γ	Set valued differential inclusion	55
\mathcal{D}	Dissipation functional	30
λ_i	Lagrange multipliers	26

Supervisory Control

$\sigma_e(t)$	Environmental switching in time	125
$\sigma_c(t)$	Controller switching in time	121
τ_d	Upper bound on time delay	125
$N_\sigma(t_0, t)$	Number of switches σ_x experiences in time (t_0, t)	125
p^*	The <i>actual</i> process	120
A_p	Matrix describing dynamics for plant p	120
ϵ_μ	Monitoring signal constant	121
μ_p	Monitoring signal	121
\mathbb{P}	Uncertain process	120
\mathbb{C}	Candidate controllers	120
\mathbb{E}	Multi-estimator	120
\mathbb{M}	Monitoring signal generator	121

§	Switching logic	121
Ⓓ	Environmental signal generator	124

Bibliography

- [1] R. Abraham, J.E. Marsden, and T.S. Ratiu. *Manifolds, Tensor Analysis, and Applications*. Addison–Wesley, 1988.
- [2] M. Adams and V. Guillemin. *Measure Theory and Probability*. Birkhäuser, 1996.
- [3] J.C. Alexander and J.H. Maddocks. On the kinematics of wheeled vehicles. *The International Journal of Robotics Research*, 8(5):15–27, October 1989.
- [4] B.D.O. Anderson, T.S. Brinsmead, F. De Bruyne, J.P. Hespanha, D. Liberzon, and A.S. Morse. Multiple model adaptive control. I. finite controller coverings. *George Zames Special Issue of the Int. J. of Robust and Nonlinear Control*, 10(11-12):909–929, Sep 2000.
- [5] E. Asarin, O. Bournez, T. Dang, O. Maler, and A. Pnueli. Effective synthesis of switching controllers for linear systems. *Proc. IEEE*, 88(7):1011–1025, July 2000.
- [6] J.P. Aubin. *Viability Theory*. Birkhäuser, 1991.
- [7] K. Bhattacharya and R.D. James. A theory of thin films of martensitic materials with applications to microactuators. *J. Mech. Phys. Solids*, 47:531–576, 1999.
- [8] A.M. Bloch, P. S. Krishnaprasad, J.E. Marsden, and R.M. Murray. Nonholonomic mechanical systems with symmetry. *Arch. Rational Mech. Anal.*, 136(1):21–99, 1996.

- [9] K.F. Böhringer, R. G. Brown, B. R. Donald, J.S. Jennings, and D. Rus. Sensorless manipulation using transverse vibrations of a plate. In *Proc. IEEE Int. Conf. on Robotics and Automation*, pages 1989–1996, Nagoya, Japan, 1995.
- [10] K.F. Böhringer and H. Choset, editors. *Distributed Manipulation*. Kluwer, 2000.
- [11] K.F. Böhringer, B. Donald, and N. MacDonald. Upper and lower bounds for programmable vector fields with applications to mems and vibratory plate parts feeders. In *Algorithms for Robotic Motion and Manipulation*, pages 255–276. A.K. Peters, Ltd., 1997.
- [12] K.F. Böhringer, B.R. Donald, L.E. Kavraki, and F. Lamiroux. A distributed, universal device for planar parts feeding: unique part orientation in programmable force fields. In *Distributed Manipulation*, pages 1–28. Kluwer, 2000.
- [13] K.F. Böhringer, R.G. Donald, N.C. MacDonald, G.T.A. Kovacs, and J.W. Suh. Computational methods for design and control of mems micromanipulator arrays. *IEEE Computer Science and Engineering*, pages 17–29, 1997.
- [14] W.M. Boothby. *An Introduction to Differentiable Manifolds and Riemannian Geometry*. Academic Press, 1986.
- [15] M.S. Branicky. Multiple Lyapunov functions and other analysis tools for switched and hybrid systems. *IEEE Trans. Automatic Control*, 43(4):475–482, April 1998.
- [16] R. Brockett. *Stabilization in Differential Geometric Control Theory*, chapter Asymptotic Stability and Feedback Stabilization, pages 181–191. Birkhäuser, 1983.
- [17] R.W. Brockett. *New Directions in Applied Mathematics*, chapter Control Theory and Singular Riemannian Geometry. Springer-Verlag, New York, 1981.
- [18] W.L. Chow. Über systeme von linearen partiellen differentialgleichungen erster ordnung. *Math Ann.*, 117:98–105, 1939.

- [19] F.H. Clarke. *Optimization and Nonsmooth Analysis*. SIAM, 1990.
- [20] F.H. Clarke, Y.S. Ledyaev, R.J. Stern, and P.R. Wolenski. *Nonsmooth Analysis and Control Theory*. Springer, 1998.
- [21] E.A. Coddington and N. Levinson. *Theory of Ordinary Differential Equations*. Krieger, 1955.
- [22] M. Coutinho and P. Will. The intelligent motion surface: a hardware/software tool for the assembly of meso-scale devices. In *IEEE Int. Conf. on Robotics and Automation (ICRA)*, 1997. Albuquerque, New Mexico.
- [23] R.W.R. Darling. *Differential Forms and Connections*. Cambridge University Press, 1994.
- [24] W.P. Dayawansa and C.F. Martin. A converse Lyapunov theorem for a class of dynamical systems which undergo switching. *IEEE Trans. Automatic Control*, 44(4):751–760, Apr. 1999.
- [25] K. Deimling. *Multivalued Differential Equations*. Walter de Gruyter, 1992.
- [26] M.A. Erdmann and M.T. Mason. An exploration of sensorless manipulation. *IEEE Journal of Robotics and Automation*, 4(4), 1988.
- [27] A.F. Filippov. *Differential Equations with Discontinuous Right-Hand Sides*. Kluwer, 1988.
- [28] T. Frankel. *The Geometry of Physics: An Introduction*. Cambridge University Press, 1997.
- [29] H. Fujita. Group work of microactuators. In *International Advanced Robot Program Workshop on Micromachine Technologies and Systems*, pages 24–31, Tokyo, Japan, 1993.
- [30] K.Y. Goldberg. Orienting polygonal parts without sensing. *Algorithmica*, 143 (2/3/4):201–225, 1993.

- [31] Luis Goncalves and Enrico Di Bernardo. Software for motion tracking. Developed at the Caltech Vision Lab, 2000.
- [32] B. Goodwine and J.W. Burdick. Controllability of kinematic control systems on stratified configuration spaces. *IEEE Trans. on Automatic Control*, 46(3): 358–368, 2000.
- [33] S. Goyal, A. Ruina, and J. Papadopoulos. Planar sliding with dry friction. Part 1. limit surface and moment friction. *WEAR*, 143:307–330, 1991.
- [34] S. Goyal, A. Ruina, and J. Papadopoulos. Planar sliding with dry friction. Part 2. dynamics of motion. *WEAR*, 143:331–352, 1991.
- [35] J.P. Hespanha, D. Liberzon, and A.S. Morse. Logic-based switching control of a nonholonomic system with parametric uncertainty. *Systems Control Lett.*, 38:167–177, 1999.
- [36] J.P. Hespanha, D. Liberzon, A.S. Morse, B.D.O. Anderson, T.S. Brinsmead, and Franky De Bruyne. Multiple model adaptive control, part 2: Switching. *Int. J. of Robust and Nonlinear Control Special Issue on Hybrid Systems in Control*, 11(5):479–496, April 2001.
- [37] J.P. Hespanha and A. S. Morse. Stability of switched systems with average dwell-time. In *Proc. IEEE Int. Conf. on Decision and Control*, 1999.
- [38] J.P. Hespanha and A.S. Morse. Stability of switched systems with average dwell-time. Technical report, EE-Systems, University of Southern California, 1999.
- [39] I. Kolmanovsky and N.H. McClamroch. Developments in nonholonomic control problems. *IEEE Control Systems Magazine*, pages 20–36, December 1995.
- [40] P. Krulevitch, A.P. Lee, P.B. Ramsey, J.Trevino J. Hamilton, and M.A. Northrup. Thin film shape memory alloy microactuators. *Journal of Micro Electro Mechanical Systems*, 5(270), 1996.

- [41] R. Howe K.S.J. Pister, R. Fearing. A planar air levitated electrostatic actuator system. In *Proceedings IEEE Workshop on Micro Electro Mechanical Systems (MEMS)*, pages 67–71, Napa Valley, California, 1990.
- [42] J.P. LaSalle. Stability theory for ordinary differential equations. *J. Diff. Eq.*, 4:57–65, 1968.
- [43] A.P. Lee, C.F. McConaghy, P. Krulevitch, G.E. Sommargren, and J. Trevino. Electrostatic comb drive for vertical actuation. In *Proceedings of Micromachined Devices and Components, SPIE 1997 Symposium on Micromachining and Microfabrication*, volume 109, Austin, Texas, 1997.
- [44] A.D. Lewis. When is a mechanical control system kinematic? In *Proc. 38th IEEE Conf. on Decision and Control*, pages 1162–1167, Dec. 1999.
- [45] A.D. Lewis. Simple mechanical control systems with constraints. *IEEE Transactions on Automatic Control*, 45(8):1420–1436, 2000.
- [46] A.D. Lewis, R.M. Murray, and J.W. Burdick. Nonholonomic mechanics and locomotion: the snakeboard example. In *Proc. IEEE Int. Conf. on Robotics and Automation*, pages 2391–2397, May 1994.
- [47] D. Liberzon and A.S. Morse. Basic problems in stability and design of switched systems. *IEEE Control System Mag.*, 19(5):59–70, 1999.
- [48] J. Luntz and W. Messner. Closed-loop stability of distributed manipulation. In *Proc. American Control Conference (ACC)*, 2000.
- [49] J. Luntz, W. Messner, and H. Choset. Stick-slip operation of the modular distributed manipulator system. In *Proc. American Control Conference (ACC)*, 1998.
- [50] J. Luntz, W. Messner, and H Choset. Velocity field design on the modular distributed manipulator system. In *Proceedings, Workshop on the Algorithmic Foundations of Robotics*, 1998.

- [51] J. Luntz, W. Messner, and H. Choset. Open loop orientability of objects on actuator arrays. In *Proceedings of the IEEE International Conference on Robotics and Automation (ICRA)*, 1999.
- [52] J. Luntz, W. Messner, and H. Choset. Closed-loop distributed manipulation using discrete actuator arrays. In *Workshop on the Algorithmic Foundations of Robotics (WAFR)*, 2000.
- [53] J. Luntz, W. Messner, and H. Choset. Closed-loop operation of actuator arrays. In *Proc. IEEE Int. Conf. on Robotics and Automation*, 2000.
- [54] J. Luntz, W. Messner, and H. Choset. *Distributed Manipulation*, chapter Discreteness Issues in Actuator Arrays. Kluwer Academic Publishers, 2000.
- [55] H. Fujita M. Ataka, A. Omodaka. A biomimetic micro motion system. In *Transducers - Digest International Conference on Solid State Sensors and Actuators*, pages 38–41, 1993. Pacifico, Yokohama, Japan.
- [56] M.D.P. Monteiro Marques. *Differential Inclusions in Nonsmooth Mechanical Problems*. Birkhäuser, 1993.
- [57] R.T. M'Closkey III. *Exponential Stabilization of Driftless Nonlinear Control Systems*. PhD thesis, California Institute of Technology, January 1995.
- [58] MEMS Exchange. Current challenges. <http://www.mems-exchange.org/>, April 2001.
- [59] J.J. Moreau and P.D. Panagiotopoulos (editors). *Nonsmooth Mechanics and Applications*. Springer-Verlag, 1988.
- [60] K. A. Morgansen, V. Duijndam, R. J. Mason, J. W. Burdick, and R. M. Murray. Nonlinear control methods for planar carangiform robot fish locomotion. In *Proc. IEEE Int. Conf. on Robotics and Automation*, Seoul, Korea, 2001.
- [61] T. D. Murphey and J. W. Burdick. Issues in controllability and motion planning for overconstrained wheeled vehicles. In *Proc. Int. Conf. Math. Theory of Networks and Systems (MTNS)*, Perpignan, France, 2000.

- [62] T. D. Murphey and J. W. Burdick. A controllability test and motion planning primitives for overconstrained vehicles. In *Proc. IEEE Int. Conf. on Robotics and Automation*, Seoul, Korea, 2001.
- [63] T. D. Murphey and J. W. Burdick. Global stability for distributed systems with changing contact states. In *Proc. IEEE Int. Conf. on Intelligent Robots and Systems*, Hawaii, 2001.
- [64] T. D. Murphey and J. W. Burdick. On the stability and design of distributed systems. In *Proc. IEEE Int. Conf. on Robotics and Automation*, Seoul, Korea, 2001.
- [65] T. D. Murphey and J. W. Burdick. A controllability test for multiple model systems. In *Proc. IEEE American Controls Conference (ACC)*, Anchorage, Alaska, 2002.
- [66] T. D. Murphey and J. W. Burdick. Global exponential stabilizability for distributed manipulation. In *Proc. IEEE Int. Conf. on Robotics and Automation*, Washington D.C., 2002.
- [67] T. D. Murphey and J. W. Burdick. Nonsmooth controllability and an example. In *Proc. IEEE Conf. on Decision and Control (CDC)*, Washington D.C., 2002.
- [68] R.M. Murray, Z. Li, and S.S. Sastry. *A Mathematical Introduction to Robotic Manipulation*. CRC Press, 1994.
- [69] R.M. Murray and S.S. Sastry. Steering nonholonomic systems in chained form. In *Proc. Int. Conf. on Decision and Control (CDC)*, pages 1121–1126, 1991.
- [70] R.M. Murray and S.S. Sastry. Nonholonomic motion planning: Steering using sinusoids. *IEEE Transactions on Automatic Control*, 38:700–716, 1993.
- [71] G.J. Pappas, G. Laffierier, and S. Sastry. Hierarchically consistent control systems. *IEEE Trans. Automatic Control*, 45(6):1144–1160, June 2000.

- [72] M. A. Peshkin and A. C. Sanderson. Minimization of energy in quasistatic manipulation. *IEEE Transactions on Robotics and Automation*, 5(1), February 1989.
- [73] M.A. Peshkin. *Planning Robotic Manipulation Strategies for Sliding Objects*. PhD thesis, Carnegie-Mellon University, 1986.
- [74] L.S. Pontryagin, V.G. Boltyanskii, and R.V. Gamkrelidze. *The Mathematical Theory of Optimal Processes*. Wiley, New York, 1962.
- [75] F. Rampazzo and H. J. Sussmann. Set-valued differentials and a nonsmooth version of Chow's theorem. In *Proc. of 40th Conf. Decision Control*, 2001.
- [76] S. Sastry. *Nonlinear Systems: Analysis, Stability, and Control*. Springer, 1999.
- [77] K.P. Seward, P. Krulevitch, H.D. Ackler, and P. Ramsey. A new mechanical characterization method for microactuators applied to shape memory films. In *10th International Conference on Solid State Sensors and Actuators, Transducers '99*, Sendai, Japan, 1999.
- [78] S.M. Song. and K.J. Waldron. *Machines that walk: the Adaptive Suspension Vehicle*. MIT Press, 1989.
- [79] A. Sudsang and L. Kavraki. A geometric approach to designing a programmable force field with a unique stable equilibrium for parts in the plane. In *Proc. IEEE Int. Conf. Robotics and Automation*, Seoul, Korea, 2001.
- [80] H.J. Sussmann. Multidifferential calculus: Chain rule, open mapping and transversal intersection theorems. In *Optimal Control: Theory, Algorithms, and Applications*, pages 436–487. Kluwer, 1998.
- [81] H.J. Sussmann. *New theories of set-valued differentials and new versions of the maximum principle of optimal control theory*, chapter Nonlinear Control in the Year 2000. Springer-Verlag, London, 2000. A. Isidori, F. LamnabhiLagarrigue, and W. Respondek, Eds.

- [82] A.R. Teel, R.M. Murray, and G. Walsh. Nonholonomic control systems: From steering to stabilization with sinusoids. *Int. J. of Control*, 62(4):849–870, 1995.
- [83] V.I. Utkin. *Sliding Modes and Their Applications in Variable Structure Theory*. Mir Publishers, 1978.
- [84] K.J. Waldron and C.J. Hubert. Control of contact forces in wheeled and legged off-road vehicles. In *Preprints, 6th Symp. on Experimental Robotics*, pages 265–274, Sydney, Australia, March 1999.
- [85] F.W. Warner. *Foundations of Differentiable Manifolds and Lie Groups*. Springer-Verlag, 1971.
- [86] S. Wiggins. *Introduction to Applied Nonlinear Dynamical Systems and Chaos*. Springer Verlag, 1990.
- [87] M. Zefran and J.W. Burdick. Design of switching controllers for systems with changing dynamics. *Proc. Conf. on Decision and Control*, 1998.